Old materials with new tricks: multifunctional open-framework materials

Daniel Maspoch,[ab] Daniel Ruiz-Molina[a] and Jaume Veciana*[a]

Received 4th October 2006
First published as an Advance Article on the web 8th February 2007
DOI: 10.1039/b501600m

The literature on open-framework materials has shown numerous examples of porous solids with additional structural, chemical, or physical properties. These materials show promise for applications ranging from sensing, catalysis and separation to multifunctional materials. This *critical review* provides an up-to-date survey to this new generation of multifunctional open-framework solids. For this, a detailed revision of the different examples so far reported will be presented, classified into five different sections: magnetic, chiral, conducting, optical, and labile open-frameworks for sensing applications. (413 references.)

1 Introduction

Since the discovery of the excellent properties and applications of aluminosilicate zeolites in the areas of ion-exchange, separations, and catalysis,[1,2] the science of porous materials has become one of the most challenging issues for chemists, physicists and nanotechnologists over the last 30 years. Along all these years, the number of new synthetic porous solids has increased significantly. The most remarkable breakthrough was materialized in 1982, when Flanigen and co-workers reported the synthesis of the first zeolite-analogue, the microporous aluminophosphates solids ($ALPO_4$-*n*, where *n* refers to a structural type).[3] This pioneering zeolite-like family stimulated the discovery of novel inorganic porous materials,[4] most of them based upon oxygen-containing inorganic materials. In addition to the family of phosphates with a large list of different metal ions (gallium,[5] tin,[6] iron,[7] cobalt,[8,9] vanadium,[10] indium,[11] boron,[12] manganese,[13] molybdenum,[14] *etc.*), more recently new oxygen-containing porous materials such as phosphites,[15] oxofluorides and oxochlorides,[16] fluorides,[17] nitrides,[18] sulfates,[19] sulfides,[20] selenites,[21] halides,[22] germanates,[23] arsenates,[24] and cyanides[25] have been obtained.

Along with the progress of purely inorganic porous solids, another innovation for the synthesis of porous materials emerged at the beginning of the 1990s with the introduction of organic molecules as constituents of the structure. Such polytopic organic ligands, generally nitrogen- and oxygen-donor ligands, connect "inorganic" frameworks along the space in the appropriate topology to originate connected void volumes in the structure. These new porous materials can be classified into different families according to the dimensionality of the inorganic framework: (i) organic–inorganic hybrid materials (2-D and 1-D), (ii) coordination polymers (0-D), and (iii) pure organic materials. A schematic

[a]*Institut de Ciència de Materials de Barcelona (CSIC), Campus Universitari de Bellaterra, 08193, Cerdanyola, Spain. E-mail: vecianaj@icmab.es; Fax: (34) 935805729; Tel: (34) 935801853*
[b]*Actual address: Institut Català de Nanotecnologia, Campus Universitari de Bellaterra, 08193, Bellaterra, Spain*

Daniel Maspoch Comamala

Daniel Maspoch Comamala was born in L'Escala, Catalonia, Spain in 1976. He received his BSc degree in Chemistry from Universitat de Girona. He earned his PhD in Materials Science at the Universitat Autònoma de Barcelona (UAB) and at the Institut de Ciència dels Materials de Barcelona (ICMAB-CSIC) under the supervision of Prof. Jaume Veciana, Prof. Concepció Rovira and Dr Daniel Ruiz Molina in the field of magnetic porous molecular materials. After receiving his PhD degree in 2004, he joined Prof. Chad A. Mirkin's group at Northwestern University as a postdoctoral research associate. His project involved the study and formation of nanostructures on surfaces by Dip-Pen Nanolithography. In 2006, he moved to the Institut Català de Nanotecnologia, Bellaterra, Spain thanks to the financial support of the Ramon y Cajal Program . His current fields of interest include metal–organic chemistry, porous materials, molecular magnetism, nano-lithographic techniques, and nanomaterials.

Daniel Ruiz-Molina

Daniel Ruiz-Molina was born in Barcelona, where he received his PhD in 1996 working with Prof. Veciana at the Institute of Materials Science of Barcelona (ICMAB). In 1997, he joined Hendrickson's Group at UCSD for three years as a postdoctoral research fellow. Afterwards he returned to the ICMAB, where he has held a permanent position since July 2001. His main interests are the preparation and characterization of multifunctional molecular materials and switches (optical and magnetic properties) and the preparation of molecular ordered arrays on surfaces (2-D).

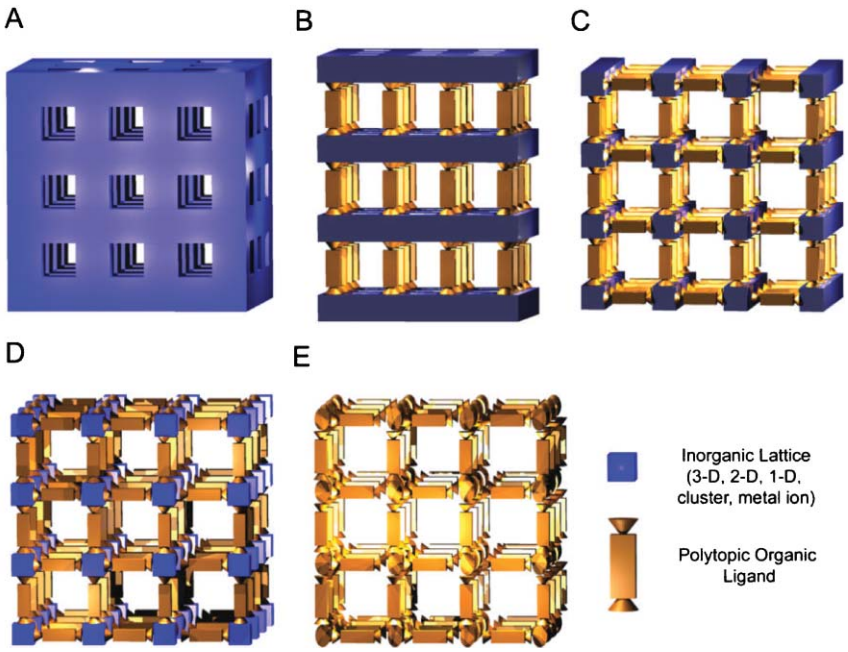

Fig. 1 Schematic representation of the evolution of the dimensionality of the inorganic lattice in open-framework materials. (A) 3-D inorganic framework. (B) Hybrid framework formed by 2-D inorganic layers pillared by organic ligands. (C) Hybrid framework constructed from 1-D inorganic chains linked by organic ligands. (D) Coordination polymer created by 0-D clusters or isolated metal ions connected through polytopic organic ligands. (E) Purely organic framework formed by organic molecules interlinked through non-covalent bonds such as hydrogen-bonds or π-π interactions. The design of this figure has been inspired from [*Chem. Mater.*, 2001, **13**, 3084] reported by Prof. Gérard Férey.

representation of such classification is shown in Fig. 1, where pure inorganic materials have also been included for comparison purposes.

Jaume Veciana

Jaume Veciana was born in San Salvador (Rep. El Salvador) and studied chemistry at the University of Barcelona (Spain) where he obtained his PhD in 1977 working on physical organic chemistry with Manuel Ballester. He was appointed as Colaborador Cientifico of the CSIC in 1979 and in 1982/1983 moved to The Johns Hopkins University, MD (USA), with Dwaine O. Cowan, as a Postdoctoral fellow working on molecular conductors and organic metals. In 1991 he moved to the Institut de Ciència de Materials de Barcelona (CSIC) where was promoted to Full Professor in 1996. He has been co-author of more than 320 journal articles and book chapters and has edited and co-edited two books, receiving in 2001 the Solvay Award and in 2004 the Real Sociedad de Quimica Española Award for his research in chemistry. In 2005 he received the DuPont Award for his contributions in Molecular Nanoscience and Nanotechnology. His research interests focus on molecular functional materials and molecular nanoscience and in particular the fields of molecular magnetism, metal–organic porous materials, electron transfer phenomena and processing of molecular functional materials.

Porous networks constructed from the connection of "inorganic" layers or chains through di-, tri- or tetratopic organic ligands are generally referred to as organic–inorganic hybrid porous structures. The idea was initiated by Johnson and Jacobson and co-workers,[26] who proposed the use of linear diphosphonates or functionalized monophosphonates as bridging organic ditopic ligands. Later on, Férey, Bujoli and co-workers specially contributed to their expansion, with a series of porous hybrid phosphates solids formed by the use of linear diphosphonates and dicarboxylates,[27] whereas Rao, Cheetham and co-workers described a new family of porous oxalato-phosphates.[28] Furthermore, no less important was the synthetic approach proposed by Zubieta and co-workers, who described the MOXI-*n* family, a series of solids constructed from molybdenum oxides and nitrogen-donor ligands with a rich variety of transition-metal ions.[29]

Open-framework coordination polymers are made from 0-D "inorganic" clusters or isolated metal ions connected by bridging organic multitopic ligands *via* more or less covalent metal–ligand bonding.[30] One of the most representative examples of porous coordination polymers is the family of complexes discovered by Yaghi and co-workers,[31] formed by octahedral zinc clusters linked through rigid linear dicarboxylate ligands. In this study, robust open-framework structures with diverse pore sizes (3.8 to 28.8 Å) and functionalities decorating the pores were obtained by modifying the length and nature of the ditopic ligands. This method opened the way to the synthesis of modular porous solids, a rational design that has been extensively developed by innumerable researchers along the last six years. The low cost (only classical organic, supramolecular and coordination chemistry is required), the potentiality of organic chemistry to design

flexible organic multitopic ligands, the versatile chemistry of metals ions and the important applications found for these porous coordination polymers (methane and hydrogen storage,[32] vide infra) are some of the reasons that explains the rapid expansion of this research around the world. In fact, since the beginning of the 2000s, thousands of publications describing open-framework coordination polymers with diverse topologies, pore sizes, shapes, and natures have been reported.[33–40]

The final step for the incorporation of organic molecules as constituents of the porous structures is the generation of purely organic porous materials. Basically, these open-frameworks are formed by polytopic organic tectons connected through supramolecular interactions, such as hydrogen-bonding or π–π interactions. Based on these interactions, many organic open-frameworks have been described.[41,42] However, even though most of these materials show a channel-like structure, they are not stable in absence of solvent guest molecules due to the relative weakness of supramolecular interactions. To our knowledge, only a few examples of robust purely organic porous materials are found in the literature. The supramolecular arrangement of the natural product gossypol discovered by Ibragimov *et al*. was the first robust purely organic H-bonded porous structure.[43] After this example, only a few other organic porous solids have been reported.[44] Among them, it is notable a polymorph of tris(*o*-phenylenedioxy)cyclophosphazene that is able to absorb xenon gas atoms and conducting iodine molecules.[45] Another interesting example was recently reported by Wuest and co-workers.[46] The crystallization of a series of tetraphenylborates form robust H-bonded networks in which the cations can be exchanged with retention of crystallinity and with selectivities similar to those observed in typical zeolites.

Such a variety of synthetic methodologies has been crucial not only for the description of new structural motifs and architectures but also for the continuous discovery of new properties and applications. For instance, Kitagawa, Yaghi and co-workers showed the remarkable ability of some metal-ion porous materials in the sorption of methane[31,47] and hydrogen.[32] Such results aim us to expect the development of gas storage devices in a not-too-distant future,[45,48,49] based on the selective sorption, sensing and separation of gases.[50] Important improvements in the field of ion-exchange,[51,52] separation processes,[53] and catalysis,[2,54] have also been successfully reported. However, as far as properties is concerned, the major revolution comes from the large diversity of elements (especially metal ions) used in the direct composition of the walls of the open-framework. This situation opens news perspectives in the design of a second generation of multifunctional porous materials[55] that combine classical applications of zeolites associated to their inherent porosity character, with the development of novel chemical and physical properties, such as magnetic, conductivity and/or optical properties.

In this Review, we aim to give a general overview of such a new generation of multifunctional porous materials showing additional structural, chemical, or physical properties. For this, a detailed revision of the different examples so far reported will be presented, classified into five different sections: (2) magnetic, (3) chiral, (4) conducting, (5) optical and (6) labile open-frameworks for sensing applications. Among them, magnetic porous materials are highlighted, and the comprehensive list of references provides links to the most up-to-date information.

2 Magnetic open-frameworks

Magnetic open-framework materials probably are the most abundant multifunctional porous materials reported up to date. Indeed, a pretty large number of pure inorganic materials, organic–inorganic hybrid materials and coordination polymers with magnetic properties have been reported thanks to the use of constitutive open-shell transition-metal ions within the framework of the structure. More limited is however the number of pure organic porous magnetic materials so far reported, because of the difficulties in handling the organic magnetic carriers; *i.e.*, the free organic radicals. A detailed description of the most representative examples of each one of the families previously described is given next.

2.1 Inorganic open-frameworks

There are several examples so far reported of magnetic pure inorganic open-frameworks. Among them, most abundant are inorganic networks with the following anions: (i) phosphates, (ii) borophosphates, (iii) phosphites, (iv) arsenates, (v) sulfates and (vi) cyanides. All of them are summarized next.

2.1.1 Phosphates. The formation of open-framework structures with transition-metal phosphates was first reported for iron in 1986.[56] After this work, other groups opened up a rich chemistry with various metal ions such as molybdenum,[57] vanadium,[58] copper[59] and cobalt.[60] In addition to the diversity of structural motifs and topologies found on these studies, the incorporation of paramagnetic transition-metal ions allowed scientists to report the first magnetic studies on open-framework materials. For instance, weak ferromagnetic ordering at 5.2 K for the vanadium phosphate samples, $[(VO)_3(OH)_2(H_2O)_2(PO_4)_2]\cdot C_3N_2H_{12}$[61] and $K_4[V_{10}O_{10}(H_2O)_2(OH)_4(PO_4)_7]\cdot CNH_5\cdot 4H_2O$,[10] was reported early in 1993. One year later, a cobalt phosphate $[CoPO_4]\cdot 0.5C_2N_2H_{10}$ or DAF-2 (where DAF-*n* refers to Davy Faraday series) showed a 3-D porous network with channels between 3.9 and 4.7 Å and an antiferromagnetic ordering at 2 K.[62] Antiferromagnetic interactions were also observed in a family of copper phosphonates.[63] However, all the previous cases were isolated examples and it was not until 1996 when the first detailed study of an extensive family of open-framework phosphates with remarkable magnetic properties, was reported. It was the family of porous iron(III) oxyfluorinated or oxide-centered phosphates, which exhibited antiferromagnetic interactions and long-range magnetic orderings at temperatures in the range of 10–37 K. This family included the ULM-*n* series (where ULM refers to University of Le Mans), MIL-*n* series (where MIL refers to Materials of Institut Lavoisier) as well as other nameless materials.[64]

The interest raised up by the pioneering works previously described, attracted the attention of the scientific community. Since then, several reports on metal phosphate open-framework structures with interesting magnetic properties have been reported. Most of the examples are iron-based phosphates although other interesting examples include cobalt,

manganese and nickel phosphates. A detailed description of such structures is presented in the following sections.

2.1.1.1 Iron phosphates. Most iron phosphates open-framework structures so far described have been synthesized under mild hydrothermal conditions (110–180 °C) from appropriate mixtures of an iron source (Fe_2O_3, FeO(OH), $FeCl_3$, $Fe(OH)_3$, $Fe(NO_3)_3{\cdot}6H_2O$ or $Fe(acac)_3$), H_3PO_4, HF (only for the synthesis of fluorophosphates) and amines, in water or organic solvents.[65] Besides other purposes, amine molecules are acting as structure-directing templates for the generation of openings on these structures. Moreover, depending on the reaction conditions (temperature, proportion of reactants, amine, pH, solvent, *etc.*), a large number of open-frameworks composed of octahedral iron centers linked by fluorine atoms (Fe–F–Fe), oxygen atoms (Fe–O–Fe) or phosphate groups (Fe–O–P–O–Fe) have been prepared. The nature of the bridge is not only important on dictating the topology of the resulting structure but also, from a magnetic point of view, for the coexistence of different type of magnetic interactions. Whereas strong magnetic exchange interactions between iron centers linked through fluorine or oxygen bridges take place, weaker superexchange interactions between iron centers linked through phosphate groups are observed. In addition to the nature of the bridge, other structural parameters have been found to be crucial on the modulation of the magnetic exchange coupling. Indeed, in the early 1990s, Goodenough described that systems like Fe–F–Fe and Fe–O–Fe shows anti- or ferromagnetic superexchange interactions depending on the valence of iron metal ions and angle between the three centers.[66] For Fe(III) metal ions, d^5–d^5 superexchange is predicted to be antiferromagnetic for angles between 90 and 180°. However, when this interaction implies a mixed valence Fe(II)/Fe(III) system, the d^6–d^5 superexchange is mainly antiferromagnetic for angles close to 180°, whereas the interactions are ferromagnetic if the angle is close to 90°. A similar behaviour is predicted for Fe(II) ions, in which the d^6–d^6 superexchange is antiferromagnetic and weak ferromagnetic for angles close to 180 and 90°, respectively. On the other hand, the superexchange interactions between d orbitals of two Fe ions coupled through phosphate groups (Fe–O–P–O–Fe) are generally antiferromagnetic and are weaker. However, these antiferromagnetic interactions can be stronger when the configuration of this system is almost planar.[67] Finally, the intramolecular interactions (*e.g.* Fe–F···F–Fe, *etc.*) are usually very weak and in most of the cases they are considered negligible.

In the following, the different examples of iron phosphates open-framework structures so far reported in the literature will be revised and classified according to the dimensionality and strength of the magnetic exchange interaction between the iron centres. More precisely, since the strongest magnetic interactions take place through Fe–X–Fe (X = F or O) bonds, the repetitive building blocks that have been used to classify the structures are constituted by iron centres connected through fluorine or oxygen atoms. The dimensionality of such building blocks, which are recurring along the whole porous structure connected through phosphate groups, range from (in terms of the connectivity of the iron centres through F or O atoms): (i) isolated octahedral iron units, (ii) connected Fe–X–Fe clusters, (iii) connected Fe–X–Fe chains, and (iv) connected Fe–X–Fe layers.

"Isolated octahedral iron units". From a structural point of view, the simplest building unit is an isolated octahedral FeO_6 unit. A representative example is complex $[Fe_3(H_2PO_4)_6(HPO_4)_2]{\cdot}NH_4{\cdot}4H_2O$, which exhibits a 2-D structure where each layer is formed by iron octahedra connected to other four iron centres through six phosphate groups (Fig. 2(A)).[68] As shown in Fig. 2(B), this creates 12-membered ring channels, where the NH_4^+ molecules are placed. A similar connectivity gave an open-framework 3-D structure formulated as $[Fe(HPO_4)_2]{\cdot}NH_4$.[69] This material shows a 2-D channel network filled with the NH_4^+ molecules. Isolated octahedral iron centers are also connected through phosphate groups in $[Fe_2(HPO_4)_4]{\cdot}C_2N_2H_{10}$.[70] However, the 3-D structure in this

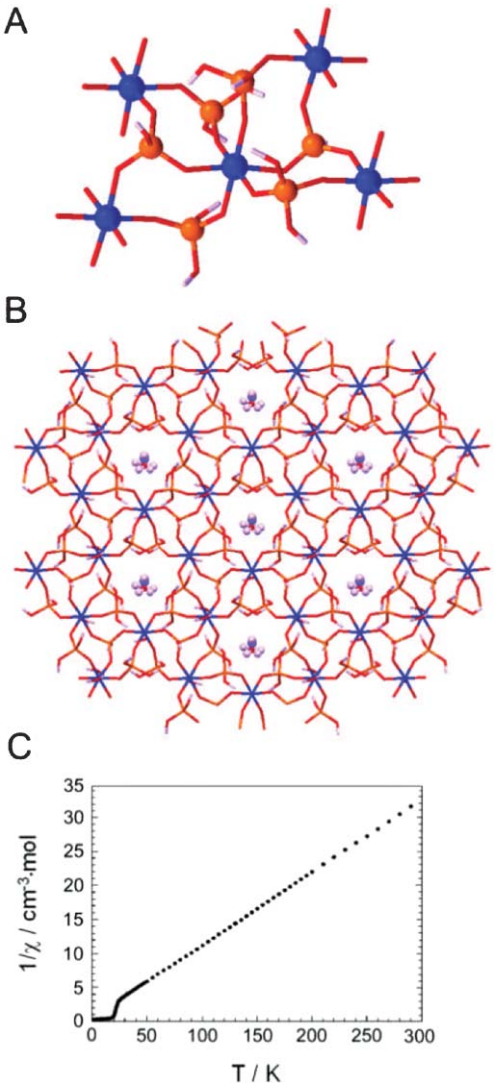

Fig. 2 (A) Connectivity of the iron centers through phosphate groups in $[Fe_3(H_2PO_4)_6(HPO_4)_2]{\cdot}NH_4{\cdot}4H_2O$. (B) View of the 12-membered ring channels in where the NH_4^+ molecules are placed. (C) Temperature variation of the inverse molar susceptibility ($1/\chi$) (Fe, blue; P, orange; O, red; N, light blue; H, white. In (A) Fe and P, and in (B) NH_4^+ molecules are represented as spheres). (Reprinted with permission from ref. 68. Copyright 1999, Elsevier.)

case is formed connecting each iron center to other eight iron centres through six phosphate groups, leading to the formation of 8-membered ring channels.

Due to the lack of Fe–X–Fe (X = F or O) bonds, the magnetic properties of this family of phosphates is governed by the superexchange coupling between Fe ions through phosphate groups (Fe–O–P–O–Fe). Previous magnetic measurements on non-porous iron phosphates showed that a large diversity of interactions, in terms of magnetic strength, *via* Fe–O–P–O–Fe can be found. For instance, whereas weak superexchange interactions between 4.2 and 3.9 K were reported in the $KBaFe_2(PO_4)_3$ sample,[71] stronger interactions have been observed in $NaFeP_2O_7$,[72] $Na_3Fe_2(PO_4)_3$,[73] and orthorhombic $FePO_4$,[74] with Néel temperatures (T_N) of 29, 47 and 15 K respectively. Such diversity of magnetic superexchange interactions has also observed on the related open-framework phosphates. For instance, the 2-D complex $[Fe_3(H_2PO_4)_6(HPO_4)_2]\cdot NH_4\cdot 4H_2O$ shows weak antiferromagnetic interactions ($\theta = -5$ K) with a spontaneous magnetization down to 30 K, suggesting either ferromagnetic or canted antiferromagnetic order (Fig. 2(C)). On the contrary, stronger antiferromagnetic interactions with θ values of -84 and -50 K with long-range magnetic ordering (T_N = 30 and 18 K) were measured on $[Fe_2(HPO_4)_4]\cdot C_2N_2H_{10}$ and $[Fe(HPO_4)_2]\cdot NH_4$, respectively.

"Connected Fe–F–Fe/Fe–O–Fe clusters". The use of fluorine opened novel avenues for the synthesis of open-framework iron phosphates.[75] In addition to its mineralizing effect, the presence of fluoride can stabilize specific structures, which in turn gives rise to novel 3-D network topologies with a wide diversity of structural connected Fe–F–Fe units. For example, complex $[Fe_3F_2(PO_4)_3]\cdot X$, where X stands for $NH_3(CH_2)_4NH_3$ (ULM-3) or $CH_3NH_3\cdot H_2O$ (ULM-4), showed a 3-D structure formed by trimeric clusters of iron centers linked *via* two fluorine ligands with a Fe–F–Fe–F–Fe disposition.[76,77] The central Fe site is linked to the adjacent iron centers by two fluorine bridges and three phosphate groups (Fig. 3(A)). Clusters are then linked by these phosphates groups, generating a 3-D structure with 10-membered ring channels along one direction in ULM-3 (Fig. 3(B)) and a 2-D porous network with 10- and 8-membered ring channels in ULM-4. A similar trimeric unit was detected in $[Fe_3F_6(HPO_4)_2(PO_4)]\cdot C_8N_4H_{26}\cdot H_2O_3$,[78] whereas $[Fe_5F_4(PO_4)(HPO_4)_6]\cdot C_2N_2H_{10}$ is composed of five iron centers defined by the coupling of five iron centers through one fluorine atom with a Fe–F–Fe–F–Fe–F–Fe–F–Fe disposition.[79] This last compound shows a structure with 8-membered ring channels that accommodate the guest diamine molecules.

Oxygen atoms can also act as bridging units between iron centres. The building unit of the mixed valence (Fe(II)/Fe(III)) $[Fe_4O(PO_4)_4]\cdot 2C_2N_2H_{10}\cdot H_2O$ phosphate is a cluster of four trigonal bipyramidal iron metal ions connected by a centred oxygen atom and four phosphate groups that connect each iron to the other three iron centres.[80] The 3-D structure is thus constructed by linking the tetramers to eight neighbouring clusters *via* phosphate groups, forming 8-membered ring channels that are filled by the diamine and water molecules. The 3-D phosphate $[Fe_2(OH)(H_2O)(PO_4)_2]\cdot NH_4\cdot H_2O$ is also constructed from a tetrameric cluster,[81] whose connectivity through phosphate groups creates a framework with 8-membered ring channels (6.6 × 6.3 Å). A remarkable characteristic is that this material acts as a porous material desorbing (443 K) and reabsorbing water or methanol molecules.

Other structures are composed of more than one Fe–X–Fe units. Indeed, $[Fe_4F_2(PO_4)_4(H_2O)_3]\cdot C_6N_2H_{14}$ or ULM-12 and isostructural $[Fe_4F_2(PO_4)_4(H_2O)_4]\cdot C_5N_2H_{14}$is built up from two types of clusters: a trimer of iron centers similar to that shown by ULM-3 or ULM-4 and an isolated octahedral iron center formulated as $[FePO_7(H_2O)]$.[82,83] Each trimeric cluster is connected to two others by four phosphate groups and

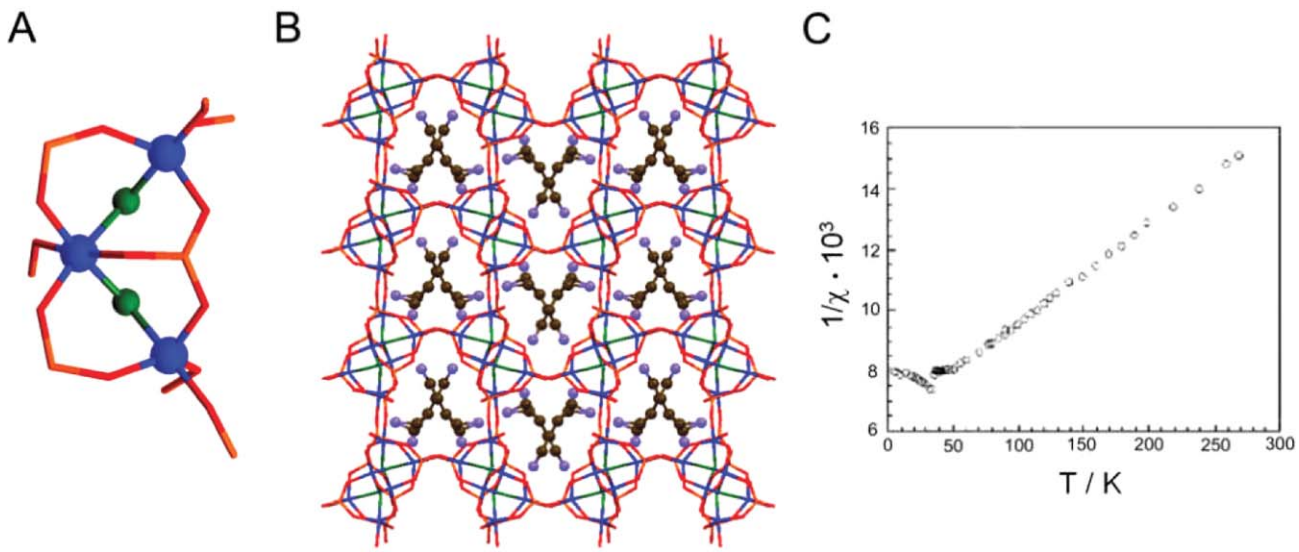

Fig. 3 (A) Fe–F–Fe connected trimeric cluster in $[Fe_3F_2(PO_4)_3]\cdot C_4N_2H_{14}$ (ULM-3). (B) Projection of the structure showing the 10-membered ring channels in which the diamine molecules are located. (C) Temperature variation of the inverse molar susceptibility ($1/\chi$) (Fe, blue; P, orange; O, red; F, green; N, violet; C, brown. In (A) Fe and F, and in (B) diamine molecules are represented as spheres). (Reprinted with permission from ref. 76. Copyright 1996, Elsevier.)

forms infinite chains. These chains are then bridged together by the isolated iron octahedron, leading to the formation of 8-membered ring channels and large cages delimited by 22 faces. These cages are filled with the protonated amine molecules. In addition, thermogravimetric studies performed on ULM-12 showed that the completely loss of water molecules occurs at 260 °C. This leads to the formation of an anhydrous phase $[Fe_4F_2(PO_4)_4]\cdot C_6H_{14}N_2$ or ULM-19.[84] The simple removal of water ligands modifies both trimeric and isolated iron units and opens new 6-membered ring channels.

Similarly, the fluorophosphate of composition $[Fe_5F_4(H_2PO_4)(HPO_4)_3(PO_4)_3]\cdot C_4N_3H_6\cdot C_4N_3H_5\cdot H_2O$ shows a 3-D open-framework composed of a linear tetrameric cluster and an isolated iron octahedron connected through phosphate groups.[85] The linear tetramer consists of four different crystallographic iron centers linked by fluorine atoms. Both central iron centers of this tetramer are connected to each other by two phosphate groups, whereas two more phosphate groups connect them with their corresponding external iron centers. These clusters are then connected to each other and through the isolated octahedral iron centers *via* phosphate groups, which originates an open-framework structure with very large 24-membered ring channels (15.3 × 4.5 Å) (Fig. 4(A)).

All the above open-framework iron phosphates show antiferromagnetic interactions with long-range magnetic orderings at temperatures between 9 and 37 K. For ULM-3, Fe–F–Fe angles of trimeric clusters have values of 120.5 and 127.6° that indicate antiferromagnetic superexchange couplings. Then, clusters are three-dimensionally connected one to the other by phosphate groups. This means that clusters are antiferromagnetically coupled at low temperatures with a special characteristic: the O–P–O connection between lateral iron centers of the same and different trimers leads to frustrated antiferromagnetic couplings. Overall, this magnetically frustrated system shows a canted antiferromagnetic behaviour with a T_N of 38 K (Fig. 3(C)). This magnetically frustrated behaviour is very similar to that observed in ULM-4 (T_N = 25 K), and $[Fe_2(OH)(H_2O)(PO_4)_2]\cdot NH_4\cdot H_2O$ (T_N = 22 K) Fe(III) phosphates. Strong antiferromagnetic interactions (θ = −148 K) with a rapid rise in susceptibility below 40 K were also observed in $[Fe_3F_6(HPO_4)_2(PO_4)]\cdot C_8N_4H_{26}\cdot 3H_2O$.[86] On the contrary, $[Fe_5F_4(H_2PO_4)(HPO_4)_3(PO_4)_3]\cdot C_4N_3H_6\cdot C_4N_3H_5$ shows strong antiferromagnetic interactions (θ = −185 K) within the pentamer and adjacent pentamers, but no long-range magnetic ordering was detected. Finally, the mixed valent $[Fe_4O(PO_4)_4]\cdot C_2N_2H_{10}\cdot H_2O$ shows intra- and intercluster antiferromagnetic super- and super-superexchange interactions at lower temperatures such that a 3-D order occurs (T_N = 12 K).

Besides its large channels, $[Fe_5F_4(H_2PO_4)(HPO_4)_3(PO_4)_3]\cdot C_4N_3H_6\cdot C_4N_3H_5$ exhibits an unusual spin-crossover behaviour. Indeed, magnetic susceptibility measurements showed that the magnetic moment increases gradually from 2.0 μ_B around 20 K to 6.0 μ_B around 250 K, corresponding to the transition between low-spin Fe(III) ($^2T_{2g}$) and high-spin Fe(III) ($^6A_{1g}$) (Fig. 4(B)). Mössbauer spectra confirmed this behaviour that could be due to internal pressure being exerted on the Fe–O polyhedra.

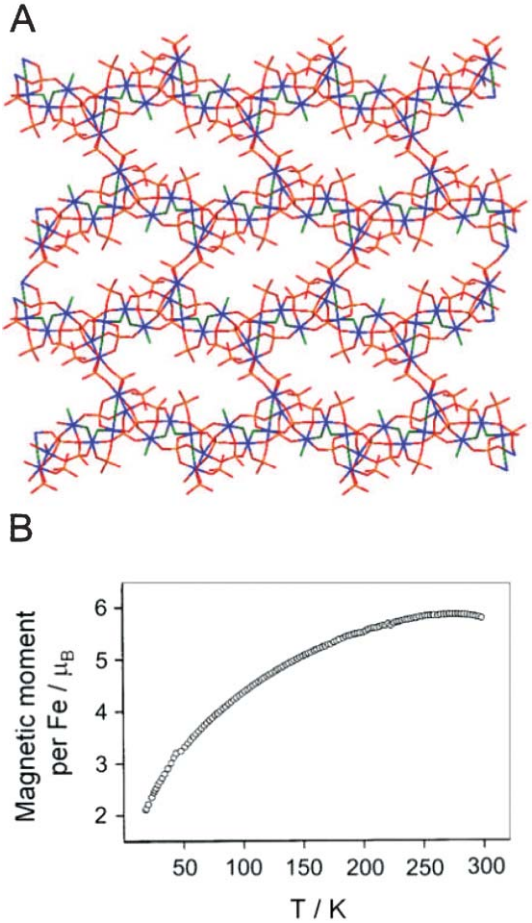

Fig. 4 (A) Structure of $[Fe_5F_4(H_2PO_4)(HPO_4)_3(PO_4)_3]\cdot C_4N_3H_{16}\cdot C_4N_3H_{15}$, showing the elliptical tunnels (Fe, blue; P, orange; O, red; F, green. Amine molecules are omitted for clarity). (B) Temperature variation of the magnetic moment. (Reprinted with permission from ref. 85. Copyright 1999, Royal Society of Chemistry.)

"Connected Fe–F–Fe/Fe–O–Fe chains". Simple Fe–F–Fe–F chains are basic structural elements in $[FeF(HPO_4)_2]\cdot C_3N_2H_{12}\cdot 0.2H_2O$ (ULM-14),[87] $[FeF(HPO_4)_2]\cdot C_5N_2H_{16}$,[88] and $[Fe_2F_2(HPO_4)_4]\cdot 2C_5N_2H_{14}\cdot 2H_2O$.[83] These compounds show 1-D structures formed by chains of octahedral iron centers linked by two fluorine ligands and four phosphate groups with the two adjacent iron centers. Similar chains observed in ULM-14 are present in $[Fe_4F_3(PO_4)(HPO_4)_4(H_2O)_4]\cdot C_3N_2H_{12}$ (ULM-15).[89] ULM-15 is composed of Fe–F–Fe–F chains and dimeric iron clusters. The discrete dimers are composed of two octahedral iron centers linked by one fluorine atom and one phosphate group. The connectivity of the remaining positions of these dimers plays a crucial role to explain the three-dimensionality of this structure. First, the dimers are linked together *via* forming chains running along the direction of the Fe–F–Fe–F chains. Second, they link the Fe–F–Fe–F chains *via* four phosphate groups forming 2-D layers. And third, adjacent layers are connected through dimers of each layer *via* phosphate groups that forms a 3-D structure with 16-membered ring channels inside which the protonated diamines are inserted.

Chains of iron centers connected with fluorine atoms shows strong antiferromagnetic interactions. Indeed, although ULM-14 and $[FeF(HPO_4)_2]\cdot C_5N_2H_{16}$ behave as paramagnets up to 2 K with relatively "weak" antiferromagnetic interactions ($\theta = -130$ and -160 K, respectively), ULM-15 show stronger interactions with a θ value of -250 K. ULM-15 shows a 3-D antiferromagnetic behaviour (T_N = 22 K) due to the presence of antiferromagnetic interactions along the chains and dimers (*via* Fe–F–Fe), and between chains and dimers (*via* Fe–O–P–O–Fe). This connectivity originates the 3-D magnetic behaviour with a certain degree of frustration as occur in ULM-3 or ULM-12.

Differently, the octahedral iron centers forming the chains in $[Fe(OH)(PO_4)]\cdot 0.5C_2N_2H_{10}$ are connected to each adjacent iron center through two oxygen atoms in a $Fe–O_2–Fe–O_2$ fashion (one oxygen corresponds to a phosphate group and the other to a hydroxide group) and one phosphate group.[90] These chains are connected to each other by phosphate groups, forming 2-D inorganic sheets. The overall structure shows distinct channels that are occupied by the diamine cations. This solid shows antiferromagnetic interactions with θ values of -107 K. The overall behaviour suggests a magnetic ordering at 30 K due to canted antiferromagnetism. The net moment implied for such a canted antiferromagnetic ground state was clearly mirrored in the hysteresis of the magnetization at 10 K.

More sophisticated chains can be found in other phosphates, which combine the presence of Fe–F–Fe and Fe–O–Fe interactions in the same chain. One example is $[Fe_5F_3(PO_4)_6(H_2O)_3]\cdot 3C_4N_2H_{14}\cdot 2H_2O$ or MIL-4 that shows a 2-D structure constructed from the alternation of inorganic and organic-templated layers.[91] The inorganic layers are built up from helicoidal chains of iron centers linked by fluorine and oxygen atoms. The repetitive unit in these chains is a cluster formed by five iron centers that are connected *via* fluorine atoms, oxygen atoms, and phosphate groups. The chains are then linked to each other by phosphate groups and form an undulated 2-D inorganic layer with two types of cavities (Fig. 5(A)). Interestingly, a higher degree of frustration was detected on MIL-4 that behaves as a ferrimagnet with a critical temperature of 7 K (Fig. 5(B)). This compound shows strong antiferromagnetic interactions with a θ value of -214 K.

"Connected Fe–F–Fe/Fe–O–Fe layers". A full layered structure has been synthesized by Natarajan and co-workers.[92] The mixed valent $[Fe(III)_{3-x}Fe(II)_xF_2(PO_4)(HPO_4)_2]_2\cdot C_6N_4H_{21}$ ($x \sim 0.5$) fluorophosphate shows a 2-D sheet of iron centers linked by fluorine and oxygen atoms. This layer can be seen as parallel chains linked together by octahedral iron centers. These chains consist of iron centers coupled with alternating double-bridge fluorine and oxygen atoms; in a $–Fe–O_2–Fe–F_2–Fe–O_2–$ fashion (Fig. 6(A), left). The linkage of these chains takes place in a way that each octahedral iron center links them *via* two three-connected fluorine bridges (Fig. 6(A), right). This creates a layer of iron centers directly coupled through fluorine/oxygen atoms and phosphate groups, with pseudo-channels located in the interlayers (Fig. 6(B)). Furthermore, it behaves as a ferrimagnet at a critical temperature of 25 K, with a very large hysteresis loop at 4.5 K defined by a coercive field of 2300 Oe and a saturated magnetization of 2.3 μ_B (Fig. 6(C)).

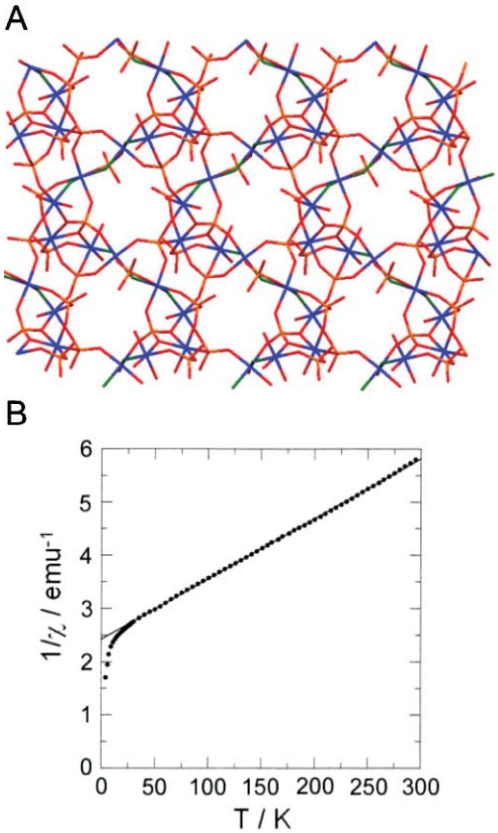

Fig. 5 (A) View of the cavities shown in the inorganic layer in $[Fe_5F_3(PO_4)_6(H_2O)_3]\cdot C_4N_2H_{14}\cdot 2H_2O$ (MIL-4) (Fe, blue; P, orange; O, red; F, green. Diamine and water molecules are omitted for clarity). (B) Temperature dependence of the inverse magnetic susceptibility. The line represents the fitting following the Curie–Weiss law. (Reprinted with permission from ref. 91. Copyright 1998, American Chemical Society.)

2.1.1.2 Cobalt phosphates. Cobalt(II) can adopt a tetrahedral coordination environment identical to that exhibited for silicon and aluminium in the formation of zeolites. This analogy provides the appropriate structural conditions to create zeolite-like Co(II) frameworks, with important porosity characteristics and additional magnetic properties. Structurally, it is well known that the redox properties of Co(II) sites enhance the catalytic properties of porous materials.[93] From a magnetic point of view, Co(II)–Co(II) magnetic interactions can give rise interesting magnetic properties, similar to those described above for iron phosphates. Based on these expectations, many efforts have been focused on the synthesis of Co(II) phosphates in recent years. This has led to the synthesis of a relatively large number of open-framework Co(II) phosphates exhibiting antiferromagnetic transitions. Some exceptions show ferromagnetic ordering.

Open-framework Co(II) phosphates are synthesized from a mixture of a cobalt source (*e.g.* $CoCO_3\cdot xH_2O$, $CoCl_2\cdot 6H_2O$), H_3PO_4 and amine molecules (for organic template) or inorganic salts (*e.g.* NaOH, KOH, NH_4OH, RbOH, and $NaHCO_3$; for inorganic template) in water or organic solvents exposed to mild hydrothermal conditions (423–463 K). An alternative synthetic methodology is the so-called amine phosphate route.[94] Amine phosphates may act as

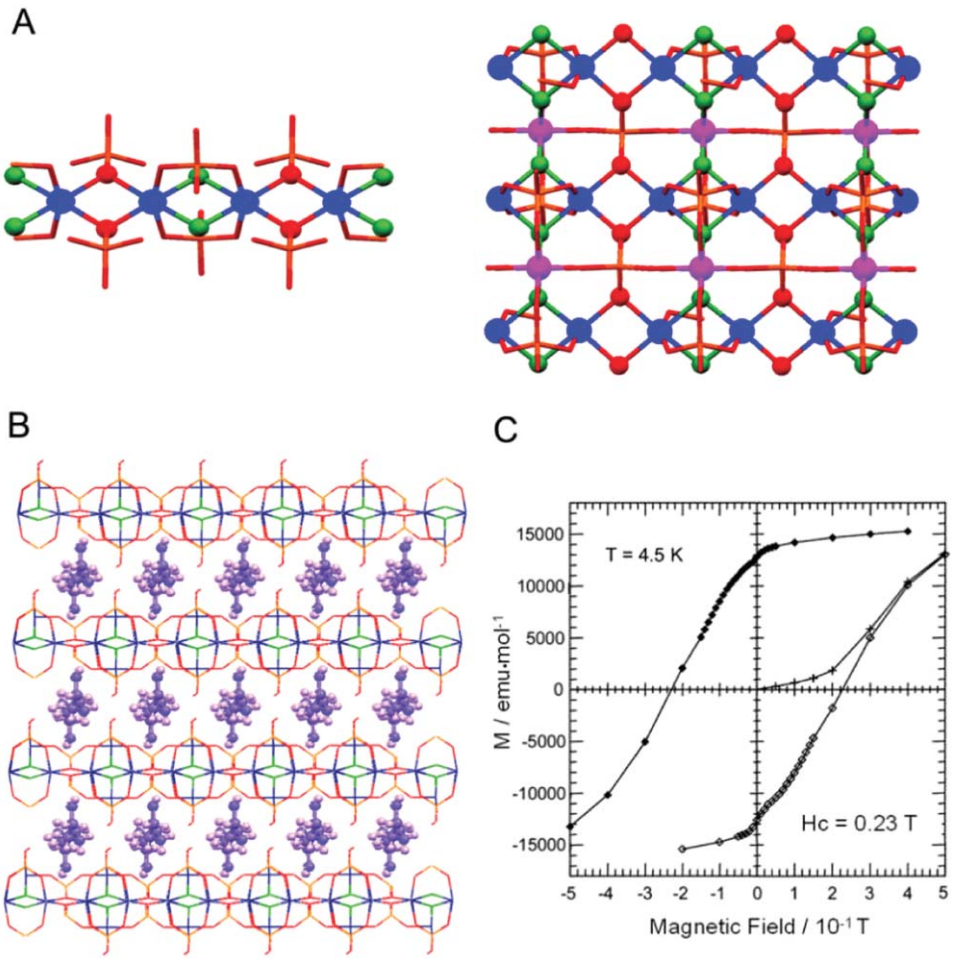

Fig. 6 (A) Representation of the Fe–O_2–Fe–O_2–Fe chain (left) and the 2-D Fe–F–Fe/Fe–O–Fe connected layer (right). (B) View of the structure of $[Fe(III)_{3-x}Fe(II)_xF_2(PO_4)(HPO_4)_2]\cdot C_6N_4H_{21}$, showing the pseudo-channels. (C) Magnetic hysteresis at 4.5 K (Fe, blue; P, orange; O, red; F, green. In (A), Fe and bridged F and O atoms are represented as balls. In the right image, octahedral Fe centers that link these chains are represented as purple balls. In (B), amine molecules are represented as violet spheres). (Reprinted with permission from ref. 92. Copyright 2002, American Chemical Society.)

intermediates in the formation of open-framework metal phosphates. Accordingly, the reaction of amine phosphates with a cobalt source (*e.g.* $CoCl_2\cdot 6H_2O$) yields Co(II) open-framework phosphates.[95] A last alternative for the synthesis of organically templated Co(II) phosphates is the direct reaction of an amine cobalt complex (*e.g.* $[Co(NH_2(CH_2)_2NH_2)_3]Cl_3$) with H_3PO_4.[96] Using these routes, different open-framework phosphates with Co(II) polyhedra linked *via* oxygen bridges and/or phosphates groups have been prepared.[97] Thus, the magnetic properties of these materials are intimately related to this structural connectivity, similar to the iron phosphates. The magnetic coupling between two adjacent Co(II) sites can be either through Co–O–Co or Co–O–P–O–Co pathways. In general, the coupling through the phosphate is weak and is seldom observed beyond temperatures of 3 K. At temperatures higher than 3 K, the magnetic coupling in Co(II) phosphates is mostly through Co–O–Co bridges.

"Isolated tetrahedron cobalt units". As stated above, the ability of Co(II) ions to exhibit tetrahedral CoO_4 coordination allows the obtaining of Co(II) phosphates with structures similar of those exhibited by zeolites, in which 3-D structures of alternating tetrahedral CoO_4 centers and phosphate groups are formed. The first example was the above mentioned $[CoPO_4]\cdot 0.5C_2N_2H_{10}$.[62] The framework consists of a 3-D 8-membered ring channel network (3.9 × 4.7 Å) formed by the connection of each CoO_4 tetrahedra to other ten cobalt centers through four phosphate units. Two related open-framework structures, $[Co_2(HPO_4)_3]\cdot C_3N_2OH_{12}$[98] and $Na[Co_2(PO_4)_2]\cdot NH_4\cdot H_2O$,[99] built up from the CoO_4 tetrahedra linked by phosphate groups have been recently reported. The three compounds show different connectivity between tetrahedra (Co/P) units, which lead to the formation of different channel networks. The last two structures have 2-D 12-membered and 3-D 4- and 8-membered ring channel networks, respectively.

However, one of the main contributions to the development of zeolite-like Co(II) phosphates was made by Stucky and co-workers with the description of five inorganic/alkali templated compounds with zeolite related frameworks.[100] $M[CoPO_4]$ ($M = Rb^+$ and NH_4^+) shows a 3-D framework with the same topology as zeolite ABW,[101] whereas $M[CoPO_4]$ ($M = Na^+$, K^+, and NH_4^+) exhibits hexagonal structures, intermediate

between the tridymite and ABW frameworks. Thus, while the two first structures have 8-membered ring channels (Fig. 7(A)), the latter three compounds exhibit 6-membered ring channels in where the alkali and NH_4^+ cations are housed (Fig. 7(B)).

As expected, magnetic properties of such Co(II) open-frameworks are directed from the magnetic interactions between Co(II) centers through Co–O–P–O–Co pathways. In general, since these interactions have a weak antiferromagnetic character, these materials behave as paramagnets with small θ values indicating weak antiferromagnetic interactions. At lower temperatures, some of these phosphates, such as $[CoPO_4]\cdot 0.5C_2N_2H_{10}$ and $Na[Co_2(PO_4)_2]\cdot NH_4\cdot H_2O$, order antiferromagnetically with T_N of 2 and 6 K, respectively. A remarkable exception is the compound $Na[CoPO_4]$ that shows a ferromagnetic ordering at 3 K (Fig. 7(C)).

''Connected Co–O–Co clusters, chains, layers, and 3-D lattices''. Besides the tetrahedral coordination environment, Co(II) metal ions are well known for its ability to coordinate in a variety of polyhedra in its phosphates, such as trigonal bipyramids and octahedra. In all these configurations, Co(II) sites can be linked not only by phosphate groups but also by oxygen bridges. An example of this diversity was observed in a $Na[CoPO_4]$ phase.[102] The framework shows tetramers of oxo-bridged trigonal bipyramidal Co(II) sites in a Co–O–Co–O_2–Co–O–Co fashion. In this cluster, the lateral Co sites are connected to the central Co centers through two phosphate groups. The interconnection of tetramers through the phosphate groups creates 8-membered ring channels.

Co(II) phosphates with 1-, 2- and even 3-D infinite Co–O–Co–O– sublattices interconnected through phosphate groups have been prepared. $Cs_2[Co_3(HPO_4)(PO_4)_2]\cdot H_2O$ consists of an open-framework of large 16-membered ring channels built up from the interconnection of three crystallographically different oxo-bridge tetrahedral Co(II) chains through phosphate groups.[103] Related chains are present in $[Co_2(PO_4)_2]\cdot C_3N_2OH_{12}$ and $[Co(PO_4)]\cdot 0.5C_4N_2H_{14}$.[98,104] Furthermore, chains of octahedral Co(II) sites connected *via* oxygen bridges can be found in an organically templated layered Co(II) phosphate.[105]

The dimensionality of the Co–O–Co–O sublattice increases in $Na[Co_3(OH)(PO_4)_2]\cdot 0.25H_2O$.[99] Tetrahedral, trigonal bipyramidal, and octahedral Co(II) sites are bridged through oxygen atoms to form connected layers. The 3-D framework is thus formed by interconnecting the Co(II) sites through the phosphate groups, which forms 4-, 6- and 8-membered ring channels. The presence of these three Co(II) polyhedra at the same time was also found in $[Co_7(PO_4)_6]\cdot C_2N_2H_{10}$.[106,107] Remarkably, this structure can be defined as an entirely 3-D Co–O–Co–O connected framework, with additional phosphate groups connecting the Co(II) sites. As shown in Fig. 8(A), the overall structure shows large 1-D 12-membered ring channels.

Compounds with Co–O–Co bonds show paramagnetic behaviour with stronger antiferromagnetic interactions. On cooling, most of them exhibit antiferromagnetic transitions. For example, $Na[CoPO_4]$ that contains Co–O–Co–O connected clusters shows this transition at 15 K,[102] while a Co(II) phosphate made from Co–O–Co connected chains of octahedral Co(II) sites shows it at 13 K.[105] Antiferromagnetic interactions are also present in the other Co(II) phosphates formed by one- and 2-D connected Co–O–Co lattices. In all these compounds, a weak ferromagnetic state is observed below 10 K,[103] 25 K,[104] and 10 K.[99] This state likely results from the ordering of the moments generated from the pairwise canted antiferromagnetic interactions between neighbouring Co(II) sites along the connected Co–O–Co lattices. Interestingly, 3-D $[Co_7(PO_4)_6]\cdot C_2N_2H_{10}$ exhibits a different behaviour attributed to a evolution of ferrimagnetism at low temperatures (Fig. 8(B)).

2.1.1.3 Manganese phosphates. The chemistry of open-framework manganese phosphates has been mostly developed in the last six years. In 1996, Kaucic and co-workers discussed for the first time the preparation of open-framework manganese phosphates.[13] In this study, the possibility to synthesize such

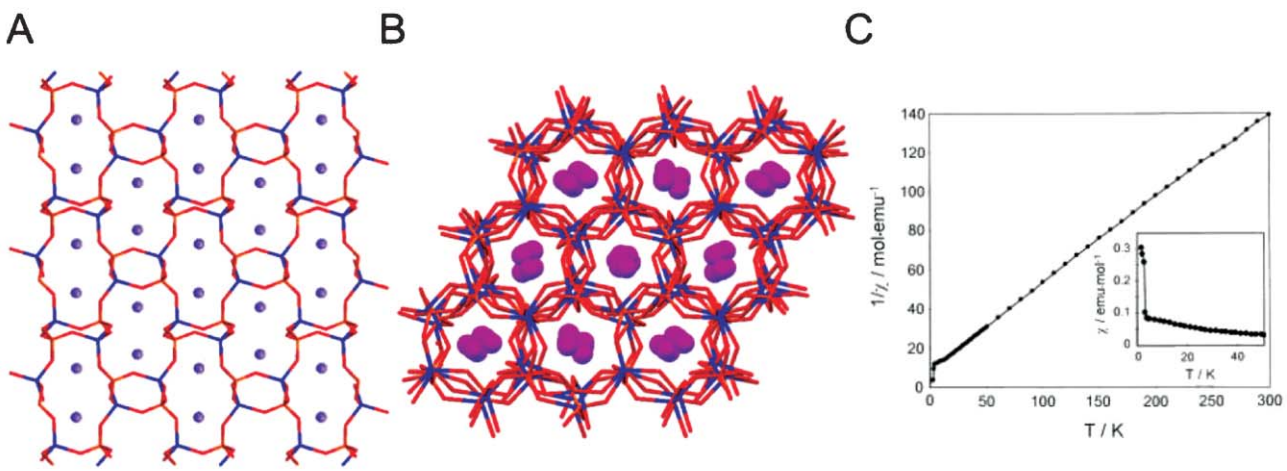

Fig. 7 Projection of the crystal structure of (A) NH_4CoPO_4-ABW and (B) $NaCoPO_4$, showing the respective channels filled with the NH_4^+ molecules and Na ions, respectively (Co, blue; P, orange; O, red; N, violet; Na, purple. NH_4^+ molecules and Na ions are represented as spheres). (C) Temperature dependence of the inverse molar susceptibility of $NaCoPO_4$. The inset shows la temperature variation of the molar susceptibility at low temperatures. (Reprinted with permission of ref. 100. Copyright 1997, Elsevier.)

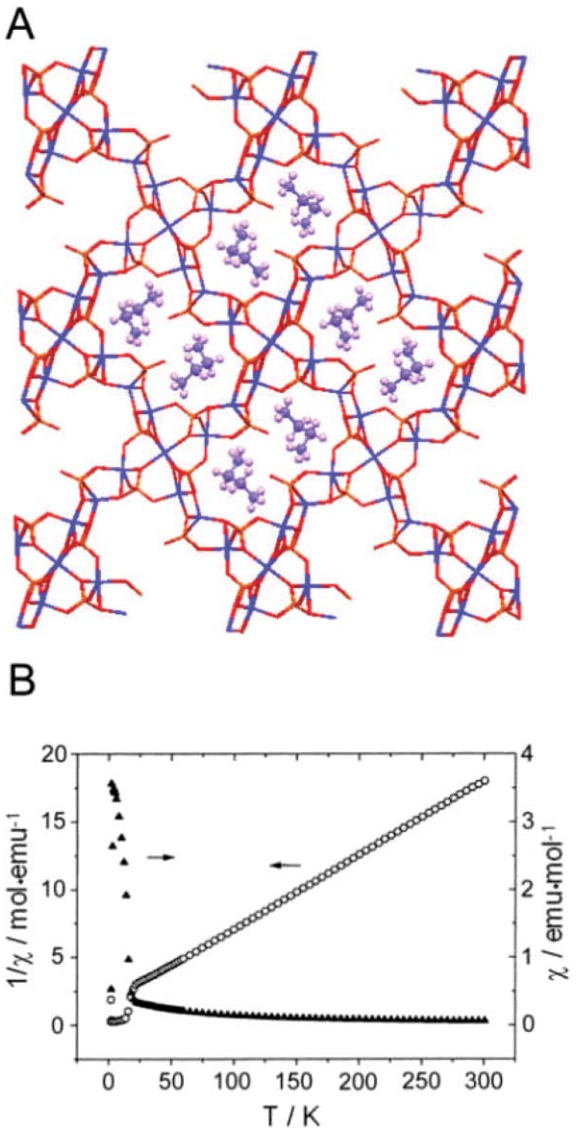

Fig. 8 (A) View of the crystal structure of $[Co_7(PO_4)_6]\cdot C_2N_2H_{10}$, showing the 12-membered ring channels (Co, blue; P, orange; O, red; N and C, violet; H, white. Diamine molecules are represented as spheres). (B) Thermal variation of the molar susceptibility and its inverse ($1/\chi$). (Reprinted with permission of ref. 106. Copyright 2000, American Chemical Society.)

phosphates using hydrothermal conditions and amine molecules as templates was pointed out. From these observations, some open-framework manganese phosphates templated by amine molecules or inorganic cations have been reported in recent emerging studies.

"Connected Mn–F–Mn/Mn–O–Mn clusters". Very few open-frameworks formed by connected Mn–O–Mn or Mn–F–Mn clusters interlinked by phosphate groups have been prepared so far. One of the first magnetic open-framework Mn(II) phosphates was $Na_7[Mn_5F_{13}(PO_4)_3(H_2O)_3]$.[108] The structure is created from a building unit defined as a triangular cluster of three octahedral Mn(II) centers bridged by a central fluorine atom and three phosphate groups. Three of those clusters are then interconnected through two isolated octahedral Mn(II) sites *via* three phosphates, creating a layered structure with 1-D channels in where most of the Na^+ cations are located. Another example is the layered $[Mn_6(HPO_4)_4(PO_4)_2(H_2O)_2]\cdot C_4N_2H_{12}\cdot H_2O$ that is formed by hexameric clusters connected through phosphate groups.[109] Each cluster is composed of two connected octahedral Mn(II) centers through two oxygen bridges, which are individually linked to one octahedral and one tetragonal bipyramidal Mn(II) *via* four oxygen atoms.

The oxidation state of manganese ions in these structures is Mn(II). From a magnetic point of view, the superexchange interactions through Mn(II)–O–Mn(II) pathways are predicted to be strongly antiferromagnetic for angles between 90 and 180°.[66] Furthermore, the superexchange interactions through the Mn–O–P–O–Mn pathway are much weaker and also with an antiferromagnetic character. For example, a manganese phosphate with isolated Mn(II) octahedra connected through phosphate groups showed very weak antiferromagnetic interactions ($\theta = -3.2$ K).[110] Thus, similar to those iron and cobalt phosphates, the magnetism of both Mn(II)) phosphates formed by connected Mn–O–Mn clusters is dominated by the strong antiferromagnetic interactions between Mn(II) ions inside each cluster. At very low temperatures, these structures show long-range antiferromagnetic order due to the weaker antiferromagnetic superexchange interactions between clusters through Mn–O–P–O–Mn pathways. T_N of 3.3 and 2.5 K were found for $Na_7[Mn_5F_{13}(PO_4)_3(H_2O)_3]$ and $[Mn_6(HPO_4)_4(PO_4)_2(H_2O)_2]\cdot C_4N_2H_{12}\cdot H_2O$, respectively.

Connected Mn–O–Mn chains, layers, and 3-D lattices. Recently reported open-framework manganese phosphates have shown layered structures with connected 1-, 2- and 3-D Mn–O–Mn sublattices. Simple $Mn–O_2–Mn–O_2$ "zigzag" chains in which each octahedral Mn(II) site is connected to each other through two oxygen bridges was found in $[Mn_3(P_2O_7)_2(H_2O)_2]\cdot 2NH_4$.[111] The interconnection of those chains through diphosphate groups forms a layered structure with the ammonium cations occupying the space between the layers. Similarly, layered $[Mn_2(HPO_4)_3(H_2O)]\cdot C_2N_2H_{10}$[112] and $[Mn_2(HPO_4)_3]\cdot 1.5C_2N_2H_{10}\cdot H_2PO_4$[113] structures are formed by 1-D connected Mn–O–Mn sublattices of corner-linked Mn_3 triangles. The chains are composed of octahedral Mn(II) sites connected to each other through two oxygen bridges and one square pyramidal Mn(II) center bridging those adjacent octahedral ions. Formation of 2-D connected Mn–O–Mn subnetworks is quite often in these compounds. $[Mn_2(PO_4)_2]\cdot C_2N_2H_{10}\cdot 2H_2O$,[114] $Ba[Mn(PO_4)(H_2O)]$,[115] and $Na_4[Mn_3(PO_4)_2(P_2O_7)]$,[116] are composed of layers of coupled Mn(II) sites through oxygen bridges and additional phosphate groups. From a structural point of view, the last compound is particularly interesting because it shows a 3-D structure with a 3-D channel-like network.

To our knowledge, only one reported open-framework $[Mn(PO_4)_3]\cdot NH_4$ phosphate can be considered a 3-D connected Mn–O–Mn network.[117] Taking into account a Mn–O distance of 2.55 Å, the framework is built up from the connection of octahedral and trigonal bipyramidal Mn(II) sites through oxygen bridges. The overall structure exhibits 1-D 6- and 7-membered ring channels containing the NH_4^+ cations (Fig. 9(A)).

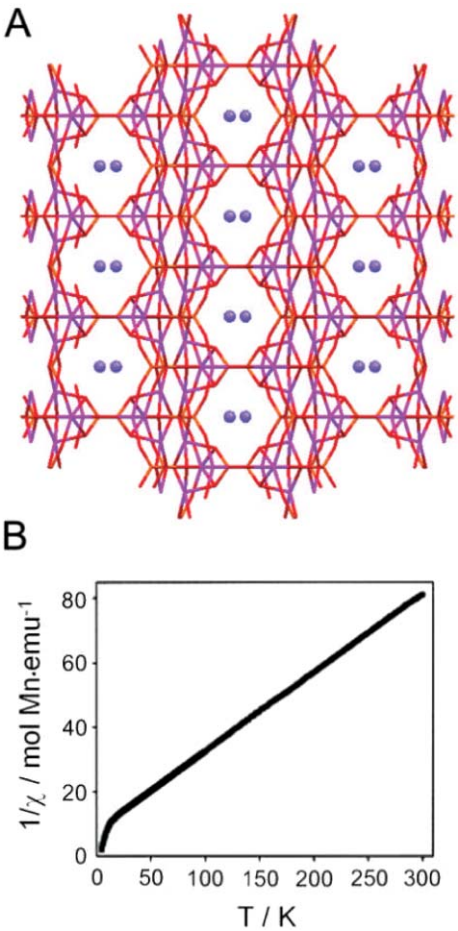

Fig. 9 (A) View of the channel-like structure of $[Mn(PO_4)_3]\cdot NH_4$(Mn, purple; P, orange; O, red; N, violet. NH_4^+ molecules are represented as spheres). (B) Thermal dependence of the inverse molar susceptibility. (Reprinted with permission of ref. 117. Copyright 2002, Elsevier.)

The magnetic behaviour of these frameworks is similar to those formed by connected Mn–O–Mn clusters. However, the temperature at which these open-frameworks are antiferromagnetically ordered tends to increase as the dimensionality of the connected Mn–O–Mn increases. Thus, whereas phosphates with zero- and 1-D connected Mn–O–Mn units order at temperatures below 5 K, those with 2-D connected Mn–O–Mn sublattices show canted antiferromagnetic transitions above 6 K. For example, $[Mn_2(PO_4)_2]\cdot C_2N_2H_{10}\cdot 2H_2O$ and $Ba[Mn(PO_4)(H_2O)]$ exhibit these transitions at temperatures of 17.5 and 16.5 K, respectively. $[Mn(PO_4)_3]\cdot NH_4$ shows the presence of antiferromagnetic interactions ($\theta = -33.5$ K), but with an interesting ferrimagnetic transition at a T_c of 17 K (Fig. 9(B)).

2.1.1.4 Nickel phosphates. Only a small number of open-framework nickel phosphates have been prepared so far. It is well known that two of the most significant open-framework nickel phosphates are two nanoporous nickel(II) phosphates, VSB-1[118] and VSB-5[119] (where VSB-*n* refers as Versailles–Santa Barbara series), with interesting magnetic properties and zeolitic characteristics, such as high BET surface area, ion exchange capacity, catalytic, and adsorption properties.

$Ni_{18}[(HPO_4)_{14}(OH)_3F_9(H_3O^+/NH_4^+)_4]\cdot 12H_2O$, or VSB-1, was hydrothermally synthesized in the presence of $NiCl_2\cdot 6H_2O$, H_3PO_4, HF (or NH_4F and KF), and an organic template such as pyridine or tris(2-aminoethyl)amine. Similar conditions (not using HF) with 1,3-diaminopropane, as the templated amine, were employed to obtain $Ni_{20}[(OH)_{12}(H_2O)_6][(HPO_4)_8(PO_4)_4]\cdot 12H_2O$, or VSB-5. More recently, free-template syntheses of both compounds under microwave irradiation have been reported.[120,121] The structure of VSB-1 is based on a 3-D network of octahedral Ni(II) sites connected through oxygen bridges with 1-D 24-membered ring channels (8.8 Å in diameter, Fig. 10(A)). Interestingly, VSB-1 becomes microporous on calcination in air at 623 K, yielding a BET surface area of 183 $m^2\ g^{-1}$, and is stable in air to approximately 823 K (Fig. 10(B)). This provides a large number of potential porosity-based applications in ion-exchange properties,[118] heterogeneous catalysis (*e.g.* conversion of butadiene to ethylbenzene),[122] and as a support for a photocatalyst.[123] Similarly, the framework of VSB-5 is formed by the 3-D connection of octahedral Ni(II) sites through oxygen bridges and shows large 1-D tunnels delimitated by 24 of those Ni(II) octahedra (10.2 Å in diameter, Fig. 10(C)). Activated for four days at 623 K, VSB-5 becomes microporous with a BET surface area of 500 $m^2\ g^{-1}$. Furthermore, it is stable up to 725 K. These characteristics lead to the possibility of using VSB-5 in several applications including selective hydrogenation, base catalysis,[119] and hydrogen storage.[124] Finally, recent studies have shown that other cations (*e.g.* Mn, Fe, Co and Zn) can be substituted for Ni in both VSB-1 and VSB-5, demonstrating that both nanoporous materials have a versatile framework to accommodate various transition-metal ions with several oxidation states and symmetries.[125]

Besides their wide porosity characteristics, both nanoporous materials exhibit interesting magnetic properties with predominant antiferromagnetic interactions. At low temperatures, both VSB-1 and VSB-5 show a canted antiferromagnetic order at a $T_N = 10.5$ K with $\theta = -71$ K, and $T_N = 14$ K with $\theta = -49.5$, respectively (Fig. 10(D)). This behaviour is consistent with the predicted antiferromagnetic interactions through Ni–O–Ni pathways and the fact that both structures may be magnetically frustrated. Dependence of magnetic properties as a consequence of doping was measured in VSB-1. Indeed, even though the doping with Mn, Co or Zn led to minor changes, the introduction of Fe increased the T_N to 20 K. From this result, one can start thinking to tune the magnetic properties of open-framework materials by changing the nature and amount of implanted metal ions.

Antiferromagnetic character and ordering have been also found in some layered Ni(II) phosphates.[126] Among them, $Na_4[Ni_3(PO_4)_2(P_2O_7)]$ is interesting for being isostructural to its Co(II) analog, with a 3-D channel system.[116] This material is formed by connected 2-D Ni–O–Ni layers and exhibits an antiferromagnetic ordering at a T_N of 12 K. Another two 3-D alkali Ni(II) phosphates showed interesting open-framework structures and similar antiferromagnetic behaviours. Both, $Na_4[Ni_5(PO_4)_2(P_2O_7)]$[127] and $Na[Ni_4(PO_4)_3]$[128] are formed by connected Ni–O–Ni chains and show antiferromagnetic transitions around 8 K and 20 K, respectively. Remarkably,

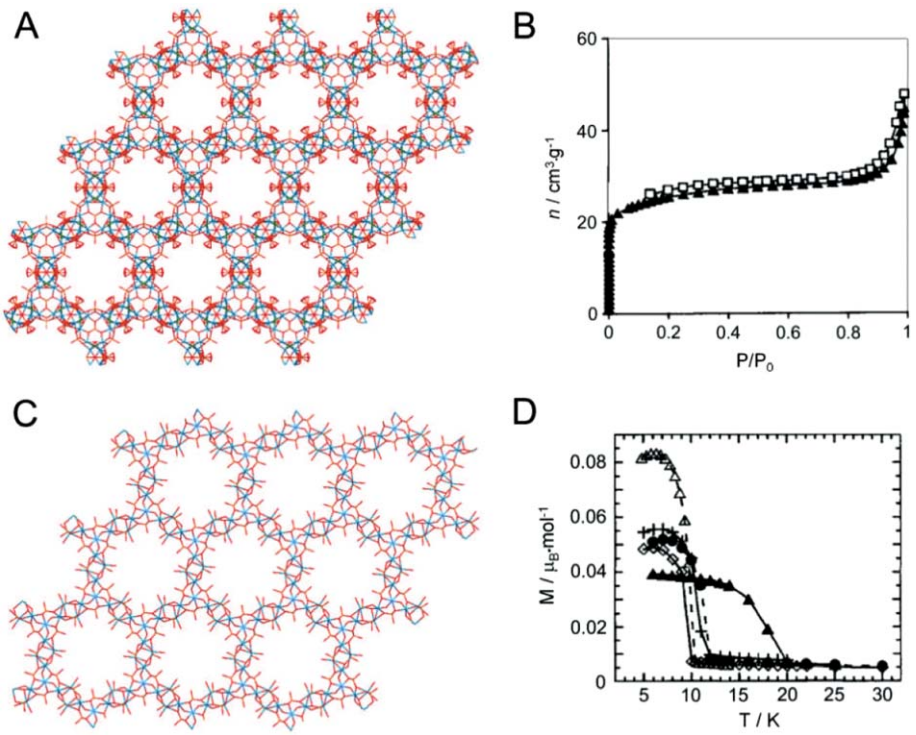

Fig. 10 (A) Projection of the porous structure of $Ni_{18}[(HPO_4)_{14}(OH)_3F_9(H_3O^+/NH_4^+)_4]$ (VSB-1). (B) Adsorption and desorption isotherms for nitrogen in VSB-1 at 77 K. (C) Projection of the porous structure of $Ni_{20}[(OH)_{12}(H_2O)_6][(HPO_4)_8(PO_4)_4]\cdot 12H_2O$ (VSB-5). (D) Low thermal dependence of the magnetization of the pure VSB-1 and samples doped with 10% atomic of Mn (+), Fe (●), Co (◇) and Zn (▲) (in (A) and (C), Ni, blue; P, orange; O, red; F, green). (Reprinted with permission of ref. 118. Copyright 1999, Académie des Sciences.)

the last compound behaves as a weak ferromagnet, with almost rectangular hysteresis loops at 14 K.

2.1.1.5 Bimetallic phosphates. The incorporation of two appropriate transition-metal ions in the structure of a phosphate could become an excellent approach to obtain open-frameworks with interesting magnetic properties. For example, by incorporating VCl_3 in the synthetic process, Grenèche and co-workers synthesized an open-framework phosphate $[Fe_{5-x}V_xF_4(H_2PO_4)_4(HPO_4)(H_2O)]\cdot NH_{2+y}(CH_2)_2NH_{2+y}$ or MIL-21 with mixed iron and vanadium metal ions that shows small cages and tunnels and behaves as a ferrimagnet below 13 K.[129] Fe(III) and V(III) metal ions are good candidates for the possibility of being ferromagnetically coupled. MIL-21 showed a 3-D structure formed by the connection of chains of randomly distributed Fe and V octahedra linked *via* fluorine ligands and isolated iron centers through phosphate groups. The origin of the ferrimagnetism is thus explained by the random distribution of Fe(III)/V(III) ions along the chains due to the expected strong antiferromagnetic Fe(III)–F–Fe(III) interactions and ferromagnetic Fe(III)–F–V(III) interactions.

Iron, cobalt, manganese and nickel ions have also been incorporated in phosphates composed of diamagnetic metal ions. Some families include gallophosphates,[130] aluminophosphates,[131] molybdenum,[132] and zinc[133] phosphates. However, even though most of these materials show interesting channel-like structures, magnetic interactions are usually very weak because magnetically active metal ions are diluted in these frameworks. Some remarkable examples include $[MnGa(HPO_4)(PO_4)]\cdot C_6N_2H_{14}$[134] and $[Zn_{4-x}Co_x(PO_4)_2(HPO_4)]\cdot 3C_3H_4N_2$.[135] The first compound is formed by clusters of two Mn(II) sites connected through four phosphate groups, which are interlinked by the tetrahedral Ga(III) sites forming a 3-D structure with 8- and 10- membered ring channels. The magnetic properties of this solid show an antiferromagnetic ordering with a T_N of 10 K due to the antiferromagnetic interactions through the Mn–O–P–O–Mn dimers. Similarly, the second example shows 10-membered ring channels, and behaves as an antiferromagnet at 5 K.

2.1.1.6 Other metallic phosphates. From a magnetic point of view, other good candidates for the development of phosphate-based magnetic open-framework structures would be titanium, chromium, vanadium, or copper. However, and in spite of interest, only a few examples of magnetic open-framework phosphates comprising transition-metal ions other than iron, cobalt, manganese, and nickel, have been reported so far. Among them, vanadium phosphates have been the most extensively studied family. Vanadium ions can be found in different oxidation states, such as V(III), V(IV) or V(V), although only the V(IV) and V(III) oxidation states have an open-shell character and are, therefore, susceptible to generate magnetic interactions. Overall, vanadium phosphates show a rich variety of channel-like networks and weak to moderate antiferromagnetic interactions (θ values around -10 to -30 K).[136] An exception is $[V(PO_4)F]\cdot NH_4$ described by Rojo and co-workers that exhibits a 2-D six-membered ring channels network with weak ferromagnetic interactions.[137]

Besides the family of vanadium complexes previously described, a few scarce examples of open-framework structures with interesting magnetic properties based on copper, chromium, and titanium phosphates have been described. In the case of titanium, different open-framework phosphates formed by Ti(IV) or a mixture of Ti(IV)/Ti(III) have been reported. However, the diamagnetic character of the Ti(IV) ions[138] disrupt any magnetic ordering even for the mixed-valence Ti(III)/Ti(IV) systems, which show a paramagnetic behaviour with almost no magnetic interactions between Ti(III) ions.[139] Even rarer are examples of copper and chromium phosphates. In fact, an amine-templated 1-D copper phosphate with 10-membered ring channels has been just recently described.[140]

2.1.2 Borophosphates. Metal borophosphates are formed by the connection of metal ions, tetrahedral or trigonal borates (BO_3 or BO_4 units, respectively), and tetrahedral phosphates (PO_4). From a structural point of view, such units do not differ considerably from the metal phosphates described in the previous section, leading us to envisage this family of compounds as good candidates to generate novel magnetic open-framework structures.

The discovery of the first open-framework borophosphate structure was reported by Sevov in 1996.[141] Since then, the family of borophosphate open-framework structures has increased significantly,[142,143] with a large number of transition-metal ions such as Co(II), Mn(II), Fe(III), Ni(II), and Cu(II). From them, it is worth to emphasize the complex $NH_4[FeBP_2O_8(OH)]$, which exhibits 1-D channels and antiferromagnetic ordering at T_N of 17 K.[144] Other examples simply behave as pure paramagnets with anti-[145] or weak ferromagnetic[146] interactions.

2.1.3 Phosphites. Open-framework structures incorporating 3d transition-metal ions can be constructed by using the pseudo-pyramidal hydrogen phosphite group $(HPO_3)^{2-}$ as connecting ligands and either inorganic alkaline earth cations[147] or organic alkyldiamine molecules[148] as templating agents. Among the first class, two transition-metal phosphites with composition $Na_2[M(HPO_3)_2]$ (M = Co(II) and Fe(II)) have been recently reported.[149] The framework is built up from isolated octahedral metal sites connected through phosphite groups, forming 4-, 6-, and 12-membered ring channels with maximum dimensions of 12.8 × 6.8 Å. Their magnetic characterization has shown the presence of relatively strong antiferromagnetic interactions between the metal ions through the M–O–P–O–M pathway, with θ values of −50 and −20 K for Co(II) and Fe(II), respectively.

Following the second approach, *i.e.*, with the use the organic diamine molecules as templating agents, Rojo and co-workers have prepared a series of: (I) 1-D $[M(HPO_3)F_3]^{2-}$ (M = Cr(III),[150] Ga(III)/Cr(III),[151] and V(III)[152]) chains exhibiting antiferromagnetic interactions,[153] (II) layered $[M_3(HPO_3)_4]^{2-}$ (M = Mn(II),[15] Fe(II),[154] Co(II),[155] and Mn(II)/Co(II)[156]) structures with interesting magnetic properties such as an antiferromagnetic ordering (T_N = 16 K) in the Fe(II) compound, and (III) 3-D open-framework structures. Among them, vanadium phosphites are the most abundant examples of 3-D open-frameworks.[157] Generally, these compounds exhibit large channels although very weak magnetic interactions. However, much stronger antiferromagnetic interactions were found in two iron phosphites. $[Fe(HPO_3)_2]\cdot 0.5C_2N_2H_{10}$ shows a 1-D 6-membered ring channel network formed by the connection of isolated iron octahedra through phosphite groups.[158] Similar 6-membered open channels are present in $[Fe(II)_2Fe(III)(HPO_3)_4]\cdot(NH_4)$.[159] This mixed-valent Fe(II)/Fe(III) structure is formed by connected Fe–O–Fe chains that are interlinked through phosphite groups. The magnetic measurements performed on both compounds showed relatively strong antiferromagnetic interactions (θ = −88 and −15 K) and magnetic ordering at T_N of 33 and 19 K, respectively. More recently, a related heterometallic V(III)/Fe(III) compound, $[V_{0.48}Fe_{0.52}(HPO_3)_2]\cdot 0.5C_2N_2H_{10}$, have shown weak ferromagnetism with a measured hysteresis loop at 2 K,[153] whereas other bimetallic open-framework Zn(II) phosphites with Co(II) or Ni(II) metal ions behave as paramagnets even at low temperatures.[160]

2.1.4 Arsenates. From a structural point of view, the tetrahedral arsenate oxyanion $[AsO_4]^-$ is very similar to the phosphate $[PO_4]^-$ group. For this reason, the chemistry, architectures and resulting magnetic properties of arsenate open-framework structures can be considered comparable to those previously described for the phosphate systems presented in section 2.1.1. More in detail, this family of open-framework structures are typically obtained under hydrothermal conditions from a mixture of arsenic acid, a metal source (*e.g.* $FeCl_3\cdot 6H_2O$, $Co(NO_3)_2\cdot 6H_2O$, *etc.*), and organic diamines molecules or inorganic cations. The role of such diamine molecules and inorganic cations is once more vital since they act as directing agents for the generation of open-frameworks. From a magnetic point of view, these metal arsenate structures can be grouped in two types according with the linkage between the two metal sites: (i) M–X–M (where X is O or F) and (ii) M–O–As–O–M linkages. Magnetically, the stronger interactions will be normally defined by the coupling of metal ions through the M–X–M exchange pathway, whereas couplings through M–O–As–O–M pathways are usually weaker and with an antiferromagnetic character. For this reason, the different open-framework arsenates can be classified according to the nature and existence of M–X–M bonds ranging from independent octahedral sites,[161–164] clusters,[165,161,166–168] chains[161,169–172] to 3-D M–X–M structures.

From this family of structures, it is important to emphasize compound $[Fe(AsO_4)F]\cdot NH_4$, which experiences a thermal transformation into a 3-D connected Fe–O–Fe framework after heating up to 798 K. As describe in Fig. 11(A), the resulting porous solid with formula $Fe(AsO_4)$ exhibits 6-membered ring channels (Fig. 11(B)).[169,170] More recently, a second related example, the mixed-valent $[Fe(II)_{1.5}Fe(III)_{1.5}F_6(AsO_4)]\cdot 0.75C_3N_2H_{12}$ compound, has been reported to exhibit an open-framework consisting of 6- and 8-membered ring channels.[173] Both structures show strong antiferromagnetic interactions with θ values of −320 and −204 K, respectively. At treatment at certain temperatures, both compounds order antiferromagnetically with T_N of 54.5 K and 6 K (Fig. 11(C)).

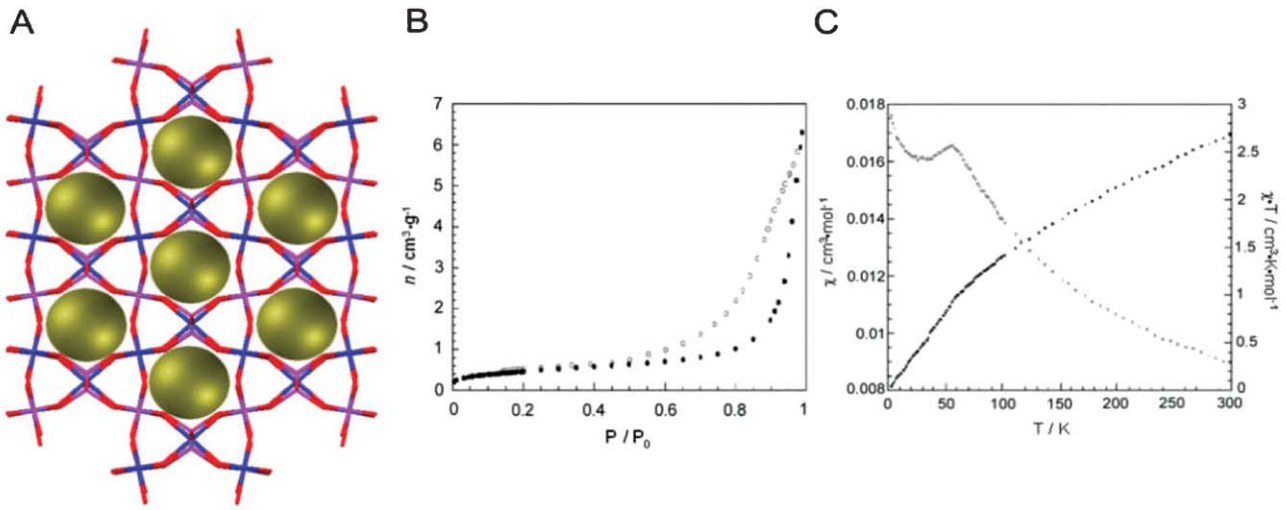

Fig. 11 (A) View of the crystal structure of $Fe(AsO_4)$ showing the 1-D channels. The void volume is represented as yellow spheres. (Fe, blue; As, purple; O, red). (B) N_2 adsorption (●) and desorption (○) isotherms measured at 77 K. (C) Thermal evolution of the molar susceptibility (χ) and the product χT at 1000 Oe. (Reprinted with permission of ref. 170. Copyright 2004, American Chemical Society.)

2.1.5 Sulfates. The interest for magnetic open-framework sulfates has been strongly fueled in the last few years by the publication of two cadmium sulfates by Rao and co-workers.[19,174] Immediately after, a considerable number of examples employing sulfate tetrahedra for the generation of open-framework transition-metal sulfates with attractive magnetic properties has been established, including a series of amine-templated sulfates with stoichiometry $[M_3F_6(SO_4)_2]$ (where M stands for Fe(II),[175,176] Co(II),[177] and a mixture of Fe(II)/Fe(III) ions).[178] These structures exhibit a Kagomé lattice with 1-D 6-membered ring channels (Fig. 12(A)), although their magnetic properties slightly differ from either the spin-glass or long-range antiferromagnetism properties, typically observed in Kagomé lattices.[179] For instance, Fe(II) and mixed-valent Fe(II)/Fe(III) sulfates undergo ferrimagnetic ordering at temperatures in the range of 15 to 19 K, whereas Co(II) compound shows weaker antiferromagnetic interactions with a possible antiferromagnetic ordering around 2.8 K (Fig. 12(B)).

The variety of these open-framework compounds has been recently expanded with the publication of several examples of iron,[180] nickel,[181] and manganese[182] sulfates. From a magnetic point of view, it is worth emphasizing the ferrimagnetic nature of the layered $[Fe_2F_2(SO_4)_2(H_2O)_2]\cdot C_2N_2H_{10}$,[180] $[Fe(III)_2Fe(II)_3F_{12}(SO_4)_2(H_2O)_2]\cdot 2C_4N_2H_{12}$,[178] and $[Ni_3F_2(SO_4)_3(H_2O)_2]\cdot C_4N_2H_{12}$[181] compounds, with critical temperatures of 22, 15, and 9 K, respectively. Even more recently, new open-framework sulfates have been synthesized including mixed transition/lanthanide and pure lanthanide metal ions.[183] These recent innovations are a clear sign that we are only at the early stages of this family, which is certainly going to offer new interesting open-framework structures with novel topologies and magnetic properties in the next few years.

2.1.6 Cyanides. Since the discovery of the Prussian blue pigment, $Fe_4[Fe(CN)_6]$ in 1704,[184,185] Prussian blue analogues are among the most known cyanide-based complexes. These

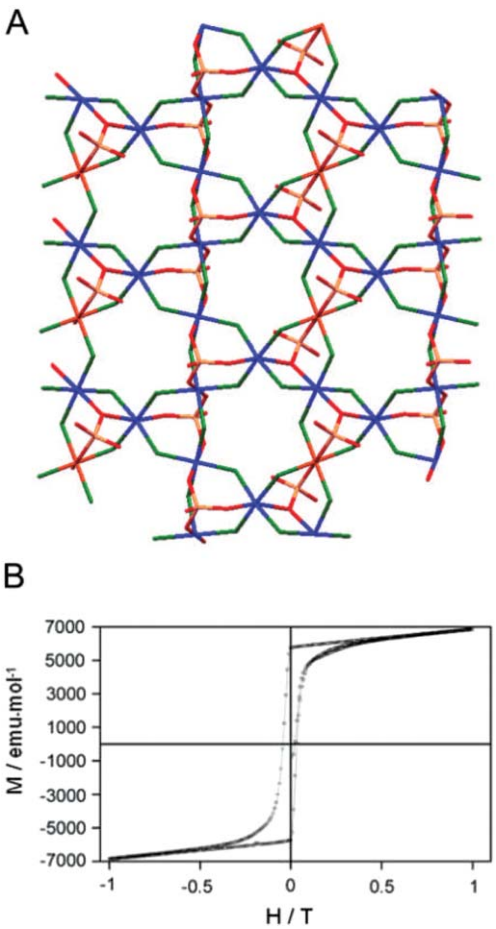

Fig. 12 (A) Structure of $[Fe_3F_6(SO_4)_2]\cdot C_6N_4H_{22}$, showing the presence of 6-membered rings. (Fe, blue; S, orange; O, red; F, green. Amine molecules have been omitted for clarity). (B) Magnetic hysteresis at 10 K. (Reprinted with permission of ref. 175. Copyright 2002, Royal Society of Chemistry.)

compounds possess structures based on a simple cubic $M_A[M_B(CN)_6]$ framework, in which octahedral $[M_B(CN_6)]^{n-}$ complexes are linked *via* octahedrally coordinated, nitrogen-bound M_A^{n+} ions. Thus, by combining M_A^{n+} with $[M_B(CN_6)]^{n-}$ complexes, numerous Prussian blue analogues have been reported with an extraordinary variety of chemical and physical properties.[186] Among them, the magnetic properties of these compounds have been extensively studied,[187] and now, using the appropriate combination of metal ions, one can prepare hexacyanometalate compounds with magnetic ordering temperatures as high as room temperature and 376 K.[188]

The crystal structures of Prussian blue derivatives offer intriguing possibilities for designing porous materials. Indeed, during last century, several authors have proved the possibility to remove the internal water molecules of several iron ferricyanites leaving their open-framework intact.[189] The earliest studies were reported by Seifer, who investigated the sorption properties of several small molecules such as water, methanol or ethanol by a series of divalent ferrocyanides. Twenty years later, Cartraud *et al.* investigated the zeolitic properties of $K_2Zn_3[Fe(CN)_6]_2{\cdot}xH_2O$,[190] and found interesting adsorption characteristics for different gas molecules, such as CO, N_2 and C_2H_4. During the same period, the molecular sieving and catalytic properties were also explored. Thus, for example, $Zn_3[Co(CN)_6]_2$ complex was used to separate C_6 isomers,[191] whereas a high capacity material for CO/CH_4 separations and a new catalyst for propylene oxide polymerizations were found in $Mg_3[Co(CN)_6]_2$ and $Zn_2[Co(CN)_6]Cl$, respectively.[192] More recently, a series of dehydrated Prussian blue analogues with formula $M_3[Co(CN)_6]_2$ (M(II) = Mn, Fe, Co, Ni, Cu, Zn and Cd) have shown promise for applications for hydrogen storage.[193]

Taking into account the large variety of magnetic and porosity properties found in these compounds, one can imagine Prussian blue derivatives as one of the ideal compounds to generate materials with both properties. However, examples of magnetic porous cyanide-type materials where both properties have been studied in concert are still limited. The porosity of most of these magnets or the magnetism of most of these porous compounds has not yet been tested. Thus far, one of the well-known examples is Prussian blue that is able to absorb small molecules such as N_2 or methanol after dehydration and orders ferromagnetically at a critical temperature of 5.5 K.[194,195] A second example was reported by Beauvais and Long.[196] The dehydration of $Co_3[Co(CN)_5]_2{\cdot}8H_2O$ generates a microporous ferrimagnet with a T_N = 38 K and a sorption capacity of 179 $cm^3\ g^{-1}$ (Fig. 13). This compound is especially important since is one of the first examples in which a long-range magnetic ordering and microporosity was rigorously demonstrated to coexist. In a recent study, Lü *et al.* have described another Prussian blue ferrimagnet, $K_{0.2}Mn_{1.4}Cr(CN)_6{\cdot}6H_2O$, with a reversible dehydration/hydration process followed by a decrease and increase of the critical temperature from 66 to 99 K.[197]

Alternatively, cyanide anions have been used for the synthesis of other molecular open-framework magnetic materials.[198] Among them, a remarkable series of expanded Prussian blue analogues have been shown to exhibit paramagnetic behaviour with weak antiferromagnetic interactions

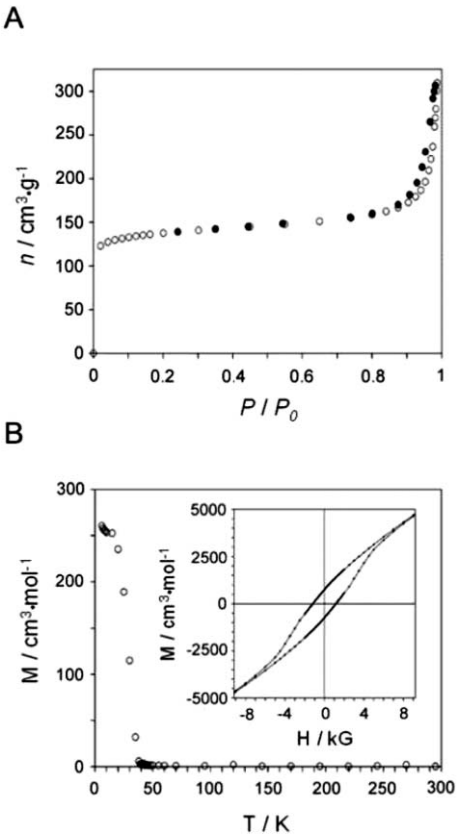

Fig. 13 (A) N_2 adsorption (○) and desorption (●) isotherms for porous $Co_3[Co(CN)_5]_2$ (after dehydration) measured at 77 K. Using the BET model, the surface area of this solid was determined to be 480 $m^2\ g^{-1}$. (B) Thermal evolution of the field-cooled magnetization at 10 G. Inset shows the magnetic hysteresis at 5 K. (Reprinted with permission of ref. 196. Copyright 2002, American Chemical Society.)

at very low temperatures.[199] Cooperative spin-crossover behaviour can also be found in some cyanide-bridge networks.[200] For example, hybrid compounds $[Fe(pyrazine)_2M(CN)_4]{\cdot}4H_2O$ (where M is Ni(II), Pd(II) and Pt(II)) show a 3-D porous structure combining strong cooperative spin transitions with T_c between 20 and 40 K.[201]

2.1.7 Other inorganic open-frameworks. In spite of the numerous inorganic families and examples of magnetic open-framework materials so far described along this review as well as their enormous progress experienced over the last 15 years, the search for new inorganic magnetic open-framework compounds can be still considered at an early stage. Indeed, recent examples of magnetic silicates,[202] germanates,[203] fluorides,[17,204] selenites,[205] polyoxovanadates,[206] sulfides[207] and oxochlorides[16] with open-framework structures seems to confirm such tendency by opening new and successful synthetic routes. From a magnetic point of view, most of them still behave as paramagnets with weak antiferromagnetic interactions at low temperatures. However new expectations have been opened in studying the magnetic properties shown by the selenite $[X]{\cdot}[Fe_2F_3(SeO_3)_2]$ (where X is $[C_4N_2H_{12}]_{0.5}$, $[C_4N_3H_{14}]_{0.5}$, and $[NH_4]$).[208] This compound with 1-D channels (5.8 × 7.6 Å) exhibits a frustrated magnetic behaviour with a critical temperature of 23 K.

2.2 Hybrid metal–organic open-frameworks

Hybrid open-frameworks are composed of "inorganic" subnetworks (identical to those structures summarized in the previous section) interconnected through multitopic organic ligands. According to this connectivity, two types of structures can be found. In a first class, the organic ligands act as pillars between "inorganic" layers, creating 3-D porous structures with pores usually defined by the void space available between the "inorganic" layers. Decreasing the dimensionality of the inorganic network, the second class of these hybrid structures are open-frameworks formed by the linkage of "inorganic" chains with organic molecules. Fig. 1(B) and (C) illustrate both types of channel-like structures. According to both composition and connectivity, the magnetic properties of these solids are usually governed by the dimensionality of the "inorganic" structures since their shorter inorganic bridges usually lead to stronger magnetic exchange interactions between paramagnetic metal ions. As a consequence, the pillared hybrid solids tend to show 2-D magnetic behaviours, whereas the second type frequently behaves as 1-D magnetic systems. Nevertheless, the capacity of the organic ligands to favour magnetic exchange interactions between inorganic structures may also play a crucial role in the presence of long-range magnetic ordering.

2.2.1 Pillared inorganic layers. Most pillared layered solids combining porosity characteristics and magnetic properties so far reported in the literature are mainly composed of layers of metal ions bridged by phosphate/phosphite groups or oxygen atoms, which in turn are pillared (connected) through a long range of organic ligands, including phosphonate,[209,210] dicarboxylate,[211–216,222,223] N,N′-dinitrogen,[217–219] and diamine[220,221] organic molecules. One of the first and most representative examples, the open-framework antiferromagnet $[Fe_3(PO_4)(HPO_4)_3(C_2O_4)_{1.5}]\cdot 1.5C_2N_2H_{10}\cdot xH_2O$ (x = 1.5–2) built up from Fe(III) phosphate layers connected through oxalate groups, was first described by Rao and co-workers.[211] This structure shows open layers defining 12-membered ring channels filled with water guest molecules that can be reversibly removed and readsorbed. The Néel temperature of this antiferromagnet ($T_N \approx 31$ K) is similar to those observed in other related iron compounds.[212–214] For example, $[Fe_3(HPO_4)_2(PO_4)(C_2O_4)_2]\cdot H_3DETA$, which is formed by iron phosphate (Fe/P/O) layers pillared by oxalate ligands and with 8-membered ring channels, exhibits a slightly higher T_N with a value of 45 K.[214] Besides iron metal ions, other metal ions have been used in the formation of such phosphate-based structures. A summary of some of these solids is shown in Table 1. Among them, remarkable are some copper compounds exhibiting interesting magnetic properties. For instance, antiferromagnetic ordering was observed in a Cu(II) hybrid solid pillared through diphosphonate ligands,[209] whereas a solid formed by Cu/P/O layers connected through pyrazine ligands showed metamagnetic behaviour.[217]

An important contribution that has contributed to fuel this family of materials was reported in 2001 by Rosseinsky and co-workers, who reported a series of cobalt-hydroxide/sulfate layered solids with formula $Co_4(SO_4)(OH)_6(A)_{0.5}\cdot xH_2O$ (where A is ethylenediamine ($C_2N_2H_8$) or 1,4-diazabicyclo[2,2,2]octane ($C_6N_2H_{12}$), and x = 1 and 3) pillared with diamine molecules (Fig. 14(A)).[220,221] These hybrid solids exhibit a metamagnetic behaviour at temperatures below 21 and 14 K (Fig. 14(B)). Furthermore, their open-frameworks are robust even after the loss of H_2O guest molecules, showing a reversible hydration/dehydration process. Higher ordering temperature was found in another cobalt–hydroxide layer structure pillared with *trans*-1,4-cyclohexanedicarboxylate ligands.[222] This compound, reported by Kurmoo, Kepert and co-workers, not only exhibits small 1-D channels (3.7 × 2.3 Å) that represent up to the 13.4% of the crystal volume (Fig. 14(C)) but also orders magnetically below 60.5 K and shows reversible dehydration (393 K)/hydration process (Fig. 14(D)).

2.2.2 Linked inorganic chains. Linked inorganic chains are one of the families of magnetic hybrid open-framework materials that probably has experienced the largest growth over the last few years. Indeed, the assembly of "inorganic" oxo-,[224–233] phosphate/phosphite-[213,215,234,235] and nitrogen-based[236] chains through organic multitopic ligands has generated multiple channel-like magnetic solids (see Table 1). One can consider that the paradigmatic example of this type of solids was reported by Riou, Férey and co-workers in 2002.[232] These authors reported the compound $[V(OH)(C_8H_4O_4)]\cdot 0.75C_8H_6O_4$ (referred as MIL-47*as*, where *as* means as-synthesized), whose structure consists of oxo-bridged V(III) chains connected through dicarboxylate terephthalate ligands (Fig. 15(A)). This connectivity forms a 3-D structure with large 1-D pores (12.0 × 7.9 Å) that are filled with terephthalate molecules. Interestingly, terephthalate guest molecules can be evacuated at 573 K, leading to a porous compound $[V(OH)(C_8H_4O_4)]$ (MIL-47) with slightly distorted channels of dimensions of 11.0 × 10.5 Å (Fig. 15(B)). Furthermore, this porosity is accompanied by an antiferromagnetic ordering at relatively high temperatures, T_N of 95 and 75 K for MIL-47*as* and porous MIL-47, respectively (Fig. 15(C)). Later, the same authors reported another compound with formula $[Cr(OH)(C_8H_4O_4)]\cdot 0.75C_8H_6O_4$ (referred as MIL-53) showing similar properties; with an antiferromagnetic behaviour at 55 K and the capability to absorb water molecules.[231]

More recently, the combination of interesting porosity and magnetic properties have been described in other hybrid solids composed of "inorganic" oxo-bridged chains linked by dicarboxylate ligands.[224–230] For example, dehydration/rehydration process followed by a ferromagnetic to antiferromagnetic transition was observed in $[Co_3(OH)_2(C_4O_4)_2]\cdot 3H_2O$.[227] A new iron compound with formula $[Fe_2O(C_2H_3O_2)_2(C_8H_4O_4)]\cdot 2CH_3OH$ (referred as MIL-85) has also been described to exhibit a frustrated magnetic behaviour and the capacity to be stable after evacuation of the methanol guest molecules, forming a porous solid with a large Langmuir area of 110 $m^2\ g^{-1}$.[225]

Finally, it is important to remark a few other hybrid solids that have been built from nitrogen- and phosphate-based ligands. Some of these examples are $[Cu_2Mo_2O_8(4,4'\text{-bpy})]\cdot 3H_2O$,[233] $[Mn(N_3)_2(titmb)]\cdot 1.5H_2O$[236] (where titmb is 1,3,5(imidazol-1-ylmethyl)-2,4,6-trimethylbenzene) and $[Fe_3(OH)_2(O_3PC_2H_4CO_2H)_2(H_2O)_4]$ (referred as MIL-38).[234] The first of these solids is composed of double helical

Table 1 Magnetic hybrid metal–organic open-framework solids[a]

Compound	Structural description	Magnetic properties	Ref.
2-D "Inorganic" phosphate/phosphite-based layers			
$[Cu_2(O_3PXPO_3)(H_2O)_2]$ (X = C_2H_4, C_8H_8; MIL-29)	3-D framework built up from 2-D Cu/P/O layers pillared by the diphosphonate ligands. The inorganic layers contain dimers of edge-sharing $CuO_4(H_2O)$ polygons.	Both compounds are antiferromagnets at 4 K.	209
$[(VO)_2(O_3PC_3H_6PO_3)(H_2O)]\cdot 2H_2O$	3-D framework formed by V/P/O layers pillared by diphosphonate ligands. The inorganic layers contain dimers of face-sharing $VO_5(H_2O)$ octahedra.	Presence of antiferromagnetic interactions, mostly between dimers.	210
$[Fe_3(PO_4)(HPO_4)_3(C_2O_4)_{1.5}]\cdot 1.5C_2N_2H_{10}\cdot xH_2O$ (x = 1.5–2)	3-D framework formed by Fe/P/O layers pillared by oxalato ligands. This compound shows 1-D 12-membered ring channels. Reversible dehydration (383 K)-hydration is observed. MeOH is adsorbed.	Antiferromagnetic ordering below 31 K.	211
$[Fe_2(HPO_4)_3(C_2O_4)]_2\cdot C_{10}N_4H_{28}$	3-D framework formed by Fe/P/O layers pillared by oxalato units forming 8-membered ring channels in which the amine molecules reside.	Antiferromagnetic ordering below 40 K.	212
$[Fe_2(HPO_4)_2(C_2O_4)(H_2O)_2]\cdot H_2O$, $[Fe_2(HPO_4)_2(C_2O_4)(H_2O)_2]\cdot 2H_2O$	3-D framework formed by Fe/P/O layers pillared by oxalato ligands, forming 1-D 4- or 6-membered and 8-membered ring channels.	Antiferromagnetic ordering below 30 and 40 K for the first and second compound, respectively.	213
$[Fe_3(HPO_4)_2(PO_4)(C_2O_4)_2]\cdot H_3DETA$	3-D framework formed by Fe/P/O layers pillared by oxalato ligands, forming 1-D 8-membered ring channels filled with the triamine cations.	Antiferromagnetic ordering below 45 K.	214
$[A][Mn_2(HPO_4)_2(C_2O_4)(H_2O)_2]$ (A = $C_6N_2H_{16}$, $C_2N_2H_{10}$, $C_3N_2H_{12}$)	3-D framework formed by Mn/P/O layers pillared by oxalato ligands, forming 1-D channels containing the diamine cations.	Presence of antiferromagnetic interactions	215,216
$[Mn_4(PO_4)_2(C_2O_4)(H_2O)_2]$	3-D framework formed by Mn/P/O layers pillared by oxalato ligands, forming a small amount of open space between oxalate pillars.	Presence of antiferromagnetic interactions.	216
$[Cu_4(CH_3C(OH)(PO_3)_2)_2(pz)(H_2O)_4]$	3-D open-framework formed by Cu/P/O layers pillared by pyrazine ligands.	Antiferromagnetic ordering below 4.2 K and metamagnetic behaviour.	217
$(VO)_4(HPO_3)_4(4,4'\text{-bpy})_2$	3-D open-framework formed by Cu/P/O layers pillared by 4,4′-bpy ligands.	Presence of antiferromagnetic interactions.	218
$[NH_4][(V_2O_3)_2(4,4'\text{-bpy})_2(H_2PO_4)(PO_4)_2]\cdot 0.5H_2O$	3-D open-framework formed by V/P/O layers pillared by 4,4′-bpy ligands. The inorganic layers contain dimers of edge-sharing V(IV,V) dimers. The 1-D channels are occupied by NH_4^+ cations and H_2O molecules.	Presence of antiferromagnetic interactions.	219
2-D "Inorganic" oxide-based layers			
$Co_4(SO_4)(OH)_6(C_2N_2H_8)_{0.5}\cdot 3H_2O$	Layers formed by edge-sharing $Co(OH)_6$ octahedra decorated by tetrahedral Co(II) sites. The layers are pillared by the diamine molecules, forming a 3-D framework with channels (4.7 × 2.8 Å, 16.5% crystal volume). The framework is robust to loss of H_2O molecules and thermally stable to 573 K.	This compound orders as a metamagnet below 14 K. The system may be magnetically frustrated.	220,221
$Co_4(SO_4)(OH)_6(C_6N_2H_{12})_{0.5}\cdot H_2O$	Similar structure than previous compound. The framework shows interconnected channels (2.5 × 2.1 Å, 5% crystal volume) running along two directions. The framework is thermally stable to 553 K. Reversible dehydration/hydration process.	This compound orders as a metamagnet below 21 K. The system may be magnetically frustrated.	221
$Co_5(OH)_8(chdc)\cdot 4H_2O$	3-D framework built up from Co(II)-hydroxide layers pillared with *trans*-1,4-cyclohexanedicarboxylate. The framework houses 1-D channels (3.7 × 2.3 Å, accessible volume of 13.4% per unit cell). Reversible dehydration/hydration process accompanied with structural changes.	Ferrimagnetic ordering below 60.5 K.	222
$[V_2(OH)_2F_2(C_8H_4O_4)]\cdot H_2O$ (MIL-71)	3-D structure formed by layers of V(III) ions linked by OH and F bridges. The layers are pillared by terephthalate ligands, forming 1-D small cavities filled with H_2O molecules.	Canted antiferromagnetic behaviour with a T_N below 20 K.	223
1-D "Inorganic" oxide-based chains			
$[Fe(C_2O_4)(OH)]_4Ba_4(C_2O_4)Cl_2$	2-D framework formed by hydroxy-bridged Fe chains connected by bridging oxalate ligands. The framework shows large channels that contain the barium, chloride and oxalate counter ions.	This compound shows a magnetic phase transition at 32 K and a strong easy plane anisotropy at all temperatures. Above the T_c the compound behaves as an $S = 2XY$ antiferromagnetic chain.	224

Table 1 Magnetic hybrid metal–organic open-framework solids[a] (*Continued*)

Compound	Structural description	Magnetic properties	Ref.
$[Fe_2O(C_2H_3O_2)_2(C_8H_4O_4)]\cdot 2CH_3OH$ (MIL-85)	3-D framework with 1-D channels built up from 1-D helical inorganic chains connected through terephthalate ligands. Guest CH_3OH molecules are removed at 473 K without destabilizing the framework. Measured Langmuir surface area is 110 $m^2\ g^{-1}$. Stable up to 548 K.	This compound exhibits a frustrated magnetic behaviour in the low temperature range.	225
$[Fe(OH)(C_{10}H_4O_8)]\cdot xH_2O$ (x = 0.88, MIL-82)	3-D framework built up from the linkage of Fe-based chains by 1,2,4,5-tetrabenzenecarboxylate ligands. Small channels filled with H_2O molecules are present.	Antiferromagnetic ordering around 5.5 K.	226
$[Co_3(OH)_2(C_4O_4)_2]\cdot 3H_2O$	3-D structure formed by brucite-like ribbons of formula $[Co_3(OH)_2]$ that are bridged by squarate dianions. The framework shows 1-D channels (3.94 × 6.76 Å, 176.8 $Å^3$ per unit cell) filled with H_2O molecules. Reversible dehydration (473 K)/hydration process, accompanied with minor structural changes.	As-synthesized sample shows antiferromagnetic transition at 8 K followed by another transition to a canted antiferromagnetic state below 6 K. Dehydrated compound orders as a ferromagnet at 8 K.	227
$[Co_2(OH)(C_9H_3O_6)(H_2O)]\cdot H_2O$	3-D pyrochlore-type structure built up from strips of corner-sharing $Co_3(\mu_3\text{-}OH)$ triangles that are bridged by 1,3,5-benzenetricarboxylate units. The framework shows 1-D channels occupied by H_2O molecules.	Presence of antiferromagnetic interactions. Possible spin-frustrated system.	228
$[Co_3(OH)_2(C_4H_2O_4)_2(H_2O)_4]\cdot 2H_2O$	3-D framework formed by inorganic chains inter-linked by bis-bidentate fumarate anions, displaying rhombic tunnels.	Presence of antiferromagnetic interactions.	229
$[Ni_3(OH)_2(C_4H_2O_4)(H_2O)_4]\cdot 2H_2O$	1-D inorganic chains connected by fumarate ligands to form a 3-D framework. Presence of 2-D pores. No porosity after removal of water molecules.	This compound exhibits a scarce ferrimagnetic behaviour below 20 K.	230
$[Cr(OH)(C_8H_4O_4)]\cdot(C_8H_6O_4)_{0.75}$ (MIL-53)	Cr(III)-hydroxide chains linked by terephthalate ligands forming a 3-D framework with 1-D channels (7.9 × 12 Å). The guest terephthalic molecules are removed at 523 K, generating $[Cr(OH)(C_8H_4O_4)]$. This compound is porous (9.4 × 11.4 Å, Langmuir surface area of 1500 $m^2\ g^{-1}$). At room temperature, hydration occurs forming $[Cr(OH)(C_8H_4O_4)]\cdot H_2O$, also a porous material.	Antiferromagnetic ordering with a T_N of 65 K. Hydrated compound shows a T_N of 55 K.	231
$[V(OH)(C_8H_4O_4)]\cdot 0.75C_8H_6O_4$ (MIL-47)	3-D structure formed by V(III)-hydroxide chains linked by terephthalate ligands forming 1-D channels (7.9 × 12 Å). The guest terephthalic molecules are removed at 573 K, generating $[V(O)(C_8H_4O_4)]$. This compound is porous (10.5 × 11.0 Å, Langmuir surface area of 1320 $m^2\ g^{-1}$). Readsorption of diethyl ether is observed.	Antiferromagnetic ordering with a T_N of 95 K. The porous compound shows a T_N of 75 K.	232
$[Cu_2Mo_2O_8(4,4'\text{-bpy})]\cdot 3H_2O$	3-D framework formed by the linkage of double helical Cu–O–Mo–O chains by 4,4′-bpy ligands. The framework shows large channels (6.7 × 11.1 Å). Guest H_2O molecules can be removed without modifying the framework. Absorption of CH_3CN is proved.	This semiconductor shows the presence of antiferromagnetic interactions.	233
1-D "Inorganic" phosphate/phosphite-based chains			
$[Fe_3(OH)_2(O_3PC_2H_4CO_2H)_2\text{-}(H_2O)_4]$ (MIL-38)	Chains of linear edge-sharing Fe(II) octahedral trimers linked by phosphate groups. The chains are then connected through the organic ligands to form an open-framework with empty channels.	The compound shows a metamagnetic behaviour below 10 K.	234
$[Fe_2(HPO_4)(C_2O_4)_{1.5}]\cdot 0.5C_4N_2H_{12}$	3-D open-framework formed by Fe/P/O chains connected through oxalato ligands, forming channels (7.1 × 5.4 Å and 5.9 × 5.7 Å).	Presence of antiferromagnetic interactions	235
$[A][Fe_2(HPO_4)_2(C_2O_4)_{1.5}]_2$ (A = $C_3N_2H_{12}$, $C_3N_2OH_{12}$)	3-D open-framework formed by Fe/P/O ladder-like chains connected through oxalato ligands. These compounds show different channels.	Antiferromagnetic ordering with a T_N of 25 K.	213
$[Mn_4(HPO_4)_2(C_2O_4)_3(H_2O)_2]\cdot C_2N_2H_{10}\cdot 2H_2O$	3-D open-framework formed by Fe/P/O chains connected through oxalato ligands.	Presence of antiferromagnetic interactions.	215
1-D "Inorganic" azide-based chains			
$[Mn(N_3)_2(titmb)]\cdot 1.5H_2O$	Inorganic chains formed by the connection of Mn ions through azide ligands with an end-to-end coordinating mode. The linkage of these chains by titmb ligands forms an open-framework, which voids are filled by H_2O molecules.	Presence of antiferromagnetic interactions.	236

[a] Abbreviations: H_3DETA, diethylenetriamine; pz, pyrazine; 4,4′-bpy, 4,4′-bipyridine; chdc, *trans*-1,4-cyclohexanedicarboxylate; titmb, 1,3,5(imidazol-1-ylmethyl)-2,4,6-trimethylbenzene.

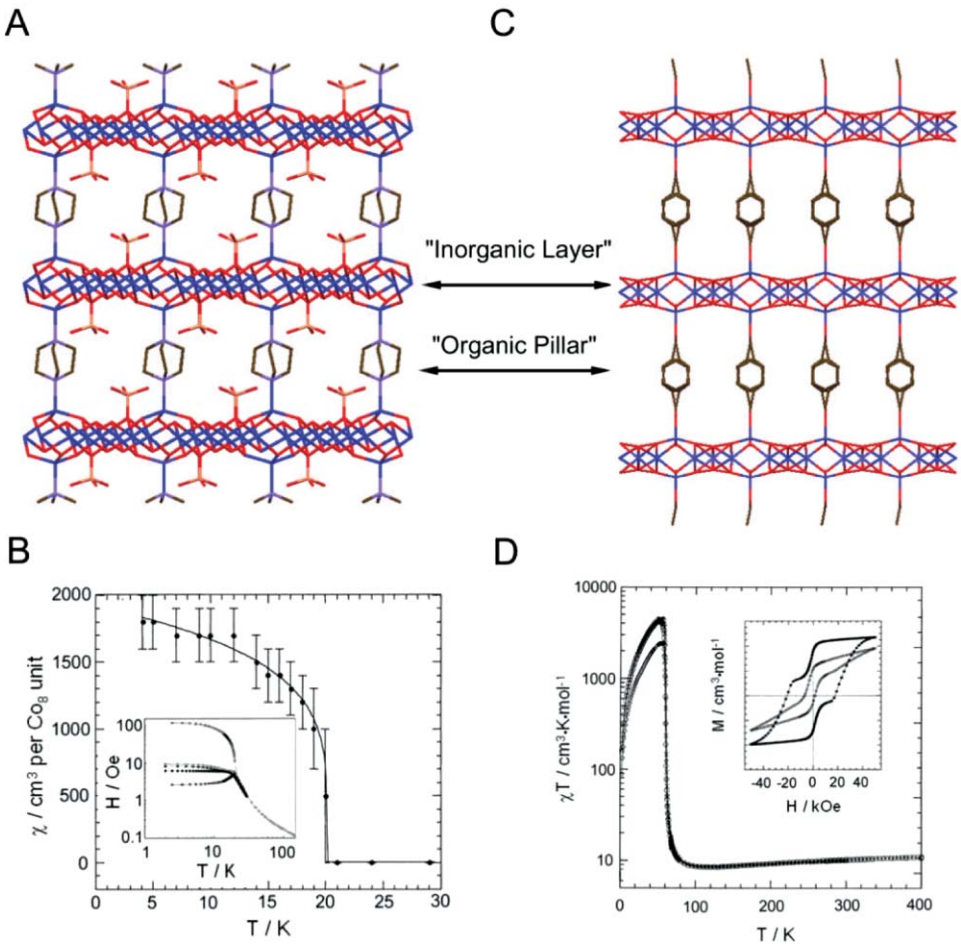

Fig. 14 (A) View of the crystal structure of $Co_4(SO_4)(OH)_6{\cdot}0.5C_6N_2H_{12}{\cdot}H_2O$ showing the 1-D channels. (B) Phase diagram for the layered metamagnet. Inset shows the thermal evolution of the molar susceptibility (χ) under an ac-applied field of 1 Oe (□) and dc-applied fields of 0.58 Oe under both filed cooled (△) and zero-field cooled (▲), 100 Oe (○), 1000 Oe (◇) and 3000 Oe (◆). (C) View of the crystal structure of $Co_5(OH)_8(chdc){\cdot}4H_2O$ (where chdc is *trans*-1,4-cyclohexanedicarboxylate). (D) Thermal evolution of the product χT for as-synthesized $Co_5(OH)_8(chdc){\cdot}4H_2O$ (○), dehydrated (×) and rehydrated (◇). Inset shows the magnetic hysteresis parallel (○) and perpendicular (●) to the *b* axes. (In (A) and (C), Co, blue; S, orange; O, red; N, violet; C, brown. H_2O solvent molecules are omitted for clarity). (Reprinted with permission of ref. 221 and 222. Copyright 2001 and 2003, American Chemical Society.)

oxo-bridged copper/molybdenum chains. The connection of these chains through 4,4′-bipyridine ligands creates a 3-D open structure with large channels (6.7 × 11.1 Å) that can be dehydrated forming a porous structure able to absorb solvent molecules such as acetonitrile. Furthermore, this porous solid behaves as a semiconductor with the presence of antiferromagnetic interactions. The second of these 3-D open-frameworks is built up from the linkage of manganese chains by three-connecting titmb ligands. In this case, the ''inorganic'' bridges are azide ligands that connect the Mn(II) ions in an end-to-end mode. This bonding originates the presence of antiferromagnetic interactions in this material. Phosphate groups can also act as linkers to create this type of hybrid solids. For example, MIL-38 is an iron open-framework formed by carboxyethylphosphonate ligands that shows 1-D empty channels and behaves as a metamagnet below 10 K.

In our opinion, the diversity of structures and magnetic behaviours shown by hybrid solids, in spite of its early stage development, symbolizes the continuous development that these materials are experiencing as well as justify the great expectations raised up for the near future.

2.3 Coordination polymers

As in many other aspects related to the molecular magnetism field, Kahn's group can be considered pioneers in the discovery of coordination polymers combining both porosity characteristics and magnetic properties.[237] In their manuscript published on 1999,[238] these authors first introduced the concept of a ''molecular magnetic sponge'' for a coordination polymer. As an example of these sponge-like polymers, the compound $[CoCu(obbz)(H_2O)_4]{\cdot}2H_2O$ (where obbz is *N*,*N*′-bis(2-carboxyphenyl)oxamido) shows a two-step reversible hydration/dehydration process followed by a dramatic change of the magnetic properties.[239] As a consequence of a first dehydration at 373 K, the discrete units link themselves forming a 1-D structure that behaves as a ferrimagnet with no ordering down to 2 K. A second dehydration process takes place after heating the sample up to 473 K. The resulting presumably 2-D structure still behaves as a ferrimagnet, but

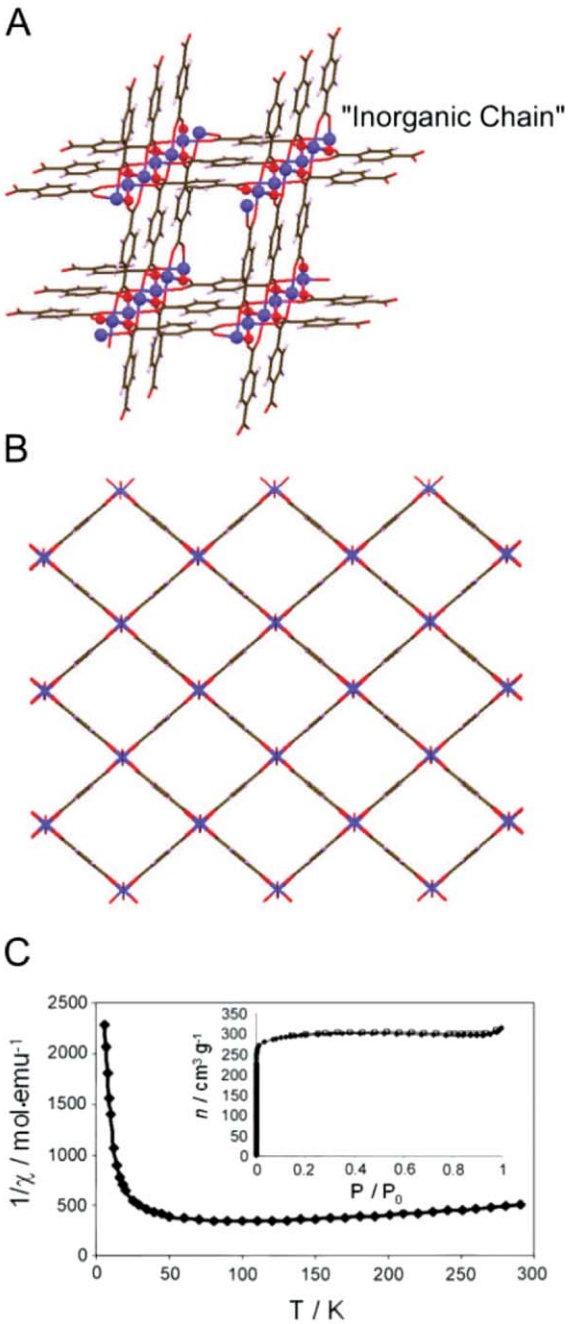

Fig. 15 (A) Projection of the "inorganic" V–O–V–O chains connected through the terephthalate ligands in $V(OH)(C_8O_4H_4)$. (B) View of the pores. (C) Thermal dependence of the reciprocal magnetic susceptibility for the as-synthesized antiferromagnet. The inset shows the N_2 sorption (◆) and desorption (□) isotherms measured at 77 K. (In (A) and (B), V, blue; O, red; C, brown; H, white. In (A), V and O atoms are represented as spheres). (Reprinted with permission of ref. 232. Copyright 2002, Wiley Interscience).

with a critical temperature of 30 K. As described in Fig. 16, all these processes are completely reversible, and the material can be rehydrated after cooling with the recovering of the initial magnetic properties.

The coordination polymers or 0-D zeotype systems, according to Ferey's classification (Fig. 1(D)), have experienced a gigantic evolution the last few years. The interest for this approach is fourfold. First, the endless versatility of molecular chemistry provides chemists with a huge variety of polytopic ligands, most of them carboxylic-based and nitrogen-based molecules. Second, these ligands have been proved to be good superexchange pathways for magnetic couplings. Third, the chemistry that needs to be applied for the synthesis of coordination polymers (reactants, instrumentation, *etc.*) is inexpensive and, in consequence, scientists all around the world can contribute to their expansion. And last but not least, they may profit from crystal engineering techniques to arrange transition-metal ions and organic tectons within a wide variety of patterns with open-framework structures that not only allow to control pore sizes and functionalities,[31,33] but also favor magnetic exchange interactions, since they coordinate in a predictable way.

In this section, we will revise representative examples of magnetic porous coordination polymers. All these examples have been selected for combining a contrasted porosity and relevant magnetic properties, evolving from the presence of strong magnetic exchange interactions and/or any type of magnetic ordering. Furthermore, since the strength of the magnetic superexchange interactions between metal ions through organic ligands is strongly dependent on their relative orientation and, especially, on the distance between interacting ions, we found convenient to divide the coordination polymers

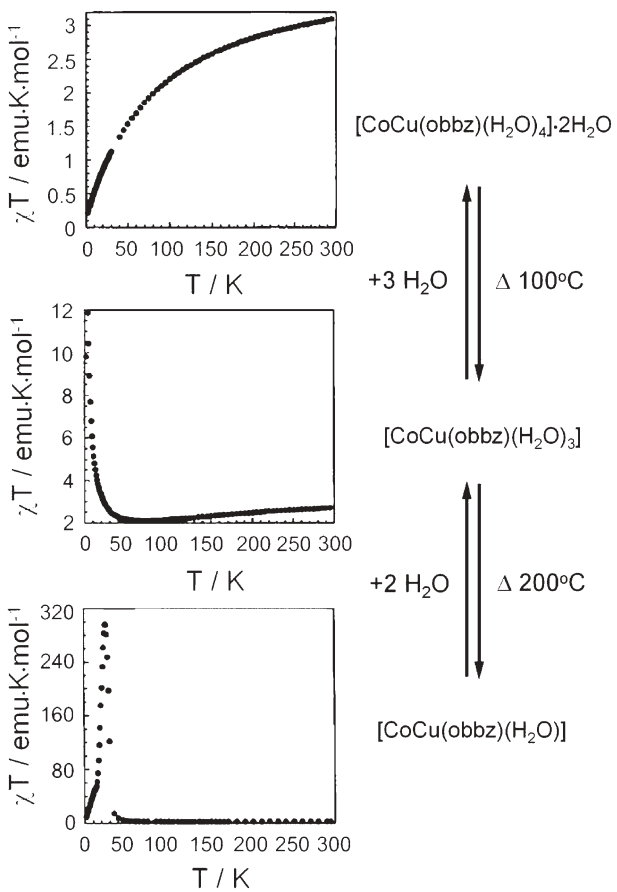

Fig. 16 Reversible hydration/dehydration processes followed by changes in the magnetic properties of $[CoCu(obbz)(H_2O)_4]\cdot 2H_2O$ (where obbz is *N*,*N*′-bis(2-carboxyphenyl)oxamido). (Reprinted with permission of ref. 238. Copyright 1999, Wiley Interscience.)

by the connectivity of metal ions. First, examples of magnetic porous metal-organic frameworks formed by 1-D, 2-D and 3-D connected M–O–C–O–M/M–O–M carboxylate-based subnetworks that can be linked by multitopic organic ligands will be described. In this type of solids, the ability of the carboxylate groups to link more than one metal ion provide M–O–C–O–M and M–O–M magnetic pathways, which usually leads to strong interactions in comparison with the pathways defined by bridged metal ions through a multitopic organic ligand involving more than one of its functional groups. As a consequence, the magnetic behaviour of these polymers is generally governed by the magnetic exchange interactions between the M–O–C–O–M and/or M–O–M subnetworks.

The second subsection will be devoted to review coordination polymers formed by connected organo-polymetal clusters through polytopic organic ligands. Similar to the first class of polymers, the magnetic properties of this family are related to the inherent magnetic properties of the clusters, and only if the organic ligands facilitate the magnetic interactions between the clusters, long-range magnetic properties are observed. Finally, the third subsection will be dedicated to review metal–organic open-framework structures based on isolated metal ions connected through multitopic organic ligands. In this third family, the magnetic properties are closely dependent on the distance between metal ions. Therefore, organic ligands that space the metal ions with long distances are expected to decrease, or in the worst of the cases disrupt, the superexchange pathway between the metal ions. When this occurs, the coordination polymers behave as pure paramagnets with only weak ferro- or antiferromagnetic interactions that are exhibited only at very low temperatures. For example, the use of larger ditopic-N,N′ organic molecules (*e.g.* 4,4′-bipyridine, *etc.*) has yielded a series of coordination polymers with different paramagnetic metal ions that exhibit interesting porosity characteristics, but only very weak antiferromagnetic couplings at very low temperatures due to the long-distances between bridged metal ions.[240]

2.3.1 1-D, 2-D, and 3-D M–O–C–O–M/M–O–M carboxylate-based networks. An excellent review on metal carboxylates with open architectures has been recently published.[40] As stated above, from a magnetic point of view, the use of short organic ligands mediates the magnetic interactions between metal ions, and is essential for obtaining channel-like polymers with intense and long-range magnetic behaviour. For this reason, some of the most used ligands are formate, malonate, oxalate, succinate, fumarate, and glutarate. These are short ligands that tend to bridge metal ions through M–O–C–O–M or M–O–M type linkages, facilitating magnetic exchange in one-, two-, and three-dimensions. In this section, we include a compilation of magnetic porous solids that possess frameworks built up from carboxylate-based 1-D, 2-D, and 3-D M–O–C–O–M and/or M–O–M subnetworks. Also, examples of frameworks formed by "inorganic" bridged discrete clusters connected *via* carboxylato-based M–O–C–O–M/M–O–M type bonds are considered. The various features of many representative examples are described below and in Table 2.

Several magnetic open-framework metal formates have been reported.[245–249,260,273] The formate ion, $HCOO^-$, is the smallest and simplest carboxylate ligand, with a small stereo effect beneficial for the formation of polymers. The short $HCOO^-$ bridge, a three-atom connector, is very effective for the magnetic coupling between magnetic metal sites, compared to other small "inorganic bridges" such as CN^-, N_3, *etc.* Indeed, the absence of any bulky organic group on the formate ion favours an *anti-anti* mode of coordination that tends to promote effective magnetic exchange pathways between the magnetic moment carriers. More recently, this bridging formate ligand has been incorporated in the formation of porous structures, most of them with a high thermal stability even in the absence of the solvent guest molecules.[241] The porous compound $Mn_3(HCOO)_6{\cdot}CH_3OH{\cdot}H_2O$ reported by Kobayashi, Kurmoo and co-workers possesses a diamondoid framework with high stability and flexibility for the inclusion of many types of guests.[248] This framework exhibits 1-D channels with dimensions of 4 × 5 Å (32% of the total volume cell), where each node is occupied by $MnMn_4$ tetrahedral building units built up from a central Mn(II) ion connected to four Mn(II) ions at the apices. The resulting 3-D network is thermally robust up to 533 K, even after evacuation of guest molecules (Fig. 17(A)), and exhibits a rich guest-modulated magnetic behaviour (for more details, see Section 6). The initial synthesized and evacuated materials show a long-range magnetic ordering with a critical temperature close to 8 K (Fig. 17(B)). The presence of long-range order in open-framework formates has also been reported in the series $M(HCOO)_3{\cdot}NH_2(CH_3)_2$ (M = Mn, Co, Ni),[246] $[M(HCOO)_2]{\cdot}1/3HCOOH$ (M = Fe, Co, Ni),[247] $[AmineH^+]{\cdot}[Mn(HCOO)_3]$,[245] $Co(HCOO)_2(HCONH_2)_2$,[260] $M(HCOO)_2(4,4'\text{-bpy}){\cdot}5H_2O$ (M = Co, Ni),[273] and $Mn(HCOO)_3{\cdot}0.5CO_2{\cdot}0.25HCOOH{\cdot}0.75H_2O$.[249] Among them, the last complex reported by Sessoli and co-workers exhibits very interesting porosity characteristics: this material traps CO_2 molecules in their cavities.

Similarly, the oxalate ions, a dicarboxylate ligand that acts as a rigid ambidentate ligand, facilitates the formation of extended channel-like coordination polymers and mediates the magnetic coupling between bridging metal ions. To date, the use of oxalate ligand has allowed the synthesis of several mixed-valent polymers with common formula $(A){\cdot}[M(II)M(III)(C_2O_4)_3]$ (where A refers to ammonium cations, alkali-metal cations, or $Cp_2M(III)$, and Cp is cyclopentadiene).[261,262] The crystal structure shows an organically templated framework formed by alternating M(II) and M(III) metal ions in a 2-D honeycomb lattice, bridged by the bidentate oxalate ions, and in which the cations are located to the 1-D channels (Fig. 18(A)). Other related oxalate-based polymers are the 3-D networks of the type $[M(II)_2(C_2O_4)_3]$, $[M(I)M(III)(C_2O_4)_3]$, and $[M(II)M(III)(C_2O_4)_3]$.[251] The structure of these compounds consists of an oxalate-bridged metallic chiral (10,3)-network that hosts the tris-chelated transition-metal diimine $[M(II)(bpy)_2]^{2+}$ complexes into the 1-D channels (Fig. 18(B)). From a magnetic point of view, depending on M(II) and M(III) metal ions, the near-neighbour exchange in all these compounds may be ferro- or antiferromagnetic, leading to long-range anti-, ferro- or ferrimagnetic behaviours.[250] Thus far, however, not many of these compounds have been

Table 2 Magnetic channel-like coordination polymers based on connected *M–O–C–O–M* and/or *M–O–M* carboxylato-based networks[a]

Compound	Structural description	Magnetic properties	Ref
3-D M–O–C–O–M/M–O–M network			
$[Mn(HCOO)_3]\cdot[AmineH^+]$	3-D NaCl-type framework formed by the connection of Mn(II) ions *via* formate groups. The channels are occupied by alkylammonium cations. The channels size can be modulated by changing the size of the alkylammonium cation.	All compounds behave as antiferromagnets below 9 K.	245
$M(HCOO)_3\cdot NH_2(CH_3)_2$ (M = Mn, Co, Ni)	3-D distorted perovskite-like structure formed by the connection of metal ions through formate ligands. Dimethylamine molecules are located in the cages of the network.	All compounds behave as canted weak ferromagnets with T_c = 8.5 K (Mn), 14.9 K (Co) and 35.6 K (Ni), and for Co and Ni complexes spin reorientation take place at 13.1 and 14.3 K, respectively.	246
$[M(HCOO)_2]\cdot 1/3HCOOH$ (M = Fe, Co, Ni)	3-D framework built up from M–O–M and M–O–C–O–M type linkages. The structure shows 1-D channels with an accessible volume of 505 $Å^3$ per unit cell, or 30.5% of the unit cell volume.	Fe(II) compound undergoes 3-D ordering below T_c = 16 K. The Co(II) complex is dominated by antiferromagnetic interactions.	247
$[Mn_3(HCOO)_6]\cdot CH_3OH\cdot H_2O$	3-D diamond-type framework formed by the connection of Mn(II) ions *via* formate ligands. The framework exhibits 1-D channels of 4 × 5 Å (32% of the total volume cell). Guest solvent molecules can be removed below 373 K, and the framework is thermally stable up to 533 K.	Magnetic ordering below 8.1 K. The critical temperature of this complex is modulated by the nature of the guest molecules.	248
$Mn(HCOO)_3\cdot 0.5CO_2\cdot 0.25HCOOH\cdot 0.75H_2O$	3-D framework built up from connected Mn(II) metal ions through formate ligands. Interestingly, the framework includes CO_2 and HCOOH guests in the cavities.	Antiferromagnetic transition below 27 K.	249
$(A)\cdot[M(II)_2(C_2O_4)_3]$, $(A)\cdot[M^IM(III)(C_2O_4)_3]$, and $(A)\cdot[M(II)M(III)(C_2O_4)_3]$ ($A = [M(II)(2,2'\text{-bpy})_3]^{2+}$)	3-D oxalate-bridged metallic chiral (10,3)-network exhibiting 1-D channels. Tris-chelated metal diimine complexes are hosted into the channels.	Depending on the metal ions, the near-neighbor exchange in all these compounds may be ferro- or antiferromagnetic, leading to long-range anti-, ferro- or ferrimagnetic behaviour. For more details see reference.[250]	251
$[Fe_2(C_2O_4)_2OCl_2]\cdot 2NH_4\cdot 2H_2O$	Chiral 3-D framework of oxalate-bridged Fe(III) chains connected by single oxo bridge. The structure shows helical channels (~12 × 6 Å) in which ammonium and water molecules are located.	Magnetic ordering below 40 K.	252
$[Fe_2(C_2O_4)_2(OH)Cl_2]\cdot EtNH_3\cdot 2H_2O$	Similar 3-D structure. $EtNH_3$ and H_2O molecules are located into the channels. Irreversible solid–solid transformation (proton transfer) to a new complex $[Fe_2(C_2O_4)_2(O)Cl_2]\cdot EtNH_3\cdot H_3O\cdot H_2O$ in contact with the air.	Behaves as a magnet below 70 K.	253
$[Fe_2(C_2O_4)_2(O)Cl_2]\cdot EtNH_3\cdot H_3O\cdot H_2O$	Similar 3-D structure. The symmetry of the channels has decreased.	Behaves as a magnet below 70 K.	253
$K[Cr(C_2O_4)_3][Cu(trans[14]dien)]$	3-D structure formed by oxalate-bridged alternated K and Cr metal ions. The framework shows large channels (21.2 × 9.3 Å) that are occupied by the Cu(II) complexes.	Presence of antiferromagnetic interactions.	254
$[Co_7(C_2O_4)_3(OH)_8(ppz)]$	3-D framework formed by the connection of heptanuclear $Co_7(OH)_8$ clusters *via* oxalate (through Co–O–C–O–Co bonds) and ppz ligands. The framework contains small triangular 1-D channels.	Behaves as an antiferromagnet with T_N of 26 K. $M(H)$ plot is characteristic of metamagnetism.	255
$K_2MnU(C_2O_4)_4\cdot 9H_2O$	3-D diamond-like structure formed by alternating Mn and U metal ions linked by oxalate ligands. 1-D square-shaped channels are present.	Presence of weak antiferromagnetic interactions.	256
$[Cu(C_3H_2O_4)(DMF)]$	3-D chiral diamond-like open-framework formed by Cu(II) ions connected *via* –O–C–O– bridges.	Ferromagnetic ordering below 2.6 K.	257
$[Ni_7(C_4H_4O_4)_6(OH)_2(H_2O)_2]\cdot 2H_2O$.	3-D honeycomb structure formed by Ni–O–Ni type linkages. This framework shows 1-D pores formed by wide cavities (8 Å) and narrow apertures (4 Å). Thermochemically stable up to 673 K. Reversible dehydration/hydration.	Paramagnet down to about 5 K. This compound may be magnetically frustrated.	258
$[Ni_{20}(C_5H_6O_4)_{20}(H_2O)_8]\cdot 40H_2O$	3-D framework constructed from infinite Ni–O–Ni type linkages (bridging H_2O and glutarate ligands). Presence of very large intersecting 20-membered ring tunnels that are filled with H_2O molecules. Reversible dehydration/hydration without significant structural changes and shows a surface area of 346 $m^2\ g^{-1}$.	Behaves as a pure ferromagnet at 4 K.	259

Table 2 Magnetic channel-like coordination polymers based on connected *M–O–C–O–M* and/or *M–O–M* carboxylato-based networks[a] (*Continued*)

Compound	Structural description	Magnetic properties	Ref
2-D M–O–C–O–M/M–O–M network			
$Co(HCOO)_2(HCONH_2)_2$	2-D square lattices of Co(II) metal ions linked by formate ligands. Hydrogen bonds between formate and formamide ligands link the sheets together forming a 3-D structure.	Long-range magnetic ordering below 9 K.	260
$(A)\cdot[M(II)M(III)(C_2O_4)_3]$ (A = ammonium cations, alkali-metal cations, or $Cp_2M(III)$; M(II) = divalent metal ion; M(III) = trivalent metal ion)	2-D honeycomb-like framework formed by the connection of metal ions through oxalates. Cationic molecules or ions are located into the 1-D channels.	Depending on M(II) and M(III), the near-neighbour exchange in all these compounds may be ferro- or antiferromagnetic, leading to long-range anti-, ferro- or ferrimagnetic behaviours. For more details see reference x.	261,262
$Mn_2(C_3H_2O_4)_2(4,4'\text{-bpy})\cdot H_2O_2$	2-D Mn–O–C–O–Mn layers pillared by 4,4′-bpy ligands, forming 1-D channels.	Presence of weak antiferromagnetic interactions.	263
$[Cu_3(C_3H_2O_4)_2(bpe)_3(H_2O)_2](NO_3)_2\cdot 2H_2O$	3-D framework that consists of Cu–O–C–O–Cu connected layers that are linked by bpe ligands as molecular pillars. The structure shows intersecting channels of 4.1 × 8.5 Å and 4.5 × 6.5 Å. Dehydration/rehydration process is observed.	Overall ferromagnetic interactions.	264
$[Cu_4(C_3H_2O_4)_4(bpe)_3]\cdot 6H_2O$	3-D structure made up of corrugated Cu–O–Cu and Cu–O–C–O–Cu layers linked through bpe molecules. 1-D channels filled with H_2O are present.	Overall ferromagnetic behaviour.	265
$[M_2(C_3H_2O_4)_2(H_2O)_2(hmt)]$ (M = Co, Cu, Mn)	3-D framework that consists of M–O–C–O–M layers linked by hmt ligands as molecular pillars. The dimensions of the 1-D channels are 2.2 × 5.2 Å.	Both compounds show the presence of antiferromagnetic interactions.	266
$[Co_3(C_4H_4O_4)_{2.5}(OH)]\cdot 0.5H_2O$	2-D layers formed by Co(II) ions connected *via* OH and succinate ligands. The layers are pillared by succinate ligands, forming an open-framework with hourglass-shaped 1-D channels.	Presence of strong antiferromagnetic interactions.	267
$Fe_5(OH)_2(C_4H_4O_4)_4$	3-D framework built up from 2-D layers of Fe–O–Fe type linkages (through OH and succinate ligands). The layers are stacked by succinate ligands, forming channels between the layers.	No magnetic measurements at low temperatures were performed.	268
$[Mn(C_4H_4O_4)(4,4'\text{-bpy})(H_2O)]\cdot 0.5(4,4'\text{-bpy})$	3-D framework formed by 2-D sheets of connected Mn(II) ions through succinates. The layers are sustained by 4,4′-bpy ligands to form channels filled by free 4,4′-bpy molecules.	Paramagnet with weak antiferromagnetic interactions.	269
$Co(C_5H_6O_4)$	3-D structure that consists of connected Co–O–C–O–Co layers stacked by the coordinated glutarate alkyl chain.	Predominant antiferromagnetic interactions below 14 K.	270
$[Co_2(C_{10}H_2O_8)(H_2O)_4]\cdot 2H_2O$	3-D framework made up from connected Co–O–C–O–Co layers linked by 1,2,4,5-benzenetetracarboxylate molecules. The structure shows 1-D channels filled by H_2O molecules.	Paramagnet with weak antiferromagnetic interactions.	271
$[Co_3(IDC)_2(4,4'\text{-bpy})_3]\cdot 6H_2O\cdot DMF$	3-D structure generated from 2-D connected Co–O–C–O–Co layers pillared by 4,4′-bpy. Hexagonal channels (12.6 × 11.6 Å, 39.3% accessible volume) filled with DMF and H_2O are found.	Presence of antiferromagnetic interactions.	272
1-D M–O–C–O–M/M–O–M network			
$M(HCOO)_2(4,4'\text{-bpy})\cdot 5H_2O$ (M = Co, Ni)	3-D $CdSO_4$-type framework formed by metallic bridged formate chains running along the *ac* direction that are interconnected *via* 4,4′-bpy molecules. This compound has large 1-D channels with a void volume of 27%.	The Co(II) compound is an antiferromagnet with T_N = 3.0 K, and the Ni(II) is a weak ferromagnet below 20 K.	273
$M(C_2O_4)(4,4'\text{-bpy})$ (M = Fe, Co, Ni)	2-D square grid framework formed by the linkage of oxalato-based Co(II) chains *via* 4,4′-bpy. The stacking of these layers creates rectangular 1-D channels.	Antiferromagnetic ordering with some canting features at transition temperatures of 12 K (Fe), 13 K (Co), and 26 K (Ni).	274,275
$[M_2(C_2O_4)_2(bpm)]\cdot xH_2O$ (M = Cu, Mn)	2-D hexagonal layers formed by the connection of oxalato-based metal chains *via* bpm molecules. Water molecules fill the 1-D channels.	Predominant antiferromagnetic interactions in both complexes.	276
$[Ni_7(C_4H_4O_4)_4(OH)_6(H_2O)_3]\cdot 7H_2O$ (MIL-73)	2-D framework formed by connected Ni–O–Ni chains linked by succinato ligands. The stacking of the layers creates three types of channels. Reversible dehydration (453 K)/hydration.	Behaves as a ferromagnet below 20 K.	277
$[M_3(CTC)_2(H_2O)_4]\cdot 5H_2O$ (M = Co, Ni)	The structure is formed by 1-D chains of H_2O-bridged Co(II) trimers connected through carboxylate groups. Each chain is connected one another by CTC units, forming a 3-D framework with channels along the three directions.	Competing anti- and ferromagnetic interactions are present in both compounds. In Ni(II) complex, long-range magnetic ordering may occur below 2 K.	278

Table 2 Magnetic channel-like coordination polymers based on connected *M–O–C–O–M* and/or *M–O–M* carboxylato-based networks[a] (*Continued*)

Compound	Structural description	Magnetic properties	Ref
$K[M_3(BTC)_3]\cdot 5H_2O$ (M = Fe, Co) MIL-45	3-D framework built up from the linkage of carboxylato-bridged Co(II) chains *via* BTC ligands. The structure shows 1-D channels filled with K^+ cations and H_2O molecules.	Both compounds exhibit ferromagnetic behaviour below 10 K for the Co phase and below 20 K for the mixed-metal Co–Fe phase.	279
$K[Co_3(BTC)(HBTC)_2]\cdot 5H_2O$	Carboxylato-bridged Co(II) chains linked by BTC ligands to form a 3-D framework with rectangular channels. The channels are filled with H_2O molecules. Reversible dehydration/rehydration process.	Paramagnet.	280
$Cu(isonicotinate)_2\cdot EtOH$	3-D framework formed by connected Cu–O–C–O–Cu chains *via* isonicotinate ligands. 1-D diamond-shaped channels filled with EtOH molecules are present.	Paramagnet with very weak antiferromagnetic interactions.	281
$Cu(isonicotinate)_2\cdot 2H_2O$	2-D layers formed by Cu–O–C–O–Cu chains linked by isonicotinate ligands. Stacking of the layers results in a 3-D structure with chessboard-like channels ($\sim$12.7 $\times$ 11.4 Å, accessible volume 23.3%, 318.6 Å of the unit cell volume). Dehydration without collapsing of the framework.	Paramagnet with very weak antiferromagnetic interactions.	282

[a] Abbreviations: 2,2′-bpy, 2,2′-bipyridine; trans[14]dien, 5,7,7,12,14,14-hexamethyl-1,4,8,11-tetraazacyclotetradeca-4,11-diene; ppz, piperazine; DMF, dimethylformamide; 4,4′-bpy, 4,4′-bipyridine; bpe, 1,2-bis(4-pyridyl)ethane; hmt, hexamethylenetetramine; IDC, imidazole 4,5-dicarboxylate; bpm, 2,2′-bipyrimidine; CTC, *cis*,*cis*-cyclohexane-1,3,5-tricarboxylate; BTC, 1,3,5-benzenetricarboxylate.

proved to be stable after removal of the cationic template and, thus, behave as porous materials. One exception is the compound $Na_2(N(CH_3)_3Ph)_5[Cr(C_2O_4)_3]_2Cl\cdot 5H_2O$ that maintains its structure after room-temperature cation exchange or partial thermal removal of the templates.[242]

The ability of metallic oxalates to adopt the anionic 2-D honeycomb channel-like network with a large variety of templates has been exploited by many researchers to generate

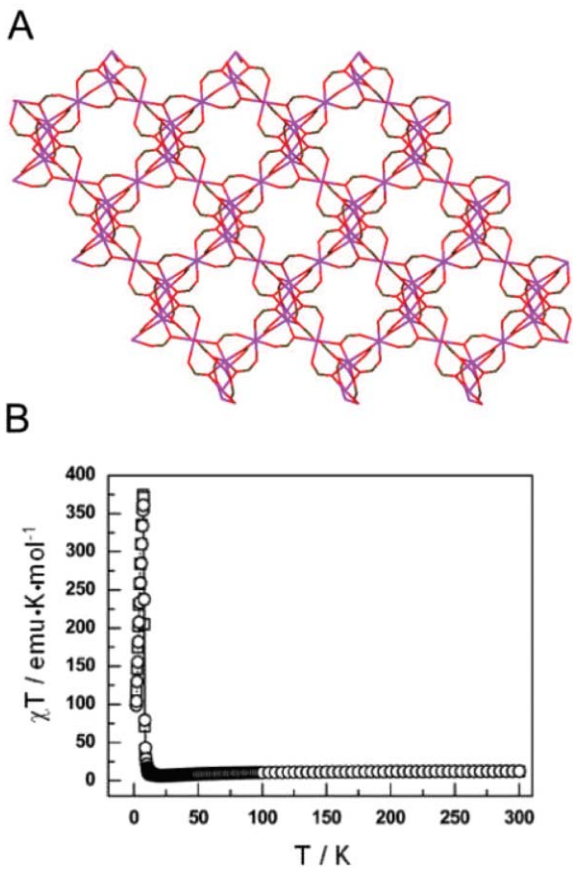

Fig. 17 (A). Structure of evacuated $[Mn_3(HCOO)_6]$ showing the 1-D channels. (Mn, purple; O, red; C, brown). (B) Temperature dependence of the χT product in an applied magnetic field of 100 Oe. Reprinted with permission of ref. 248. Copyright 2004, Royal Society of Chemistry.

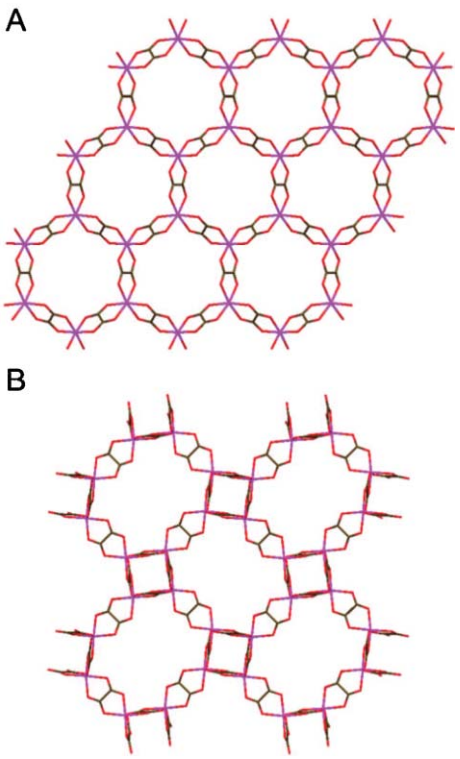

Fig. 18 Projection of the two representative templated lattices constructed from using oxalate ligands. (A) 2-D honeycomb framework of (A)·$[M(II)M(III)(C_2O_4)_3]$ (where A refers to ammonium cations, alkali-metal cations, or $Cp_2M(III)$). (B) Chiral (10,3)-network observed in $[M(II)_2(C_2O_4)_3]$, $[M(I)M(III)(C_2O_4)_3]$, and $[M(II)M(III)(C_2O_4)_3]$. (M, purple; O, red; C, brown. Cationic templates are omitted for clarity).

interesting multifunctional molecular materials. This strategy was successfully developed using the oxalate-based open-architecture as the magnetic component and the templating cations as the element that introduce the new functionality. For example, Coronado and co-workers were able to synthesize a series of magnetic conductors using this approach.[243] Perhaps the most well-known of these materials is $[BEDT\text{-}TTF]_3\cdot[MnCr(C_2O_4)_3]$ (where BEDT-TTF is bis(ethylenedithiol)tetrathiafulvalene), formed by alternating layers of the $[MnCr(C_2O_4)_3]$ as the anionic network and the BEDT-TTF molecules as the cationic templates.[244] This molecular material behaves as a ferromagnet below 5.5 K and is metallic down at least 0.2 K.

Other oxalate frameworks with different templates have reported. For example, the 3-D complex $[Fe_2(C_2O_4)_2(OH)Cl_2]\cdot EtNH_3\cdot 2H_2O$ possesses cages in where the cationic moieties and water guest solvent molecules are located.[253] Interestingly, this coordination polymer undergoes a solid–solid transformation accompanied of a color change when the crystals are exposed to the air. In this transformation, a proton transfers from the hydroxo bridge to a water molecule without collapsing the channel framework, thus forming a new compound with formula $[Fe_2(C_2O_4)_2(O)Cl_2]\cdot EtNH_3\cdot H_3O\cdot H_2O$. Magnetically, both phases behave as magnets through spin canting below 70 K. 2-D coordination polymers with a general formula of $[M(C_2O_4)(4,4'\text{-bpy})]_n$ (where 4,4′-bpy refers to 4,4′-bipyridine and M = Fe(II), Co(II) and Ni(II)) were reported by Li and co-workers in 1999.[274] These complexes are formed by the linkage of chains of metallic oxalates through 4,4′-bipyridine molecules and show robust open-frameworks with rectangular-shape channels with dimensions of 2 × 5 × 8 Å and stable up to 563–613 K. Furthermore, magnetic properties revealed a spontaneous antiferromagnetic (with certain canting structures) magnetic ordering with transition temperatures of 12 K [Fe(II)], 13 K [Co(II)] and 26 K [Ni(II)], attributed to the strong exchange interactions between the 1-D bridged metal ions through oxalate organic ligands and weaker interchain magnetic interactions. Also, an antiferromagnetic behaviour in $[Co_7(C_2O_4)_3(OH)_8(ppz)]$ (where ppz refers to piperazine) and helical tunnels with dimensions of 21.2 × 9.3 Å in $K[Cu(trans[14]dien)][Cr(C_2O_4)_3]$ (where trans[14]dien is 5,7,7,12,14,14-hexamethyl-1,4,8,11-tetraazacyclotetradeca-4,-11-diene) have been reported.[254,255] In this last polymer, the Cu complexes coordinated to the framework are located into the channels. Recently, rare-earth metal ions have also been introduced in the formation of magnetic oxalate-based open-frameworks. Thus far, $K_2MnU(C_2O_4)_4\cdot 9H_2O$, a uranate compound that exhibits a diamond-like topology with 1-D square-shaped channels, has been described, but shows very weak antiferromagnetic interactions.[256]

Many metal channel-like magnetic complexes synthesized using malonate, succinate and glutarate ligands have been reported. In most of these, a 3-D framework is formed by 2-D carboxylato-based layers pillared by difunctional ligands.[263–270] This topology usually defines 1-D channels running parallel to the layers. However, from a magnetic point of view, they rarely show long-range ordering. An exception to this topology was found in the malonate complex $[Cu(C_3H_2O_4)(DMF)]$.[257] This solid shows a 3-D chiral diamond-like open-framework formed by Cu(II) ions connected through malonate ligands. Furthermore, this complex behaves as a ferromagnet below 2.6 K. A similar pillared framework was observed in a imidazole 4,5-dicarboxylate metal complex.[272]

Especially attractive from a magnetic point of view are the open-frameworks involving infinite M–O–M type linkages. Forster and Cheetham have described a nickel succinate $[Ni_7(C_4H_4O_4)_6(OH)_2(H_2O)_2]\cdot 2H_2O$ with infinite Ni–O–Ni connectivity, exhibiting 1-D hydrophobic channels composed of wide cavities of dimensions of 8 Å and narrow apertures of 4 Å (Fig. 19(A) and (B)).[258] This material exhibits a high thermal stability up to 673 K and may be magnetically frustrated. Similarly, nickel glutarate $[Ni_{20}(C_5H_6O_4)_{20}(H_2O)_8]\cdot 40H_2O$ reported by Guillou *et al*. shows an infinite Ni–O–Ni connectivity with very large intersecting 20-membered ring channels and a pure ferromagnetic ordering at 4 K (Fig. 19(C) and (D)).[259] The porosity characteristics of this material are fascinating. This compound can be dehydrated at 423 K and slowly rehydrated under air at room temperature. Furthermore, a sample activated at 473 K shows a surface area of 346 $m^2\ g^{-1}$. Also, a open-framework ferrimagnet with 1-D connected Ni–O–Ni chains showing a reversible dehydration/hydration process has been described.[277]

2.3.2 Networks based on organo-polymetallic clusters. Discrete di-, tri-, tetranuclear and higher nuclearity organo-polymetal clusters such as the carboxylate-based paddle-wheel copper acetate and trimeric zinc or iron acetates are suitable building blocks (commonly called secondary building blocks, SBUs) for polymerization reactions involving polytopic ligands.[283] Such clusters are spaced in defined geometries depending on their own geometry and the geometry of the polytopic ligands. As a result, extended porous structures with high porosity and predictable structures are typically obtained. Using a cluster with an inherent property, one can then imagine distributing these SBUs in a desired way along the three dimensions, and create porous solids with novel functionalities. For example, catalytic clusters may be included in the skeleton of a porous structure, increasing the accessibility for these units and, therefore, enhancing their catalytic properties. From a magnetic point of view, the assembly of clusters also provides an excellent route to magnetic porous solids. The advantages of this strategy are obvious, since bigger pores can be obtained from the big cluster linkers and the functional framework inherits the interesting physical properties from the clusters.

In 1999, Williams and co-workers reported for the first time the magnetic properties of a porous structure based on the connectivity of paddle-wheel Cu(II) dimers through 1,3,5-benzenetricarboxylate ligands (Fig. 20(A)), the $[Cu_3(C_9O_6H_3)_2(H_2O)_3]$ complex (referred to as KHUST-1).[284] From this connectivity, a 3-D network of channels with fourfold symmetry and dimensions of 9 × 9 Å and stable up to 513 K is created (Fig. 20(A)). Water molecules that fill the channels can be easily removed at a temperature of 373 K without a loss of structural integrity. Resulting voids give a surface area of 917.6 $m^2\ g^{-1}$, a calculated density of 1.22 $g\ m^{-3}$

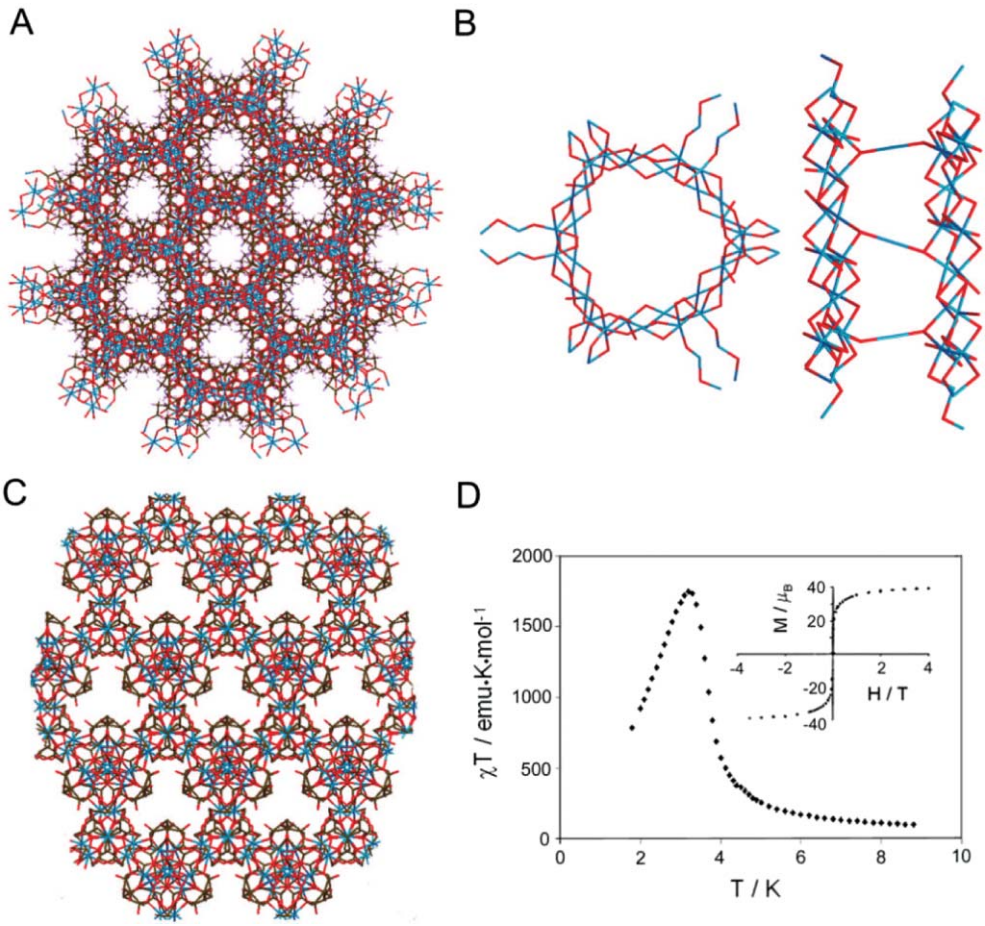

Fig. 19 (A) View of the channels of the nickel succinate $[Ni_7(C_4H_4O_4)_6(OH)_2(H_2O)_2]\cdot 2H_2O$. (B) Views of the 3-D Ni–O–Ni connectivity of this nickel succinate along two different directions. (C) View of the crystal structure of $[Ni_{20}(C_5H_6O_4)_{20}(H_2O)_8]\cdot 40H_2O$ showing the tunnels. (D) Thermal dependence of the χT product. The inset shows the magnetizations versus the applied magnetic field at 2 K, showing a fast saturation typical of a pure cooperative ferromagnet. (In (A), (B) and (C), Ni, blue; O, red; C, brown; H, white. Solvent guest molecules are omitted for clarity). (Reprinted with permission of ref. 259. Copyright 2003, Wiley Interscience.)

and an accessible porosity of nearly 41% of the total volume cell. Interestingly, additional experiments of the anhydrate KHUST-1 showed that it is possible to induce chemical functionalization without losing the overall structural information. Furthermore, the structural porosity of KHUST-1 is accompanied by interesting magnetic properties.[285] As shown in Fig. 20(B), this porous coordination polymer shows a minimum in its χ *vs.* T plot at around 70 K and an increase at lower temperatures. Fitting high-temperature data to the Curie–Weiss law gave a Weiss constant of 4.7 K. This magnetic behaviour can be explained by the presence of strong antiferromagnetic interactions within a Cu(II) dimer and weak ferromagnetic interactions between Cu(II) dimers.

Other magnetic porous solids have been prepared using the paddle-wheel Cu(II) dimer as SBUs.[286–290] Fig. 21(A) shows a molecular porous Kagomé lattice obtained by Zaworotko and co-workers.[286] In this case, the authors proposed the use of such building blocks as molecular squares linked by 1,3-benzenedicarboxylic ligands ($C_8O_4H_4$), that is, at 120°, to generate two porous frameworks, according to the self-assembly of two different SBUs: a triangular SBU, formed by three connected paddle-wheel Cu(II) dimers, or a square SBU, formed by four connected paddle-wheel Cu(II) dimers. The first of such structures was: $(Cu_2(py)_2(C_8O_4H_4)_2)_3$, generated from the self-assembly of the Cu(II) dimers with a bowl-shaped triangular topology to yield a Kagomé lattice with hexagonal channels and dimensions of 9.1 Å. The second structure $(Cu_2(py)_2(C_8O_4H_4)_2)_4$,[287] was generated from the self-assembly of Cu(II) dimers with a bowl-shaped square topology to lead a 2-D network with channels formed by narrowed windows (1.5 × 1.5 Å) and large cavities with maximum dimensions of about 9.0 × 9.0 × 6.5 Å. As for KHUST-1, the Kagomé lattice shows a high rigidity in the absence of solvent guest molecules and pyridine ligands, which can be removed at a temperature of 473 K without the loss of the crystalline character. From a magnetic point of view, its most interesting feature is the report of remnant magnetization even at room temperature due to the magnetic spin frustration associated to its triangular lattice,[288] although this result seems to be controversial according to the molecular character of this material (Fig. 21(B)). In contrast, the 2-D framework with a square-like arrangement of the dimeric units does not present any remnant magnetization due to the lack of any geometrical frustration. In such a context, its magnetic behaviour is very

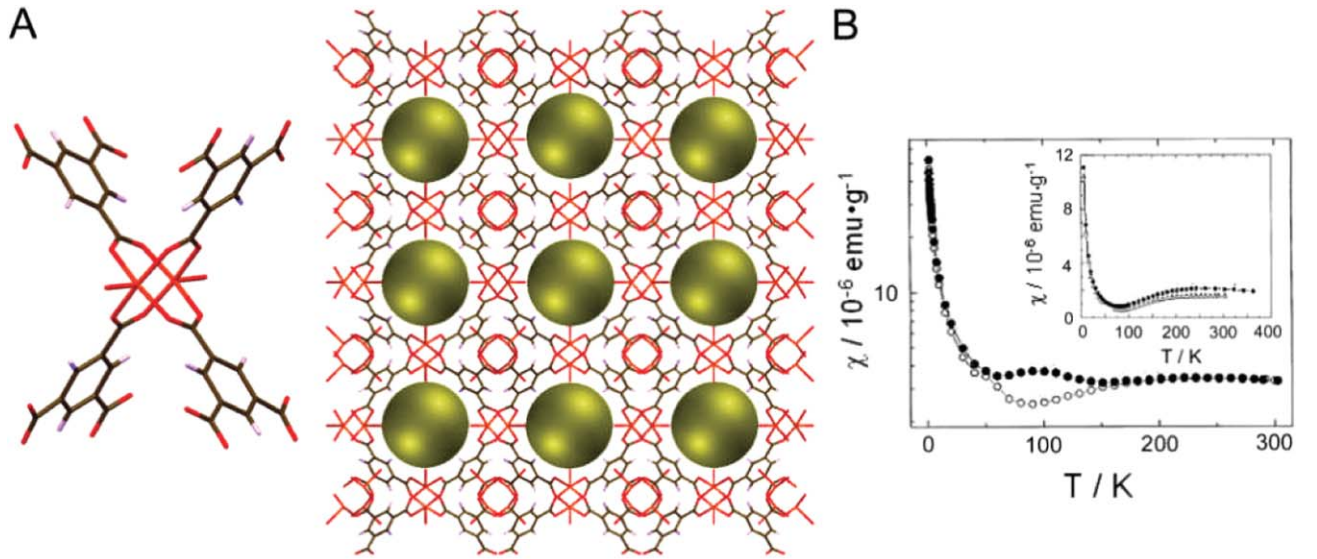

Fig. 20 (A) Paddle-wheel copper(II) tetracarboxylate building block for $[Cu_3(C_9O_6H_3)_2(H_2O)_3]$ and view of the open-framework showing nanochannels with fourfold symmetry. The empty space is represented as yellow spheres. (Cu, orange; O, red; C, brown; H, white). (B) Zero-field cooled (○) and field-cooled (●) temperature dependent magnetic susceptibility. Inset shows the temperature dependent magnetic susceptibility. (Reprinted with permission of ref. 285. Copyright 2000, American Institute of Physics.)

similar to that observed for KHUST-1, with an intradimer antiferromagnetic interaction of -380 cm^{-1} and interdimer interactions of -85 cm^{-1}.

Similarly, strong intradimer interactions up to -444 cm^{-1} were observed for another porous metal–organic coordination framework made again from paddle-wheel Cu(II) dimers building blocks linked by 1,3,5,7-adamantane tetracarboxylate ligands.[289] The resulting typical inorganic platinum sulfide-based topology shows a high porosity with a surface area of 560 m^2 g^{-1} in its dehydrated form. Finally, the same structural unit has been linked *via* 1,2,4,5-benzenetetracarboxylate ligands to form a 2-D coordination structure with rectangular pores of 6 × 7 Å and antiferromagnetic interactions.[290]

Channel-like magnetic frameworks built up from the spacing of dimers other than the paddle-wheel dimer can also be found. To date, coordination polymers composed of nitrogen-bridge,[291] oxo-bridge,[269,290,292] carboxylato-bridge,[290,293] and mixed oxo/carboxylato-bridge dimers[294] have been reported. For example, Liu *et al*. reported a family of complexes formed by dicobalt(II) building blocks linked through nicotinate ligands that shows robust open-framework structures up to 295 °C with antiferromagnetic couplings within the cobalt dimers.[294]

Besides these dimeric building blocks, a series of higher nuclearity clusters have been spaced by polytopic ligands.[295–297] An example of a trimeric structural unit was described by Barthelet *et al*.[296] $[V(III)(H_2O)]_3O(C_8O_4H_4)_3(Cl{\cdot}9H_2O)$ exhibits a 3-D framework built up from octahedral vanadium trimers joined *via* the isophthalate anionic linkers to delimit cages where water molecules and chlorine atoms are occluded. Although the trimeric clusters are connected along three directions, the 120° triangular topology of V(III) ions in each cluster induces a spin-frustration of their magnetic moments and therefore, a lowering of the temperature for magnetic ordering. More recently, Wu and co-workers have reported a very interesting porous solid constructed from tetranuclear Co(II) citrate clusters as octahedral linkers and Co(II) ions as trigonal nodes.[297] This connectivity shows an anatase topology with channels of 9.5 × 4.3 Å along two directions, leading to an apparent Langmuir surface area of 939 m^2 g^{-1} with pore volume of 0.31 cm^3 g^{-1}. From a magnetic point of view, this material behaves as a 3-D canted antiferromagnet with a magnetic hysteresis loop observed at 2 K.

2.3.3 Networks based on isolated metal ions. A variety of open-framework solids prepared using carboxylic acid ligands composed of a phenyl or cyclohexane backbone with two or more carboxylate functional groups are known.[298] However, even though the magnetic properties of many of them are not described, the magnetic exchange interactions between metal ions are expected to be weaker in comparison with the complexes described so far. For example, two complexes formed by Ni(II) macrocycles linked by 1,3,5-benzenetricarboxylate ligands show structures with large channels (~11 Å), but they only behave as paramagnets with very weak antiferromagnetic interactions at low temperatures.[299] Similarly, other coordination polymers prepared using 1,3,5-benzenetricarboxylate[291,300] and 1,2,4,5-benzenetetracarboxylate[301] ligands exhibit comparable weak interactions.

Although carboxylic ligands have been more extensively used, the use of polytopic nitrogen-based ligands has also generated some examples of magnetic open-framework structures.[302–304] For instance, Kepert and co-workers recently reported a nanoporous spin crossover coordination material based on the use of the *trans*-4,4′-azopyridine (azpy) as a ditopic ligand.[303] The crystal structure of the resulting complex $[Fe_2(azpy)_4(NCS)_4]{\cdot}EtOH$ consists of double interpenetrated 2-D grid layers built up by the linkage of Fe(II) ions by azpy ligands. As a result, two types of 1-D channels running in the same direction, filled with ethanol molecules and exhibiting

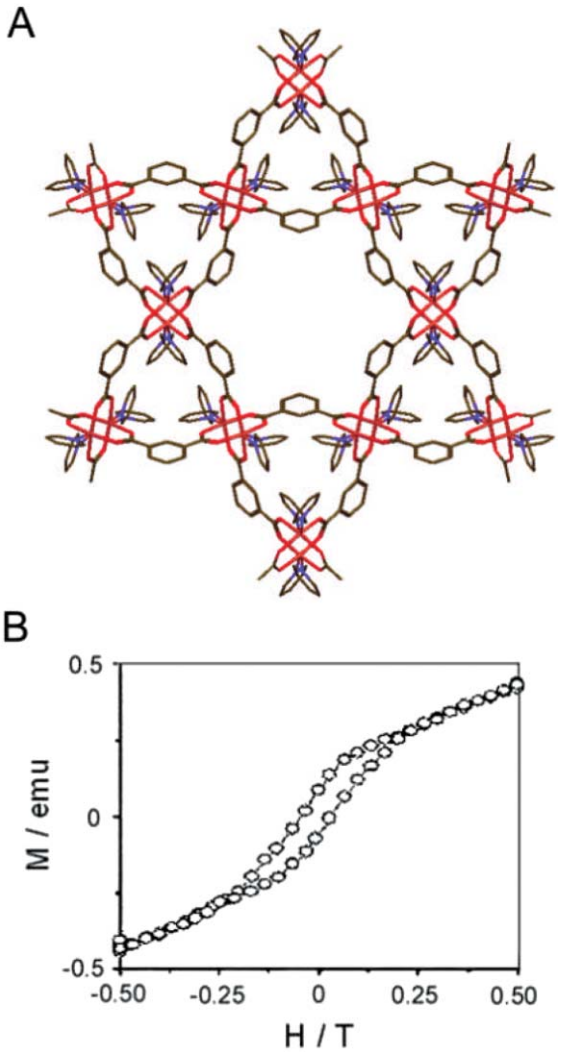

Fig. 21 (A) Kagomé-type 2-D lattice of $[(Cu_2(py)_2(C_8O_4H_4)_2)_3]$, showing the hexagonal channels. Solvent guest molecules are omitted for clarity. (Cu, orange; O, red; C, brown; N, blue). (B) Magnetic hysteresis at 5 K. (Reprinted with permission of ref. 286. Copyright 2002, Wiley Interscience.)

openings of 10.6 × 4.8 Å and 7.0 × 2.1 Å, are created. The evacuation of ethanol guest molecules takes place at 373 K and is accompanied by several reversible structural changes (for more details, see section 6). The as-synthesized sample exhibits a constant effective magnetic moment of 5.3 μ_B between 300 and 150 K. Below this temperature, the magnetic moment decreases reaching a constant value of 3.65 μ_B due to a spin-crossover interconversion coming from a fraction of the Fe(II) ions existing in the material. On the contrary, the evacuated sample does not show a spin-crossover behaviour exhibiting a constant magnetic moment around 5.1 μ_B, corresponding to two crystallographic high-spin Fe(II) ions.

Structural versatility of coordination polymers to obtain magnetic porous molecular materials was once again demonstrated by Gao, You and co-workers, who reported a family of Co(II) imidazolates (im) complexes showing a variety of open-framework structures with different magnetic behaviours.[304] In this case, the rational use of solvents and counter-ligands plays a key role to obtain a collection of polymorphic 3-D porous Co(II) structures: $[Co(im)_2]\cdot 0.5py$, $[Co(im)_2]\cdot 0.5Ch$, $[Co(im)_2]_2$, $[Co(im)_2]_4$, and $[Co_5(im)_{10}\cdot 0.4Mb]_5$ (where py, Ch and Mb refer to pyridine, cyclohexanol and 3-methyl-1-butanol, respectively). Complexes $[Co(im)_2]\cdot 0.5py$ and $[Co(im)_2]\cdot 0.5Ch$ are isostructural and formed by Co(II) centers linked into boat- and chairlike 6-membered rings connected in an infinite diamond-like net. This conformation originates 1-D channels of dimensions 5.3 × 10.4 Å and 6.6 × 8.4 Å, respectively (Fig. 22(A)). The influence of the reaction solvent and structure-directing agents was evident in the other three Co(II) imidazolate coordination polymers. The crystal structure of $[Co(im)_2]_4$ is formed by the self-assembly of 4-membered ring Co(II) units, which are doubly connected to wavelike or double crankshaft-like chains. These chains intersect with those running along the perpendicular axis by means of the common 4-rings at the wave peaks. Three of such frameworks are interwoven and linked by the imidazolates at the Co(II) ions. Fig. 22(B) shows the resulting 3-D framework with 1-D helical channels of 3.5 × 3.5 Å dimensions. Similarly, complex $[Co(im)_2]_2$ is formed by the self-assembly of identical units connected into chain units. These chains are linked to each other by the imidazolate ligands along the other two directions to give a 3-D framework with a pore opening of 4.0 × 4.0 Å (Fig. 22(C)). The fact that both structures crystallize in the absence of solvent guest molecules give them a highly structural rigidity up to 773 K. Of special structural interest is the complex $[Co_5(im)_{10}\cdot 0.4Mb]_5$, which shows an open structure with zeolitic topology (Fig. 22(D)). In all polymorphous frameworks, the imidazolates transmit the antiferromagnetic coupling between the Co(II) ions. However, the uncompensated antiferromagnetic couplings arising from the particular stoichiometries and topologies leads to spin-canting phenomena that are sensitive to the structural characteristics: compound $[Co(im)_2]\cdot 0.5py$ is an antiferromagnet with T_N = 13.1 K; $[Co(im)_2\cdot]0.5Ch$ shows a very weak ferromagnetism below 15 K (Fig. 22(E)), $[Co(im)_2]_4$ exhibits a relatively strong ferromagnetism below 11.5 K and a coercive field (H_C) of 1800 Oe at 1.8 K, and $[Co(im)_2]_2$ displays the strongest ferromagnetism of the three cobalt imidazolates and demonstrates a T_C of 15.5 K with a coercive field, H_C, of 7300 Oe at 1.8 K (Fig. 22(F)). However, compound $[Co_5(im)_{10}\cdot 0.4MB]_5$ seems to be a hidden canted antiferromagnet with a magnetic ordering temperature of 10.6 K.

In the literature there has also been described some examples of coordination polymeric architectures made by the simultaneous linkage of paramagnetic metal ions through mixed carboxylic and N-based ligands.[305–308] The most successful family is a series of polymers built up from the linkage of metallic carboxylate chains through 4,4′-bipyridine ligands. $[Cu(C_4H_4O_4)(4,4'\text{-bpy})(H_2O)_2]\cdot 2H_2O$ is formed by the connection of chains of Cu(II) metal ions bridged by succinate ligands through 4,4′-bipyridine molecules.[306] This 3-D framework shows channels in which the water molecules are located and weak ferromagnetic interactions. The connectivity in $[Fe(C_4O_4)(4,4'\text{-bpy})(H_2O)_2]\cdot 3H_2O$ is almost identical.[307] Chains of Fe(II) metal ions bridged by squarate ligands are connected through 4,4′-bipyridines and forms a framework with 1-D channels filled with water molecules that shows ferromagnetic couplings. The dehydration/rehydration process in this complex (and other isostructural polymers with other

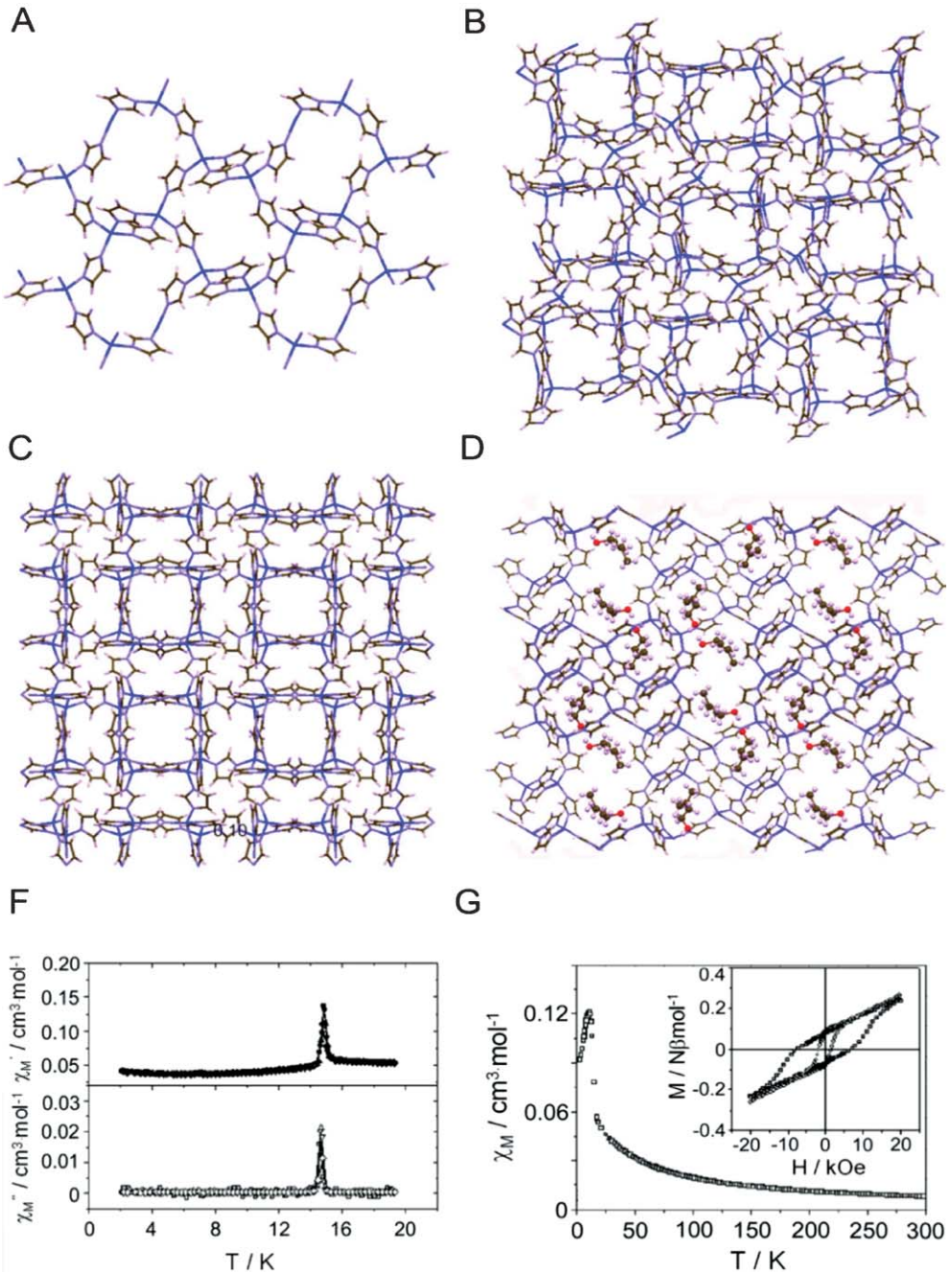

Fig. 22 Views and magnetic properties of the open-framework cobalt imidazolate structures. (A) Evacuated $[Co(im)_2]\cdot 0.5Ch$ (where Ch is cyclohexanol). (B) $[Co(im)_2]_4$. (C) $[Co(im)_2]_2$. (D) $[Co_5(im)_{10}\cdot 0.4Mb]_5$ (where Mb is 3-methyl-1-butanol). (E) Plots of temperature dependence of ac susceptibility obtained at 0.1 Oe field for $[Co(im)_2]\cdot 0.5Ch$. A peak appears at 15 K, which is indicative of the ferromagnetic character of this compound. (F) Plot of the thermal evolution of the χ_M for $[Co(im)_2]_2$ at 10 kOe field. The inset shows the hysteresis loop at 1.8 K (□) and 5.0 K (○). (Co, blue; O, red; C, brown; N, violet; H, white. Solvent guest molecules in (D) are represented as spheres). (Reprinted with permission of ref. 304. Copyright 2003, Wiley Interscience.)

metal ions) is fully reversible and accompanied with a continuous change of the colour.[308]

In all these previous examples described in this section, it can be noted that when the distance between metal ions increases, the magnetic coupling between them starts to decrease. Therefore, and since the obtaining of bigger pore sizes in coordination polymers is usually achieved by using longer organic spacers,[31] the preparation of porous materials with increasing pore size dimensions and simultaneous long-range magnetic properties is still a challenge. One strategy to overcome this has been proposed by Veciana and co-workers. This strategy is based on the combination of persistent polyfunctionalized organic radicals as polytopic ligands and magnetically active transition-metal ions. The resulting structures are expected to exhibit larger magnetic couplings and dimensionalities in comparison with systems made up from

diamagnetic polytopic coordinating ligands since the organic radical may act as a magnetic relay.[309,310] Thus, by using a persistent polytopic organic radical, such as the polychlorinated triphenylmethyl tricarboxylic acid radical ($C_{22}O_6Cl_{12}$, PTMTC),[311] a series of metal–organic radical open-framework (MOROF-*n*) have been prepared. Interestingly, the crystal structure of $Cu_3(PTMTC)_2(py)_6(EtOH)_2(H_2O)$ (MOROF-1) reveals a 2-D honeycomb (6,3) network with very large 1-D hexagonal nanopores, each composed of a ring of six metal units and six PTMTC radicals, which measure 3.1 and 2.8 nm between opposite vertices.[312] Furthermore, the long through-space distances (15 Å within the layers and 9 Å between them) between paramagnetic Cu(II) ions in MOROF-1 do not prevent a long-range magnetic ordering. Each open-shell PTMTC ligand is able to magnetically bridge three Cu(II) ions and, therefore, to extend the magnetic interactions across the infinite layers, giving a ferrimagnet behaviour with an overall magnetic ordering at low temperatures ($\sim$2 K) (see also section 6, Fig. 30(A)).

More recently, using the same paramagnetic PTMTC ligand, two new supramolecular Co(II)-based metal–organic radical open-framework, $[Co(PTMTC)(4,4'\text{-bpy})(H_2O)_3]\cdot 6EtOH\cdot 2H_2O$ (MOROF-2) and $Co_6(PTMTC)_4(py)_{17}(H_2O)_4(EtOH)$ (MOROF-3), have been reported.[313,314] The first compound shows an unprecedented $(6^3)\cdot(6^8.8^1)$ topology. Additionally, MOROF-2 exhibits helical nanochannels of dimensions 13.2 × 9.4 Å, along with antiferromagnetic interactions. The second complex exhibits a (6,3)-helical network with large 17.5 × 6.8 Å 1-D channels and a bulk magnetic ordering below 1.8 K. Other radical-based complexes exhibiting channel-like structure have been recently described.[315] For example, the molecular packing of discrete $[CuX_2(4PMNN)]_6$ units (where X refers to Br or Cl, and 4PMMM is 4-pyrimidinyl nitronyl nitroxide) exhibits 1-D honeycomb-like channels with dimensions of 11.5 Å. The magnetic properties of this compound show the coexistence of ferro- and antiferromagnetic interactions.

2.4 Pure organic open-frameworks

Purely organic magnetic open-framework materials are very scarce due to the complexity of their design and synthesis. The main limitation comes from the selection of a suitable organic radical, *i.e.*, a pure organic open shell building block or constitutive unit. First, organic radicals must be both thermally and chemically stable. Second, these radicals must be substituted with suitable functional groups to provide robust linkages between themselves. And last but not least, these radicals should exhibit a large volume and rigidity to prevent interpenetration. Even though to date different families of these radicals have been reported, such as nitroxide, nitronyl nitroxide, verdazyl and thiazyl, to our knowledge, only two purely organic magnetic open-frameworks based on polychlorotriphenylmethyl radicals are so far known. Both magnetic porous solids reported by Veciana and co-workers are based on the use of PTM radicals, previously discovered by Ballester,[316] and functionalized with carboxylic groups as organic tectons (Chart 1).[311,317,318] The advantages of these radicals are considerable: (i) they exhibit a high thermal and chemical stability; (ii) their trigonal symmetry provides a typical template for getting channels held together by hydrogen bonds through the carboxylic groups; (iii) the molecular bulkiness and rigidity of PTM radicals is expected to prevent close packing of molecular units; and (iv) besides their structural control, hydrogen bonds have been shown to favor magnetic exchange interactions between bound organic radical molecules.[319]

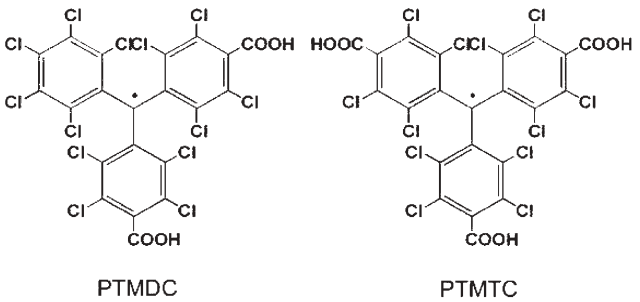

Chart 1 Polycarboxylic polychlorotriphenylmethyl (PTM) radicals.

These expectations were fully confirmed on the H-bonded self-assembly of the dicarboxylic PTMDC radical by the formation of a robust porous 2-D extended network (POROF-1, where POROF refers to as pure organic radical open-framework) with weak antiferromagnetic interactions.[317] The framework shows 1-D tunnels formed by narrowed polar windows ($\sim$5 Å in diameter) and larger hydrophobic cavities, where a sphere 10 Å in diameter can fit inside them. The combination of supercages and windows gives way to solvent-accessible voids in the crystal structure that amount up to 31% (5031 $Å^3$ per unit cell) of the total volume (16158 $Å^3$). Furthermore, it is remarkable that the structural rigidity of the framework permits evacuation of the guest *n*-hexane solvent molecules at 373 K without collapsing the packed molecules.

More recently, the crystal packing of PTMTC molecules has formed a second robust porous 2-D H-bonded magnet (POROF-2).[318] As shown in Fig. 23(A), the stacking of these H-bonded layers generates a 3-D structure that exhibits tubular highly hydrophilic channels, where a sphere of 5.2 Å in diameter can fit inside them and with solvent-accessible voids that amount up to 15% (450 $Å^3$ per unit cell) of the total cell volume. The lack of guest solvent molecules within the channels and the structural rigidity up to 573 K are excellent conditions to use this purely organic material as a new porous solid. No less remarkable are the magnetic properties of this compound, which orders ferromagnetically at very low temperatures (Fig. 23(B)).

3 Chiral open-frameworks

Of special interest for the design of porous materials has been the search for stable chiral networks due to their promising applications ranging from enantioselective sorption and separations to catalysis.[320–322] As a result of such interest, to date, several chiral porous solids have been reported, most of them summarized in Table 3. For their synthesis, three different approaches have been utilized. First, chiral open-frameworks can be built from achiral components.[325–332]

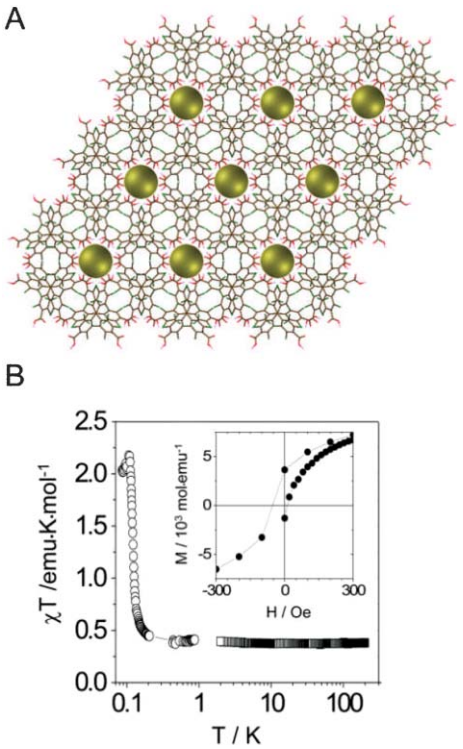

Fig. 23 (A) Crystal packing of POROF-2, showing the tubular H-bonded channels. The empty space is represented as yellow spheres. (O, red; C, brown; Cl, green; H, white). (B) Logarithmic dependence of χT function on the temperature up to 200 K, measured with an applied magnetic field of 200 Oe. The inset shows the magnetic hysteresis at 0.08 K.

However, examples of homochiral porous solids synthesized following this approach are scarce because bulk samples tend to contain a mixture of both enantiomeric crystalline forms, so the enantiopure crystals must be almost manually separated. A second approach is based on the use of an enantiopure co-ligand or template for directing the formation of homochiral porous networks.[333–335] An excellent example obtained following this approach was reported by Rosseinsky and co-workers.[323,334,335] $[Ni_3(BTC)_2(py)_6(1,2\text{-pd})_3]\cdot 11(1,2\text{-pd})\cdot 8H_2O$ (where BTC, py and 1,2-pd refer to 1,3,5-benzenetricarboxylate, pyridine and 1,2-propanediol, respectively) shows a doubly interpenetrated (10,3)-a network generated by using the diol molecules as a chiral template. The framework exhibits 1-D chiral pores with dimensions of 10.6 × 16 Å and a solvent accessible volume of 51% of the total volume cell. Interestingly, although the obtained material upon guest loss is amorphous and nonporous, it is able to react to small molecules that coordinate to the metal center. For example, reaction with EtOH leads to formation of the fourth interpenetrated (10,3)-a phase, whereas exposure to pyridine and 3-picoline leads to the layered (6,3) phase and the doubly interpenetrated (10,3)-a chiral phase, respectively.[324] This latter compound, with composition $[Ni_3(BTC)_2(3\text{-pic})_6(1,2\text{-pd})_3]\cdot 9(1,2\text{-pd})\cdot 11H_2O$, can be desolvated without destroying the framework, leading to a microporous chiral solid with surface area of 930 $m^3\ g^{-1}$ (Fig. 24). This material has been shown to enantioselectively adsorb 1,1′-bi-2-naphthol at a modest capacity of 7.3 wt% and with an enantio-enrichment (ee) value of 8.3%.

The third and most reliable approach to create homochiral porous solids is based on the use of enantiomerically pure polytopic ligands as linkers of the metal ions. Two of the first homochiral porous coordination solids with a general formula of $[Zn_3O(L_2)_6]\cdot 2H_3O\cdot 12H_2O$ (D- and D-POST-1, where L_2 refers to 2,2-dimethyl-5-[(4-pyridinylamino)carbonyl]-1,3-dioxolane-4-carboxylic acid), were described by Kim and co-workers early in 2000.[336] Such porous coordination systems are built up from oxo-bridged trinuclear zinc carboxylate building-blocks connected through the rigid chiral polytopic organic molecules. Fig. 25(A) shows the channels that have the form of equilateral triangles with dimensions of 13.4 Å and a solvent-accessible volume of 47% of the crystal volume. Furthermore, this compound revealed enantioselective catalytic activity (8% ee) for the *trans*-esterification reaction between (2,4-dinitrophenyl)acetate molecule and a racemic mixture of the chiral alcohol 1-phenyl-2-propanol (Fig. 25(B)).

This approach has been enormously popularized and developed by Lin and co-workers with the preparation of numerous examples of homochiral metal–organic porous solids by using enantiopure diphosphonate,[337–343] dicarboxylate,[344–347] and dinitrogen-donor[348–350] ligands based on 1,1′-binaphthyl framework (see Table 3). Some of these solids have shown a significant chiral separation and asymmetric catalysis. For example, the Gd compound of a series of homochiral porous lamellar lanthanide bisphosphonates with a general formula of $[M(L_3\text{-}H_2)(L_3\text{-}H_3)(H_2O)_4]\cdot xH_2O$ (where M refers to La, Ce, Pr, Nd, Sm, Gd, Tb, L_3-H_4 is 2,2′-diethoxy-1,1′-binaphthalene-6,6′-bisphosphonic acid, and x = 9–14) was used for bulk chiral separation of *trans*-1,2-cyclohexanediamine with a modest ee up to 13.6%.[338] Chiral separation of racemic 2-butanol and 2-methyl-1-butanol was also studied with an homochiral porous solid with formula $[Cd(QA)_2]$ (where QA refers to 6′-methoxyl-(8*S*,9*R*)-cinchonan-9-ol-3-carboxylic acid) reported by Xiong and co-workers.[351] This diamond-like structure showed that a crystalline sample of (*S*)-2-butanol·$[Cd(QA)_2]$ was obtained when a racemic 2-butanol and a powdered sample of $[Cd(QA)_2]$ were mixed under solvothermal reaction conditions. The optical rotation of the desorbed 2-butanol guest molecules indicated that (*S*)-2-butanol was separated with an ee value up to 98.2%. Similarly, (*S*)-2-methyl-1-butanol was separated with $[Cd(QA)_2]$ at an ee value of about 8.4%.

In the field of asymmetric catalysis, Lin's group have designed a brilliant synthetic strategy to generate enantioselective heterogeneous catalysts. This approach combines the robustness of metal phosphonate frameworks with the enantioselectivity of the metal complexes bearing pendant chiral bisphosphines. Following this approach, a series of ruthenium-containing zirconium phosphonates have shown highly enantioselective heterogeneous asymmetric hydrogenation of β-keto esters and aromatic ketones at up to 95% ee and 99.2% ee, respectively.[340,341] Similarly, zirconium phosphonates in combination with $Ti(O^iPr)_4$ have shown applications in asymmetric diethylzinc additions to a wide range of aromatic aldehydes with high conversions and ee of up to 72%.[343]

Table 3 Chiral open-framework solids[a]

Compound	Structure and porosity/chirality characteristics	Ref
$NaZnPO_4 \cdot H_2O$-I and -II	Zincophosphate framework with a tetrahedral topology that shows pear-shaped 12-ring membered channels interconnected through 8-rings and 6-rings, in which the Na^+ ions and H_2O molecules are located. Bulk sample contains both enantiomorphs.	325
$[Sn_4P_3O_{12}][CN_3H_6]$	Puckered layers of 6-membered ($Sn_3P_3O_6$) and 12-membered ($Sn_6P_6O_{12}$) rings are stacked together to form a framework that shows 12-membered ring channels (8.3 × 6.7 Å) filled with the guanidinium cations. Bulk sample contains both enantiomorphs.	326
$Zn_3(C_6H_{14}N_2)_3[B_6P_{12}O_{39}(OH)_{12}][HPO_4] \cdot C_6H_{14}N_2$	Zinc borophosphate framework with a NbO type structure. The framework shows an intersecting 3-D channel system.	327
$[Ag(hat)ClO_4] \cdot 2CH_3NO_2$	3-D (10,3)-a type framework with 1-D chiral channels (48% solvent-accessible volume of the crystal volume). The compound shows solvent exchange characteristics. Bulk sample contains both enantiomorphs.	328
$[Ni(4,4'\text{-bpy})(C_7H_5O_2)_2(MeOH)_2]$	Framework with large chiral cavities (24–28% solvent-accessible volume of the crystal volume) formed by the packing of 1-D helical polymers that consist of Ni(II) ions bridged by 4,4′-bpy ligands. Desolvation does not affect the framework. Bulk sample contains both enantiomorphs.	329
$[Ag(bpyz)](BF_4)$	3-D adamantoid coordination network with square-shaped channels (4.9 Å) and rhomboid-shaped channels (3.5 Å, totally 45.2% solvent-accessible volume of the crystal volume), filled with BF_4 anions and $MeNO_2$ molecules.	330
$[Zn(DPT)_2(H_2O)_2][Zn(DPT)_2(CH_3CN)]ClO_4 \cdot 2CH_3CN$	3-D framework formed by the interpenetration of two different 3-D coordination polymers with opposite handedness. The cavities are filled with ClO_4 anions and CH_3CN solvent molecules.	331
$[Cu(L_1)(H_2O)(SO_4)] \cdot 2H_2O$	2-D layers composed of Cu(II) ions bridged by sulfate groups. Layers are connected through L_1 ligands, forming a 3-D framework with chiral channels (20% solvent-accessible volume of the crystal volume). Robust framework after dehydration (453 K) and thermally stable up to 623 K.	332
$[Cu(L_1)(N_3)_2] \cdot 1.5H_2O$	Similar structure than the previous complex, but (4,4) sheets are formed. The framework shows 1-D channels (24.6% solvent-accessible volume of the crystal volume).	332
$[\text{D-}Co(en)_3][H_3Ga_2P_4O_{16}]$	3-D gallophosphate diamond-like framework with the metal complex included within the pores. The optically pure D-$Co(en)_3$ acts as a structural directing agent to form a homochiral structure.	333
$[Ni_3(BTC)_2(py)_6(eg)_6] \cdot 3eg \cdot 4H_2O$	Framework constructed from the interpenetration of four independent (10,3)-a networks. Large interconnected cavities (16 Å, 28% solvent-accessible volume of the crystal volume) are present. The porous structure can be desolvated (150 °C) without destroying the framework. Bulk sample contains both enantiomorphs.	334,335
$[Ni_3(BTC)_2(py)_6(1,2\text{-pd})_3 \cdot 11(1,2\text{-pd}) \cdot 8H_2O$	Homochiral framework constructed from the interpenetration of two independent (10,3)-a networks, leading the formation of chiral pores and cavities (10.6 × 16 Å, 51% with a solvent-accessible volume of the crystal volume). Reversible solvent resolvation using simple alcohols.	335
$[Zn_3O(L_2)_6] \cdot 2H_3O \cdot 12H_2O$ (L or D-POST-1)	2-D homochiral framework built up from the connection of Zn(II) trimers through L_2 ligands. The layers stack together forming 1-D chiral channels (~13.4 Å, 47% solvent-accessible volume of the crystal volume, 47 H_2O molecules per unit cell). This compound catalyzes transesterification reaction in an enantioselective manner.	336
$[M_2(\text{L-}C_4H_4O_6)_3(H_2O)_2] \cdot 3H_2O$ (M = La–Yb)	Homochiral framework built up from connected lanthanide ions through tartrate ligands, forming polar chiral channels (5 × 7 Å). Structural transformation after heating, but the complex still remains microporous.	337
$[M_2(\text{L-}C_4H_4O_6)_2(C_4H_4O_4)(H_2O)_2] \cdot 5.5H_2O$ (M = Pr)	Homochiral framework built up from connected lanthanide ions through tartrate and succinate ligands, forming large chiral channels (6 × 9 Å).	337
$[M(L_3\text{-}H_2)(L_3\text{-}H_3)(H_2O)_4] \cdot xH_2O$ (M = La, Ce, Pr, Nd, Sm, Gd, Tb; x = 9–14)	2-D lamellar homochiral structures consisting of lanthanide metal ions bridged by binaphthylbisphosphonate ligands. The framework shows large asymmetric channels (~12 Å). Heterogeneous catalysis including cyanosilylation of aldehydes and ring opening of meso-carboxylic anhydrides, and enantioselective separation studies are shown.	338
$[Mn(L_3\text{-}H_2)(MeOH)] \cdot MeOH$	3-D homochiral framework built up from the connection of Mn(II) ions through binaphthylbisphosphonate ligands, leading the formation of rhombohedral channels (5.3 × 2.7 Å) filled with MeOH molecules.	339
$[Co_2(L_3\text{-}H_2)_2(H_2O)_3] \cdot 4H_2O$	3-D homochiral framework built up from the connection of Co(II) ions through binaphthylbisphosphonate ligands, leading the formation of rhombohedral channels (3.4 × 4 Å) filled with H_2O molecules.	339
$[ZrRu(L_4)(dmf)_2Cl_2] \cdot 2MeOH$, $[ZrRu(L_5)(dmf)_2Cl_2] \cdot 2MeOH$	Porous homochiral frameworks that show highly enantioselective heterogeneous asymmetric hydrogenation of β-keto esters (with ee up to 95%). ZrRu-L_4 and ZrRu-L_5 exhibit a BET surface of 475 and 387 $m^2\ g^{-1}$, respectively.	340
$[ZrRu(L_4)(DPEN)Cl_2] \cdot 4H_2O$, $[ZrRu(L_5)(DPEN)Cl_2] \cdot 4H_2O$	Porous homochiral frameworks that show highly enantioselective heterogeneous asymmetric hydrogenation of aromatic ketones, with ee up to 99.2%. ZrRu-L_4 and ZrRu-L_5 exhibit a BET surface of 400 and 328 $m^2\ g^{-1}$, respectively.	341
$[Zr(Y)] \cdot xH_2O$ (Y = L_6, L_7 and L_8; x = 4–5)	Porous homochiral phosphonates that in combination with $Ti(O^iPr)_4$ have been used for heterogeneously catalyze the additions of diethylzinc to a wide range of aromatic aldehydes with high conversions and ee of up to 72%. These compounds exhibit BET surface areas ranging from 431 to 586 $m^2\ g^{-1}$.	342

Table 3 Chiral open-framework solids[a] (*Continued*)

Compound	Structure and porosity/chirality characteristics	Ref
$[M_2(L_9\text{-H})_2(MeOH)_8]\cdot(L_9\text{-H}_4)\cdot 3HCl\cdot 6H_2O$ (M = Nd, Sm)	Homochiral lamellar lanthanide bisphosphonates that are pillared with chiral crown ethers. Guest solvent molecules (HCl and H_2O molecules) are removed at room temperature without destroying the framework.	343
$[M_2(H_2O)(L_{10})_2(py)_3(DMF)]\cdot DMF\cdot xH_2O$ (M = Mn, Co, Ni; x = 2–3)	2-D rhombohedral grids with (4,4)-topology that are formed by the linkage of metal dimers through L_{10} ligands. The layers stack together to form small void volumes.	344
$[M_2(L_{10})_3(DEF)_2(py)_2]\cdot 2DEF\cdot 5H_2O$ (M = Gd, Er, Sm)	3-D homochiral frameworks with a $4^9 6^9$ topology that show 1-D channels (3.1 × 6.2 Å).	345
$[Cu_2(L_{11})_2(H_2O)_2]\cdot 2MeOH\cdot 4H_2O$,	H-bonded 3-D homochiral framework assembled from 1-D coordination polymer that is constructed from BDA-bridged Cu(II) paddle-wheels. The framework shows cavities (6.2 × 6.2 Å). Desolvation does not affect the framework.	346
$[HNMeEt_2]_2[Zn(L_{11})_2]\cdot 2MeOH\cdot 4H_2O$	H-bonded 3D homochiral framework assembled from 2-D rhombohedral grids with channels running along two directions (53.4% solvent-accessible volume of the crystal volume). Desolvation does not destroy the framework.	346
$[Mn(L_{11})(DEF)_2(MeOH)]\cdot Lu$, $[Co(L_{11})(DEF)(H_2O)]\cdot Lu\cdot DEF$, $[Cd(L_{11})(py)_3]\cdot py\cdot H_2O$, $[HNMe_3]_2[Cd_2Cl_2(L_{11})_2]\cdot 6H_2O$	H-bonded 3-D or 2-D homochiral frameworks assembled from 1-D coordination polymers. The last two complexes are stable after removing the guest solvent molecules. Adsorption of solvent is shown.	347
$[Cd(L_{12})(ClO_4)_2]\cdot 3EtOH\cdot H_2O$, $[Cd(L_{12})(ClO_4)(H_2O)]\cdot(ClO_4)\cdot 1.5(o\text{-}C_6H_4Cl_2)\cdot 3EtOH\cdot 6H_2O$	1-D coordination polymers further pack to form channel-like homochiral frameworks. The first compound exhibits large chiral channels (9.9 × 12.2 Å, 45.2% solvent-accessible volume of the crystal volume). Second compound also shows large channels (6.6 × 16.7 Å, 47.9% solvent-accessible volume of the crystal volume). Both compounds become amorphous after desolvation, but their crystallinity is restored by immersing the sample in EtOH.	348
$[Ni(acac)_2(L_{12})]\cdot 3CH_3CN\cdot 6H_2O$	Discrete tetragonal nanotube formed by five infinite helical chains of $Ni(acac)_2$ units bridged by L_{12} ligands. Interlocking of the nanotubes leads to a 3-D chiral framework with open channels (17 × 17 Å and 7 × 11 Å, 45.4% solvent-accessible volume of the crystal volume).	349
$[Ni(acac)_2(L_{13})]\cdot 2CH_3CN\cdot 5H_2O$	Similar structure than the previous compound with a 40% solvent-accessible volume of the crystal volume.	349
$[Cd_3Cl_6(\boldsymbol{L_{14}})_3]\cdot 4DMF\cdot 6MeOH\cdot 3H_2O$	3-D homochiral network built up from the connection of 1-D $[Cd(Cl)_2]$ chains through L_{14} ligands, forming large chiral channels (16 × 18 Å, 54.4% solvent-accessible volume of the crystal volume). Robust porous framework after desolvation at 523 K (porosity surface is 601 $m^2\ g^{-1}$). In combination with $Ti(O^iPr)_4$, this compound has been used for heterogeneously catalyze the additions of diethylzinc to a wide range of aromatic aldehydes with high conversions and ee of up to 93–94%.	350
$[Cd(QA)_2]$	3-D homochiral diamond-like structure with adamantane-type cavities. Framework stable up to 538 K. This porous solid shows enantioselective separation of small organic molecules such as racemic 2-butanol and 2-methyl-1-butanol with ee values up to 98.2 and 8.4%, respectively.	351
$[Fe_2(OH)(C_2H_3O_2)(L_{15})_2]\cdot 4H_2O$	3-D assembly of a hydroxo-bridged binuclear complex creates helical 1-D channels (7.3–9.8 Å). Using opposite chirality *S*- or *R*-L_{15} ligands, right- or left-handed helical channels are obtained. Partial dehydration occurs at 368 K under reduced pressure, leading an enantiopure porous sample (18% solvent accessible voids) that is able to absorb iodine vapor.	352
$[Cu(L_{16})_2(NO_3)_2]$	2-D grid layers stack together in a *ABCABC* fashion generating 1-D channels (8 × 8 Å, 11.8% solvent-accessible volume of the crystal volume).	353
$[Cu(NO_3)_2[12\text{-}MC_{CuN(S\text{-}\beta\text{-}pheHA)}\text{-}4]Cu_2(C_7H_5O_2)_4]$	Homochiral framework formed by the stacking of 2-D layers built up from chains of metallocrown (12-MC-4)-bridged Cu(II) paddle wheels connected through NO_3 bridges. The framework shows 1-D channels (8 × 9 Å).	354
$[Zn(sala)(H_2O)_2]_2\cdot 2H_2O$	3-D homochiral structure formed by H-bonded Zn(II) dimers. The framework shows channels (7 × 10 Å) and can be desolvated forming a new porous compound that shows a similar 3-D coordinated structure.	355
$[Cu(sala)]_2\cdot H_2O$	Similar structure and structural changes to the previous compound	356

[a] Abbreviations: hat, 1,4,5,8,9,12-hexaazatriphenylene; 4,4′-bpy, 4,4′-bipyridine; bpyz, 2,2′-bipyrazine; DPT, 2,4-di-(4-pyridyl)-1,3,5-triazine; L_1, 2,5-bis(4-pyridyl)-1,3,4-oxadiazole; en, 1,2-diaminoethane; BTC, 1,3,5-benzenetricarboxylate; py, pyridine; eg, ethylene glycol; 1,2-pd, 1,2-propanediol; L_2-H_2, 2,2-dimethyl-5-[(4-pyridinylamino)carbonyl]-1,3-dioxolane-4-carboxylic acid; L_3-H_4, 2,2′-diethoxy-1,1′-binaphthalene-6,6′-bisphosphonic acid; L_4-H_4, 2,2′-bis(diphenylphosphino)-1,1′-binaphthyl-6,6′-bis(phosphonic) acid; L_5-H_4, 2,2′-bis(diphenylphosphino)-1,1′-binaphthyl-4,4′-bis(phosphonic) acid; dmf, dimethylformamide; DPEN, 1,2-diphenylethylenediamine; L_6-H_4, 2,2′-dihydroxy-1,1′-binaphthyl-6,6′-bis(phosphonic) acid; L_7-H_4, 2,2′-dihydroxy-1,1′-binaphthyl-6,6′-bis(vinylphosphonic) acid; L_8-H_4, 2,2′-dihydroxy-1,1′-binaphthyl-6,6′-bis(styrylphosphonic) acid; L_9-H_4, 2,2′-pentaethylene glycol-1,1′-binaphthyl-6,6′-bis(phosphonic) acid; L_{10}-H_2, 6,6′-dichloro-2,2′-diethoxy-1,1′-binaphthylene-4,4′-dicarboxylic acid; DEF, *N*,*N*′-diethylformamide; Lu, 2,6-lutidine; L_{11}-H_2, 2,2′-dihydroxy-1,1′-binaphthalene-6,6′-dicarboxylic acid; L_{12}, 2,2′-dimethoxy-1,1′-binaphthyl-3,3′-bis(4-vinylpyridine); L_{13}, 2,2′-pentaethylene glycol-1,1′-binaphthyl-3,3′-bis(4-vinylpyridine); acac, acetylacetonate; L_{14}, (*R*)-6,6′-dichloro-2,2′-dihydroxy-1,1′-binaphthyl-4,4′-bipyridine; QA, 6′-methoxyl-(8*S*,9*R*)-cinchonan-9-ol-3-carboxylic acid; L_{15}-H_2, 2-(2-hydroxybenzylamino)-3-(1*H*-imidazol-4-yl)propionic acid; L_{16}, 9,9-bis[(*S*)-2-methylbutyl]-2,7-bis(4-pyridylethylnyl)fluorene; (*S*)-β-pheHA, (*S*)-β-phenylalaninehydroxamic; sala, *N*-(2-hydroxybenzyl)-L-alanine.

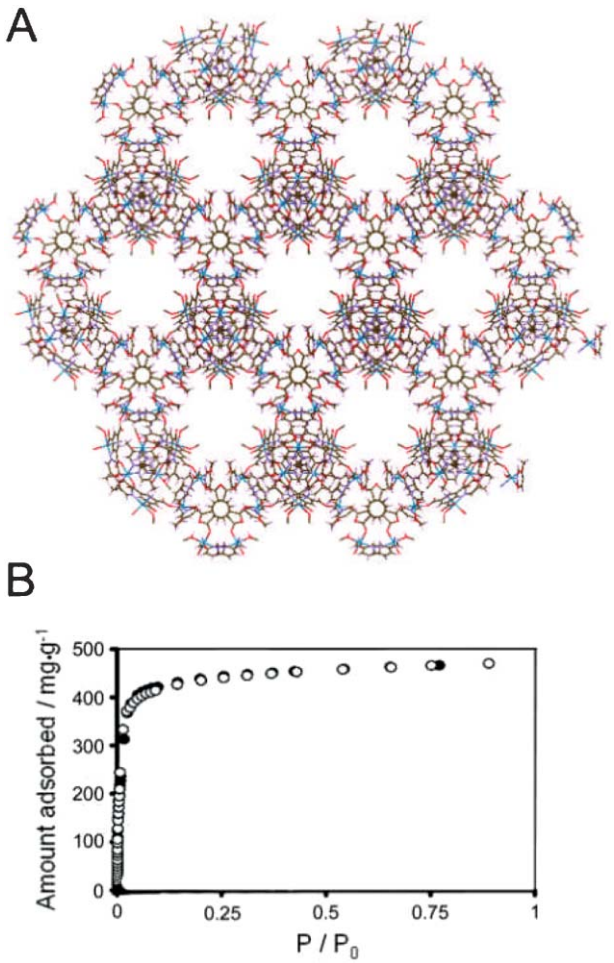

Fig. 24 (A) View of the crystal structure of the porous $[Ni_3(BTC)_2(3\text{-pic})_6(1,2\text{-pd})_3]$. (Ni, blue; O, red; C, brown; N, violet; H, white). (B) N_2 sorption (●) and desorption (○) isotherms measured at 77 K, demonstrating the microporosity of this homochiral material. (Reprinted with permission of ref. 324. Copyright 2004, American Chemical Society.)

More recently, homochiral $[Cd_3Cl_6(L_{14})_3]\cdot 4DMF\cdot 6MeOH\cdot 3H_2O$ (where L_{14} and DMF is (*R*)-6,6′-dichloro-2,2′-dihydroxy-1,1′-binaphthyl-4,4′-bipyridine and dimethylformamide, respectively) has been used to enantioselectively catalyze diethylzinc additions to aromatic aldehydes at up to 94% ee (Fig. 26).[350] The dihydroxy groups pointing out of the channels are used to bind $Ti(O^iPr)_4$ leading to a very active porous metal–organic polymeric catalyst for a wide range of aromatic aldehydes. This example opens the route to other enantioselective asymmetric catalyst derived from coordination polymers that will be certainly designed very soon.

4 Conducting open-frameworks

In spite of the fact that electrical conductivity is one of the major topics in materials science,[357] porous solids exhibiting conductivity properties are still scarce. The most probable reason is that most porous materials, such as zeolites, microporous oxides and metal–organic solids, are intrinsic electrical insulators due to their composition. An exception to this behaviour is the family of porous chalcogenides.[358,359] Open-framework chalcogenides are inorganic solids analogous to the metal oxide-based microporous materials, in which the O^{2-} anions have been replaced by chalcogens (S^{2-}, Se^{2-}, and Te^{2-}). Thus far, several 3-D chalcogenides with large channels and high porosity have been synthesized; many of them constructed from the connection of chalcogenide clusters.[360,361] Because of their composition, these materials can also exhibit semiconducting, metallic or semi-metallic properties common to solids built up from the linkage of many of the main group metals or semi-metals through sulfur, selenide and telluride bridges. Chalcogenides are then excellent candidates to integrate porosity with electrical properties, and hold promise for applications such as photoelectrodes, high-surface-area photocatalysts and sensors.

Conductivity properties in open-framework chalcogenides were first reported by Kanatzidis and co-workers, with the description of the series $(Ph_4P)[M(Se_6)_2]$ (where M is Ga, In, and Tl).[362] These solids are formed by isostructural 2-D $[M(Se_6)_2]_n^{n-}$ frameworks with 1-D channels filled with Ph_4P^+ cations. Furthermore, conductivity measurements showed a semiconductor behaviour for the In and Tl phases. Latter on, semiconductor behaviours were also reported in a cadmium and bismuth sulfide. $K_2Cd_2S_3$ and $KBiS_5$ are open-framework semiconductors with band-gaps of 2.89 and 1.21 eV, respectively, and with large tunnels that are occupied by K^+ ions.[363,364] Interestingly, the K^+ ions of the latter compound can be exchanged by Li^+, Na^+, and NH_4^+, and the resulting semiconductor phases show similar band-gaps in the range from 0.98 to 1.20 eV.[365]

Most recently, extensive studies in this family of chalcogenides have expanded the number of open-framework semiconductors.[366] For example, the indium chalcogenide $[In_{28}Cd_6S_{54}]\cdot[(CH_3)_4N]_{12}\cdot[(HSCH_2COOH)_2]_{3.5}$ behaves as a semiconductor with a band-gap of 3.0 eV.[367] Another remarkable crystalline microporous material with conductivity properties is the mineral cetineite with composition $[K_3(H_2O)_3][Sb_7O_9Se_3]$.[368] This material is a photo-semiconductor with a band-gap of 2.06 eV. Furthermore, the optical band-gap of the cetineite-type phases was found to depend on the elemental composition and is, for example, 2.5 eV in $[Na_6(H_2O)_6]\cdot[Sb_{14}O_{18}Se_6]$.[369] Later on, a narrow band-gap of 1.32 eV was found in $RbCuSb_2Se_4\cdot H_2O$, a microporous semiconductor with 1-D large channels (11.3 × 10.5 × 8.2 Å).[370] And even more recently, Palmqvist *et al*. have reported a crystalline microporous antimony(III) oxide telluride semiconductor with even a narrower band-gap of 0.25 eV (Fig. 27).[371]

As can be noticed in all these examples, the electronic band structure of an open-framework solid may be tuned by controlling the synthesis and, therefore, the framework of porous chalcogenides.[372] This control together with their inherent porosity that increases the number of active reaction sites provides the ideal conditions for using these porous semiconductors as photocatalysts, particularly in the visible-light region. This concept was demonstrated by Feng and co-workers.[373] Initially, a family of open-framework sulfides was synthesized from solutions comprising In^{3+} and S^{2-} ions and one type of transition-metal ion (*e.g.*, Cd(II), Zn(II), Mn(II), *etc*.). The resulting porous semiconductors showed different

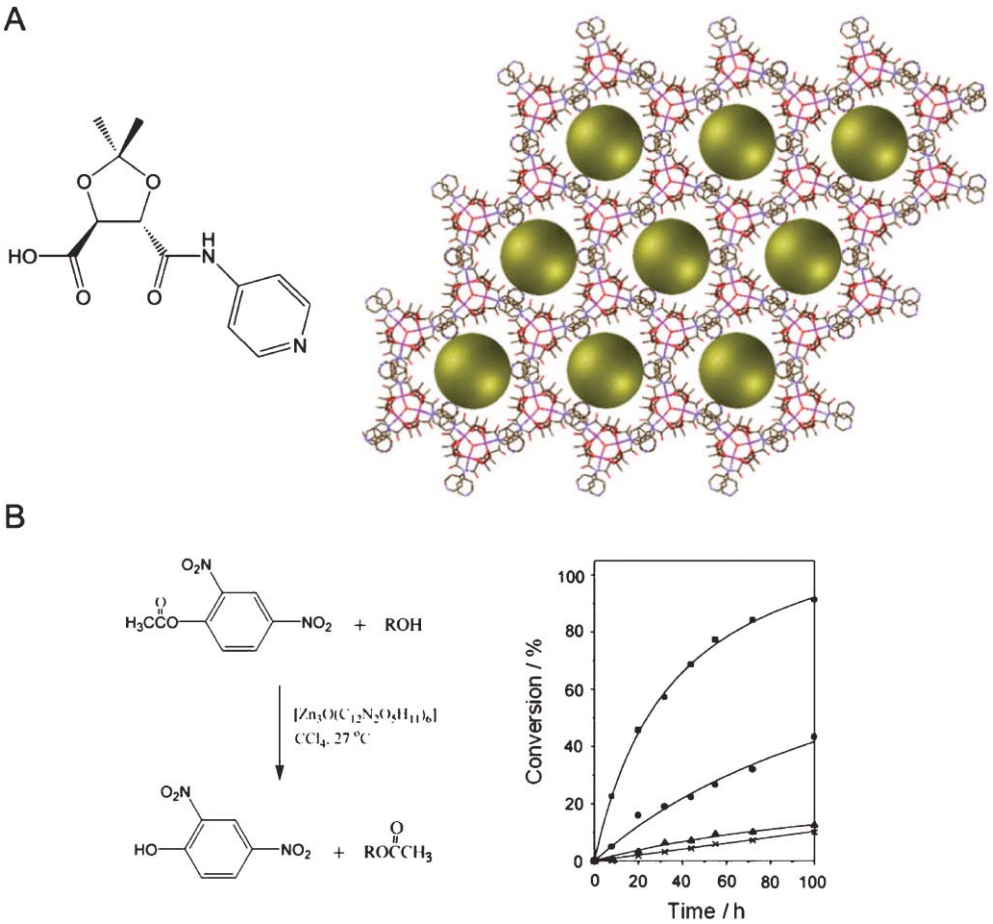

Fig. 25 (A) Diagram of the enantiomeric chiral polytopic organic ligand L_2 (2,2-dimethyl-5-[(4-pyridinylamino)carbonyl]-1,3-dioxolane-4-carboxylic acid), and view of the structure of $[ZnO(L_2)_6]$, showing the large chiral channels. Empty space is represented as yellow spheres. (Zn, purple; O, red; C, brown; N, violet). (B) Transesterification of the ester with ethanol (■), isobutanol (●), neopentanol (▲) and 3,3,3-triphenyl-1-propanol (×) in the presence of the porous metal–organic framework. (Reprinted with permission of ref. 336. Copyright 2000, Nature Publishing).

band-gaps with values ranging from 2.0 to 3.6 eV. By using the porous Cu(II) chalcogenide (referred to as ICF-5InCuSNa) with the lowest band-gap value, these authors demonstrated how this porous chalcogenide can be used as an efficient photocatalyst for the reduction of water (Fig. 28(A)). Indeed, as shown Fig. 28(B), about 18 μmol h^{-1} g^{-1} of H_2 gas was produced from a 0.5 M Na_2S aqueous solution over this catalyst under irradiation with visible light. Similar activity was observed in other members of this family.[373] Also, a recently reported germanium chalcogenide with composition $[Ge_3S_6Zn(H_2O)S_3Zn(H_2O)][Zn(C_6N_4H_{18})(H_2O)]$ has shown photocatalytic activity for hydrogen production from an aqueous solution containing Na_2SO_3.[374]

Open-framework solids containing highly mobile alkali metal cations is another approach towards combining porosity characteristics and ionic conductivity. Solids with high ionic conductivity are useful, for example, as electrode materials or solid electrolytes in electrochemical devices such as batteries, fuel cells and sensors. A recent example obtained within this strategy is the synthesis of 3-D chalcogenides containing high concentrations of mobile alkali-metal cations that behave as fast ion conductors.[375] Since chalcogenides have higher anionic framework polarizability compared to zeolites, the migration of mobile cations in this open-frameworks is facilitated. Thus far, the highest specific conductivity achieved among these open-framework chalcogenides is 0.15 $\Omega^{-1}cm^{-1}$ at 27 °C and under 100% relative humidity.[376] In addition, even though chalcogenide solids tend to exhibit higher ionic conductivities, a few other open-framework alkaline-containing solids, such as oxides, phosphates, arsenates, vanadates, and even oxalates, have also shown interesting ionic mobility and conductivity properties.[377]

5 Open-frameworks with optical properties

The combination of selective sorption and optical properties, such as fluorescent responses, have been successfully used for detecting aromatic molecules and metal ions (for more details, see section 6).[378–381] Among the different type of materials (pure inorganic, hybrid materials, *etc.*) that can be used for such purposes, over the last few years, most of the attention has been focused on the preparation and characterization of metal–organic frameworks with photoluminescent properties. Reasons are multifold.[30] First, the organic ligands ensure the presence of their inherent luminescent properties. Second, the higher thermal stability of the coordination polymers in

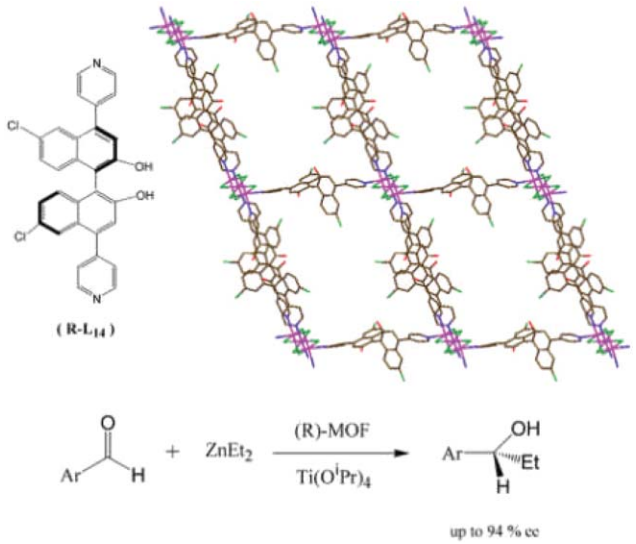

Fig. 26 Projection of the homochiral ligand L_{14} ((*R*)-6,6′-dichloro-2,2′-dihydroxy-1,1′-binaphthyl-4,4′-bipyridine), and the crystal structure of $[Cd_3Cl_6(L_{14})_3]$, showing the channels. (Cd, purple; O, red; C, brown; N, violet; Cl, green). This material has been used to enantioselectively catalyze diethylzinc additions to aromatic aldehydes.

comparison with the free organic ligands increases the probability for potential applications. And third, the coordination interaction between metal ions and organic ligands may enhance or change the luminescent properties of the free organic ligands. The origin of the photoluminescence in these complexes is thus generally due to the metal–ligand complex formation, which is typically assigned to the ligand-to-metal charge transfer (LMCT) or to the metal-to-ligand charge transfer (MLCT), and/or the intraligand fluorescent emissions.

One of the most representative families of photoluminescent open-framework structures is that of metal–organic polymeric compounds bearing d^{10} metal-ions. Following this approach, several channel-like Cd(II) and Zn(II) solids exhibiting fluorescence properties have been described; many of them exhibiting strong blue or violet fluorescence in the solid state,[382,383] although an example with strong yellow fluorescent emission has also been found.[384] Recent representative examples of this type of porous solids are $Zn_3(C_9O_6H_3)_2(DMF)_3(H_2O)\cdot DMF\cdot H_2O$ and $Cd_4(C_9O_6H_3)_3(DMF)_2(H_2O)_2\cdot 6H_2O$.[385] In both cases, the connection of Zn(II) and Cd(II) ions through 1,3,5-benzenetricarboxylate ligands creates 3-D chiral frameworks that combine the presence of large openings stable to the adsorption of solvent molecules and blue fluorescence. The stronger excitation and emission peaks for both compounds are at 341 and 410 nm and at 319 and 405 nm, respectively. These emissions are very similar to the free ligand transitions (370 nm), with a small shift probably due to the differences in metal ions and coordination environment around them.

As stated above, the connection of organic ligands and metal ions may induce the enhancement of the photoluminescence properties of metal–organic solids, leading to stronger fluorescent intensities compared to those exhibited by the free organic ligands. This phenomena has been observed, for example, in $Zn(C_6N_2O_2H_5)_2(H_2O)_{4.5}$ and $Cd(C_8O_4H_4)(py)$ solids, both exhibiting stronger intensities than free uronate and terephthalate, respectively.[386,387] The first of these compounds shows a fourfold interpenetrated diamond network with 1-D channels, which are stable after dehydration. While the free urocanate ligand displays almost no luminescence in the solid state at room temperature, this complex exhibits intense blue radiation emission maxima at wavelengths of 499 and 550 nm (λ_{ex} = 484 nm). This enhancement of the fluorescent intensity may be ascribed to the presence of the fourfold-interpenetrated frameworks which may tighten the entire skeleton, resulting in much weaker vibrations. A similar enhancement is detected in the second compound; the three-dimensionally condensed polymeric

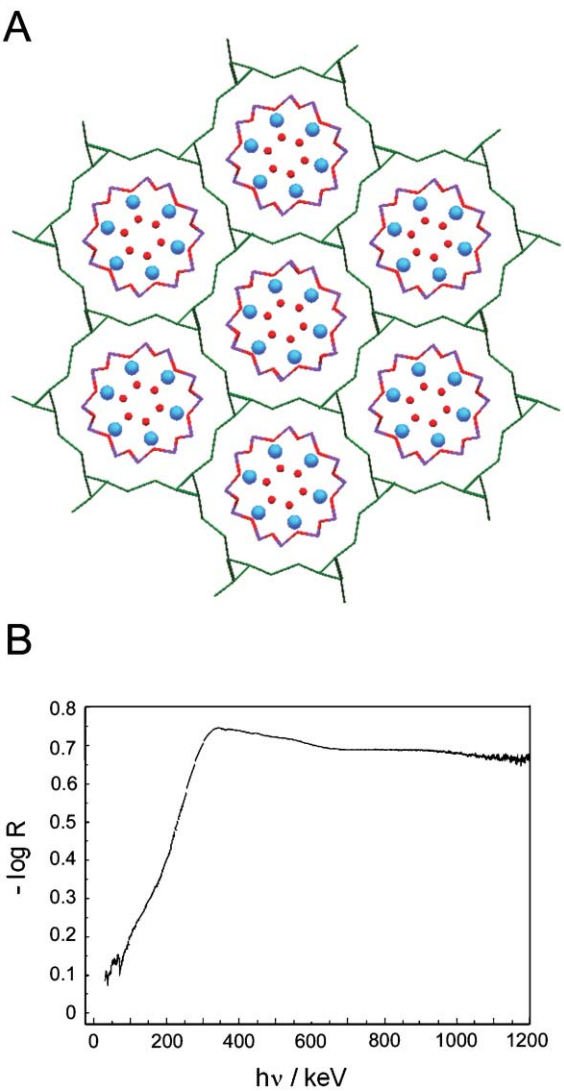

Fig. 27 (A). View of the crystal structure of $[([K_6(H_2O)_6][Sb_{12}O_{18}])_3][Te_{36}]$, showing the 24-ring tubular tellurium unit that hosts the 12-ring $\{Sb_{12}O_{18}\}$ tubular unit, which in turn hosts potassium ions and water molecules. (Te, green; Sb, purple; O, red; K, blue. Potassium and water molecules are represented as spheres). (B) Diffuse reflectance FTIR spectra showing a sharp absorption edge corresponding to an optical bandgap of 0.25 eV. (Reprinted with permission of ref. 371. Copyright 2004, Wiley Interscience.)

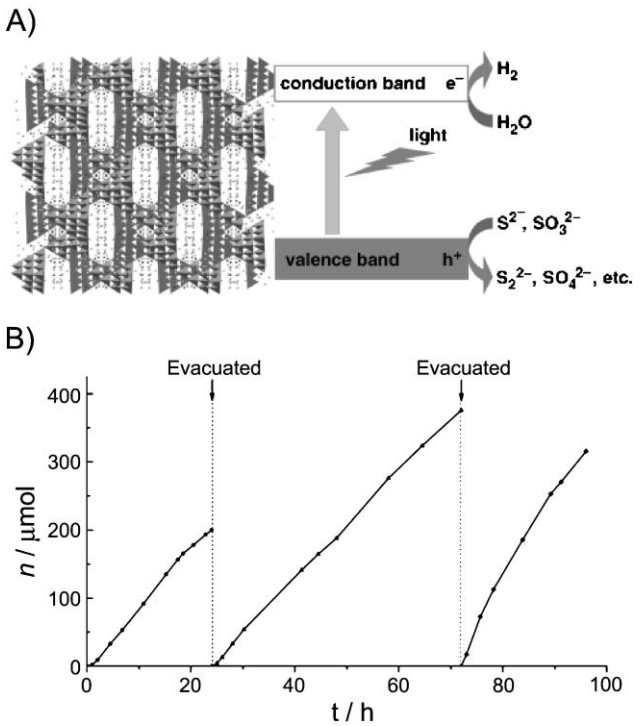

Fig. 28 (A) View of the crystal structure of Cu(II)-based chalcogenide ICF-5InCuS–Na, and the schematic representation of how this porous semiconductor acts as a photocatalyst in the reduction of water. (B) Photocatalytic evolution from an aqueous solution of Na_2S (0.5 M) over ICF-5 CuInS–Na (t is irradiation time, and n is the amount of H_2). (Reprinted with permission of ref. 373. Copyright 2005, Wiley Interscience.)

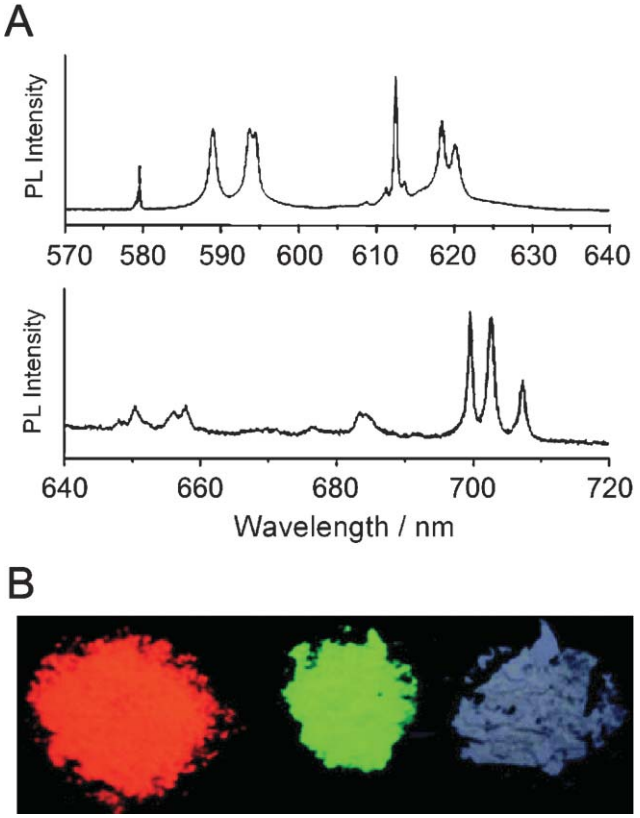

Fig. 29 (A) Fluorescence spectra of $Y_{1-x}Eu_x(C_9O_6H_3)$ ($x \sim 0.024$, MIL-78) at room temperature (excitation at 467 nm). (B) Picture of MIL-78 doped with Eu (red), Tb (green) and Dy (blue) under UV irradiation (excitation at 252 nm). (Reprinted with permission of ref. 391. Copyright 2004, Royal Society of Chemistry.)

structure leads to an almost 100 times enhancement of the blue fluorescent intensity.

Rare-earth solids are good candidates to exhibit interesting photoluminescent properties.[388,389] Thus far, Song and Mao reported a series of phosphonate-decorated lanthanide oxalates with open-framework structures exhibiting blue, red and near-IR luminescence.[390] Also, Férey and co-workers obtained a porous material with very efficient red, green and blue emission after doping the complex $Y_{1-x}Eu_x(C_9O_6H_3)$ ($x \sim 0.024$) with Eu, Tb and Dy, respectively (Fig. 29).[391] Red fluorescence has found in other lanthanide complexes,[392] while emission of green light was observed in $[Tb(C_4H_4O_4)_{1.5}(H_2O)]\cdot 0.5H_2O$.[393] Another interesting feature of lanthanide polymers is observed in $Er(bpdc)_{1.5}(H_2O)\cdot 0.5DMF$ (where bpdc is 4,4′-biphenyldicarboxylic acid) that exhibits the characteristic emission of Er(III) around 1540 nm excited at 980 nm.[394] Thus, this type of complexes could be anticipated as potential IR-emitters. Also, Ag(I) porous coordination complexes may exhibit luminescent properties,[395] most of them at low temperatures.[396]

Beside the interest in metal–organic fluorescent solids, strong photoluminescence can also be found in some pure inorganic porous materials, such as chalcogenides,[361,397] silicates,[398] and cyanides.[399] For example, a family of microporous and photoluminescent chalcogenides has been reported by Feng and co-workers.[361] These sulfide and selenide zeolite analogs show four-connected, 3-D tetrahedral porous frameworks with thermal stabilities up to at least 453 K and Langmuir surface areas that, in some cases, are as high as 807 $m^2\ g^{-1}$. Furthermore, they are strongly photoluminescent and can be excited with wavelengths from 320 to 420 nm. The emission occurs then in the range from 460 to 508 nm. More recently, interesting photoluminescence properties were reported in some lanthanide silicates with composition $Na_{1.08}K_{0.5}M_{1.14}Si_3O_{8.5}\cdot 1.78H_2O$ (where M is Eu, Tb, Sm, and Ce).[398] These materials combine microporosity with interesting photoluminescence properties, and their structural flexibility allows fine-tuning of luminescence properties, by introducing a second type of lanthanide ion in the framework.

Finally, it is worth mentioning that in addition to fluorescence, another property that has been extensively studied for open-framework inorganic materials is that of nonlinear optics. In this case, a considerable variety of non-centrosymmetrical inorganic materials have been shown to exhibit interesting second harmonic generation measurements,[400] although in some cases, third-order non-linear open-framework coordination polymers have also been reported.[401]

6 Sensing open-frameworks

Dynamic structural transformations in flexible coordination polymers, such as a selective removal and resorption of solvent molecules followed by reversible crystal transformations, have become one of the most intriguing research areas in the porous

field along the last few years[402] According to Kitagawa and Uemura, two main types of dynamic structural transformations have thus far been described. The first class is a reversible crystal-to-amorphous transformation that occurs when the framework collapses upon removal of guest solvent molecules and regenerates under the initial or similar conditions. The second type is a phase transition (crystalline-to-crystalline transformation). In this case, although removal or exchange of guest molecules results in reversible structural changes within the network, the crystalline character is maintained along the whole process.

Recently, several authors have pointed out the possibility to use these reversible structural transformations to design a novel generation of multifunctional porous solids suitable to act as potential sensors. Indeed, since most of the functionalities known in porous solids (magnetism, electronic/spin-crossover, conductivity, chromism, optical, *etc.*) are closely dependant on their crystal structure, reversible transformations upon sorption/removal of guest molecules can conveniently induce reversible modifications of the associated functionalities. This fact, together with the high selectivity usually shown for dynamic solids, provides the ideal scenario for researchers to create selective sensing open-frameworks for molecular recognition. From now on, some recent examples of dynamic porous examples exhibiting tunable functionalities will be summarized.

6.1 Solvatomagnetic switching

Besides the seminal work on molecular sponge-like coordination polymers reported by Kahn and co-workers, which change their magnetic properties after hydration/dehydration processes (Fig. 16, see section 2.3),[238] several other examples of potential sensing porous solids based on solvatomagnetic effects have been described. In 2003, Veciana and co-workers reported $Cu_3(PTMTC)_2(py)_6(EtOH)_2(H_2O)$ (referred to as MOROF-1, see also section 2.3), an open-framework coordination polymer that combines very large pores (3.1 × 2.8 nm, and a 65% void volume) with magnetic ordering around 2 K (Fig. 30(A)).[312] This material shows a reversible "shrinking–breathing" process involving up to 30% of the volume upon solvent uptake and release, which in turns induces changes in its magnetic properties. Indeed, when MOROF-1 is removed from the solution and exposed to air, the crystalline material loses guest solvent molecules very rapidly, becoming an amorphous magnet with a lower critical temperature. However, as described in Fig. 30(A), the evacuated sample of MOROF-1 experiences a transformation recovering its original crystallinity and magnetic properties after exposure to ethanol solvent. Unexpectedly, this behaviour is only observed when MOROF-1 is exposed to small alcohols, like methanol and ethanol, showing a large selectivity for this type of molecules.

Pronounced solvatomagnetic effects have also been found in several molecular porous materials reported by Kurmoo and co-workers. Reversible dehydration/rehydration in $[Co_3(OH)_2(C_2O_4)_2]\cdot 3H_2O$ and $[Ni_3(OH)_2(C_8O_2H_{10})_2(H_2O)_4]\cdot 2H_2O$ induces reversible transformations from ferromagnetic to antiferromagnetic ordering and from ferromagnetic to ferrimagnetic ordering, respectively (Fig. 30(B)).[403,404] In contrast to the large structural transformations experienced by MOROF-1, these interconversions are accompanied by subtle changes in the crystal structures. For example, the dehydration process in the first compound only involves minimum changes on its structure with almost no change in the coordination environment of the metal ions. This fact suggest that the ferromagnetic ground state in the hydrated phase may be caused by the presence of significant magnetic exchange couplings through the H-bonded water molecules located within the channels. The influence of adsorbed guest molecules in the magnetic properties was also evidenced by the discovery of another compound with formula $Mn_3(HCOO)_6\cdot CH_3OH\cdot H_2O$. This 3-D porous magnet shows a fascinating guest-modulated critical temperature.[248] Indeed, magnetic measurements of the as-synthesized or evacuated sample show a long-range magnetic ordering with a critical temperature close to 8 K. However, this critical temperature can be modulated at will from 5 to 10 K by the sorption of several types of guest molecules. This transformation can be explained by the small changes of the Mn–O–Mn bond angles (the larger the angle, the smaller the T_c) observed in this framework after absorption of guest molecules.

Prussian blue analogues can exhibit changes of their magnetic properties upon a dehydration/hydration process.[405] For example, Ohkoshi, Hashimoto and co-workers have recently reported $Co[Cr(CN)_6]_{2/3}\cdot zH_2O$, a pink ferromagnetically-coupled magnet with a T_c of 28 K that reversible transforms into a blue antiferromagnetically-coupled magnet with a T_c of 22 K after dehydration (Fig. 31).[406] Such solvatomagnetism and solvatochromism are ascribed to the adsorption and desorption of ligand water molecules onto Co ions. Such processes change the coordination geometry around the Co(II) ions from six-coordinate pseudo-octahedral 6-Co(II) to four-coordinate pseudo-tetrahedral 4-Co(II), and therefore, modulate the magnetic interactions from ferromagnetic coupling [6-Co(II)–NC–Cr(III)] to antiferromagnetic coupling [4-Co(II)–NC–Cr(III)]. A very similar explanation can be used to explain the behaviour of $Co_{1.5}[Cr(CN)_6]\cdot 7.5H_2O$.[407] When this compound is immersed in ethanol, its color turns from peach to deep blue, and its magnetic behaviour changes from a ferromagnetic-coupled to an antiferromagnetically-coupled magnet. This behaviour turns out to be reversible after re-exposing the solid to water. More recently, another example of this family with formula $K_{0.2}Mn_{1.4}Cr(CN)_6\cdot 6H_2O$ has shown a ferrimagnetic behaviour with a critical temperature of 66 K, which increases up to 99 K after dehydration.[408]

6.2 Solvatospin-state switching

Spin crossover (SCO) is a phenomenon where a given metal ion can change its electronic, and therefore spin state [high-spin (HS) ↔ low-spin (LS)], upon exposure to an external perturbation (temperature, light or pressure). Traditionally, spin-crossover compounds have been proposed for storage of information or display devices, which are important aspects of *Molecular Electronics*. Nevertheless, more recently this functionality has been incorporated into dynamic porous solids. Kepert and co-workers have reported a coordination polymer with reversible disappearance and appearance of SCO phenomena after elongation of the channels due to the

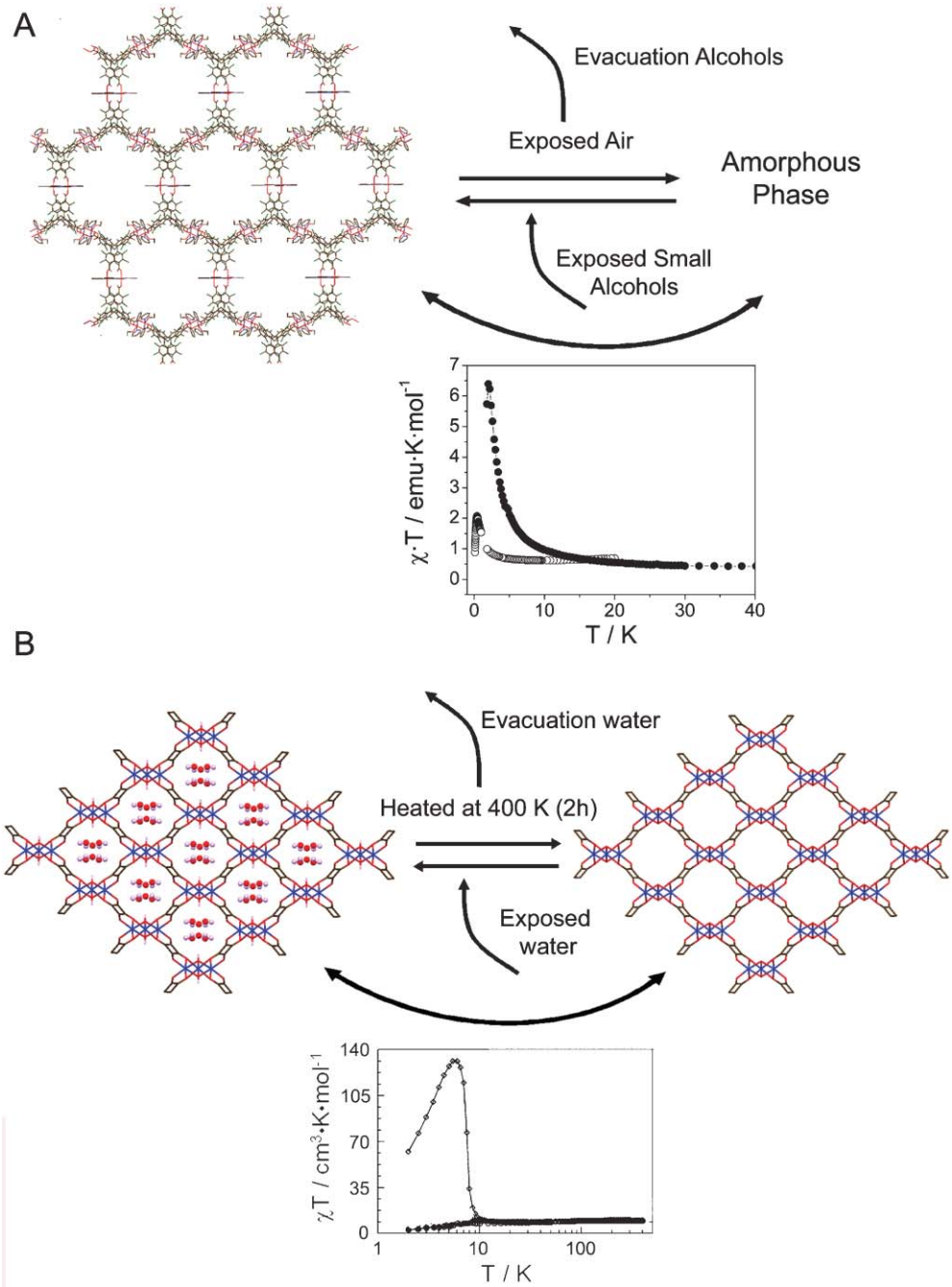

Fig. 30 Reversible solvatomagnetic effects in dynamic porous magnets. Schematic representation of the reversible structural changes of (A) $Cu_3(PTMTC)_2(py)_6(EtOH)_2(H_2O)$ (MOROF-1) and (B) $[Co_3(OH)_2(C_2O_4)_2]\cdot 3H_2O$ after evacuation/adsorption processes with their consequent changes in their magnetic properties. (Cu, orange; Co, blue; O, red; C, brown, Cl, green; N, violet, H, white. Solvent guest molecules are represented as spheres). (Reprinted with permission from ref. 403. Copyright 2005, Royal Society of Chemistry.)

evacuation/resorption of alcohol solvent molecules.[303] Briefly, the crystal structure of $[Fe_2(azpy)_4(NCS)_4]\cdot EtOH$ (where azpy is *trans*-4,4′-azopyridine) consists of double interpenetrated 2-D grid layers built up by the linkage of Fe(II) ions by azpy ligands. As a result, two types of 1-D channels (10.6 × 4.8 Å and 7.0 × 2.1 Å) filled with ethanol molecules and running along the same direction are created. Following the evacuation of ethanol guest molecules at 373 K, several structural changes are detected. The most significant modification consists in an elongation and constriction of the 1-D channels, being the new dimensions of 11.7 × 2.0 Å. This structural modification induces enormous changes in the electronic behaviour of this compound. While the as-synthesized sample exhibits a broad half SCO transition at 150 K, the evacuated sample shows a constant magnetic moment of 5.1 μB, lacking any SCO transition. Surprisingly, SCO is recovered after re-sorption of guest solvent molecules. When an evacuated crystalline sample is immersed in methanol, ethanol or propanol solvent, the magnetic properties are similar to those observed for the as-synthesized sample.

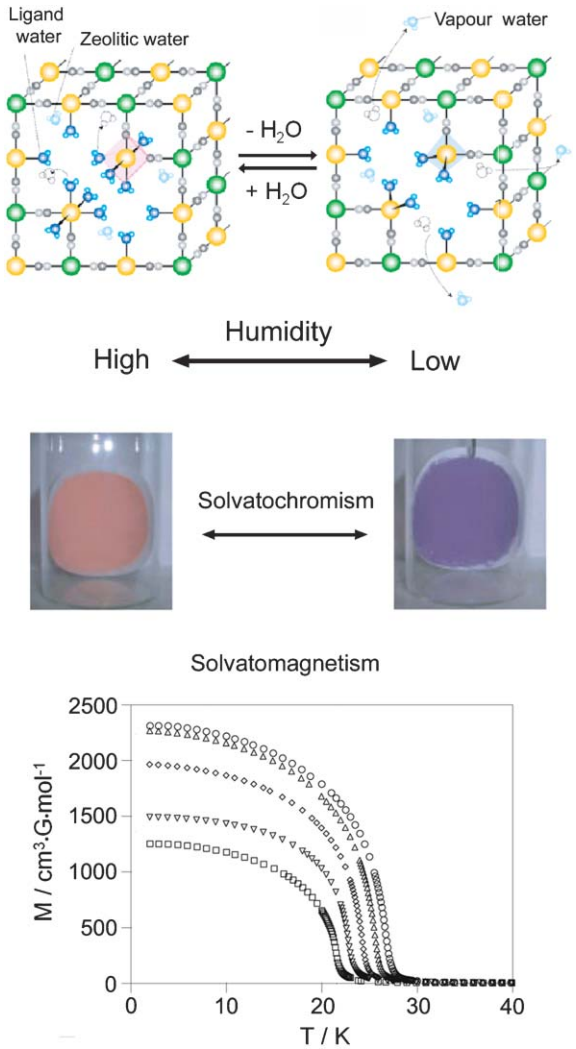

Fig. 31 Changes in color and magnetic properties of $Co[Cr(CN)_6]_{2/3}\cdot zH_2O$ depend on the humidity. Schematic illustration of the variations in the coordination geometry on Co(II) in this compound between 6-coordinate [6-Co(II)] and 4-coordinate [4-Co(II)] by adsorption and desorption of water ligand molecules in the coordination geometry of CoN_2O_4. Photographs of this compound in 80% of relative humidity (RH, pink) and 3% RH (violet). Magnetization versus temperature curves 3 (□), 7 (▽), 16 (◇), 36 (△) and 80% (○) RH at a magnetic field of 10 Oe. (Co, yellow spheres; Cr, green spheres; CN, grey spheres; H_2O, blue spheres). (Reprinted with permission from ref. 406. Copyright 2004, Nature Publishing.)

Similar reversible properties have been found in another compound reported by Real, Bousseksou and co-workers.[409,410] $[Fe(pmd)(H_2O)\{Au(CN)_2\}_2]\cdot H_2O$ (where pmd is pyrimidine) is a triple interpenetrated framework showing a sharp half SCO transition at 165 K with a hysteresis of approximately 8 K. The dehydration process induces large changes in the crystal structure. The pyrimidine ligands, which previously were bound only through one nitrogen atom, now bridge two Fe(II) ions resulting in the linkage of the three independent interpenetrated frameworks into a unique 3-D network. This conversion results in the suppression of the SCO behaviour, which can be recovered after hydration. Interestingly, the isostructural $[Fe(pmd)(H_2O)\{Ag(CN)_2\}_2]\cdot H_2O$ shows a similar reversible behaviour, but with a shift of the SCO transition to lower temperatures for the dehydrated phase.

6.3 Solvatooptical switching

A pioneering work reporting a family of open-framework tin chalcogenides with reversible solvatooptical effects for chemical sensing was published by Ozin and co-workers in 1995.[411] Among them, $QH_2Sn_3S_7$ and $A_2TEA_2Sn_3S_7$ (where QH is quinuclidinium, $C_7H_{13}NH^+$, A is NH_4^+, and TEA is Et_4N^+) become porous materials after evacuating the alkylammonium cations. Fascinatingly, both materials can absorb water with a reversible noticeable shift of approximately 20 nm in the optical absorption edge.

More recently, several other examples with reversible solvatoluminiscent properties have been proved useful for detecting molecules and metal ions. Two examples, $Cu_6L_6\cdot H_2O\cdot DMSO$ (where L is 5,6-diphenyl-1,2,4-triazine-3-thiol) and $[(ZnCl_2)_3(TPDPB)]\cdot 3CH_2Cl_2\cdot 0.25C_6H_6$ (where TPDPB is 1,3,5-tris(*p*-(2,2′-dipyridylamino)phenyl)benzene), have shown the ability to detect aromatic molecules.[378,379] Interestingly, both compounds exhibit a similar behaviour: the initial luminescence of the porous materials is quench after sorption of aromatic molecules, but it is automatically recovered after desorption of these molecules. For example, the luminescent spectrum of the first porous solid, with 1-D nanotubular channels (1.2 nm), exhibits a cluster-center band at 660 nm (excited at 460 nm) that disappears after sorption of aromatic molecules (Fig. 32). This

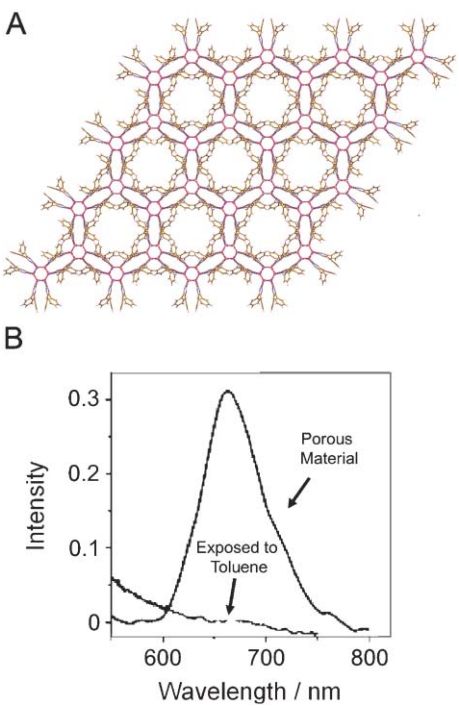

Fig. 32 (A) View of the crystal structure of $Cu_6L_6\cdot H_2O\cdot DMSO$ (where L is 5,6-diphenyl-1,2,4-triazine-3-thiol), showing the nanotubular channels. (Cu, orange; C, brown, N, violet; S, purple; H, white. Solvent guest molecules are omitted for clarity). (B) Luminiscence spectra of the porous solid and after immersing this solid in an aqueous solution of toluene (0.5 wt%). Reprinted with permission of ref. 379. (Copyright 2006, Royal Society of Chemistry.)

process is reversible, indicating that aromatic molecules can be successfully detected in a concentration as low as 0.5% in water.

The sorption of metal ions into open-framework materials can affect their luminescent properties. When this process is reversible, one can imagine the use of these porous solids as ideal chemosensors for metal ions. For instance, two coordination polymers with formula $[M(PDA)_3Mn_{1.5}(H_2O)_3]\cdot 3.25H_2O$ (where PDA is pyridine-2,6-dicarboxylic acid and M is Eu or Tb) have been revealed as luminiscent probes of Zn(II) ions.[380] Indeed, the luminiscent properties in DMF solvent of both complexes show that the emission intensity increased upon addition of Zn(II), while the introduction of other metal ions caused the intensity to be either unchanged or weakened. Similarly, a recent tryptophan-based open-framework have been investigated as a fluorescent chemosensor for Ca(II) ions, which presence induces a pronounced enhancement of the fluorescence emission.[381]

7 Conclusions and perspectives

The enormous attention attracted by multifunctional porous materials results from the diversity of potential applications and for some types of materials—like organic–inorganic hybrids, coordination polymers and purely organic materials—from their modular structure and their associated flexibility in the structural design. Besides the appealing properties of the open-framework itself which makes it interesting as a magnetic, optic, and conducting material, the open-framework can be loaded with other molecular compounds or nanoparticles—metallic or oxides—by employing classical host–guest chemistry techniques. This possibility generates a tremendous technological potentiality in applications in different fields such as catalysis and gas (H_2, CH_4, CO_2, *etc.*) storage. Nevertheless, before any practical application is achieved with these bulk materials, it is necessary to control the distinct structural and functional aspects of such materials. Among them, the most important are the following: control of sizes and shapes of void volumes and as well as their porosity, ability to govern the flexibility of the molecular frameworks, decoration of their internal walls with prefixed chemical groups, tune at will their physical—magnetic, optical, conducting, *etc*.—functionalities, increase their thermal stability and ageing. While all these applications refer to bulk properties of open-framework materials, new and even more promising applications may emerge when such materials are properly attached to surfaces. Sensors and actuators are examples where host–guest chemistry offers a wide range of possibilities to open-framework functional materials but only if these materials are conveniently interfaced to a transducer to communicate with the external world. This can be done if the open-framework functional structure is covalently bound to substrate surfaces either by growing crystalline structures on nanopatterned molecular self-assembled monolayers, used as templates, or by employing a molecular layer-by-layer multilayer formation of the open-framework functional material. Seminal works on both approaches have been recently reported by Fisher,[412] van der Boom,[413] and others deserving a more extensive future development. Another area of interest for open-framework multifunctional materials is related with the future of electronics where the fabrication of devices with length scales below 20 nm requires technological alternatives beyond well established concepts of today's microelectronics industry. In this sense, porous functional materials bear the potential not only as building-blocks for molecule-based electronics but also as templates for control of electronic connections on the ultrasmall length scale.

Acknowledgements

We thank the financial support provided by DGI, Spain (Projects MAT2003-04699 and CTQ2006-06333/BQU) and DGR Catalonia (Project 2001SGR00362). D. M. is also grateful to the Generalitat de Catalunya for a postdoctoral grant.

References

1 D. W. Breck, *Zeolite Molecular Sieves: Structure, Chemistry and Use*, J. Wiley and Sons, New York, 1974; P. B. Venuto, *Microporous Mater.*, 1994, **2**, 297.
2 A. Corma, *Chem. Rev.*, 1995, **95**, 559.
3 S. T. Wilson, B. M. Lok, C. A. Messina, T. R. Cannan and E. M. Flanigen, *J. Am. Chem. Soc.*, 1982, **104**, 1146.
4 A detailed review of inorganic-based porous materials can be consulted in: A. Cheetham, G. Férey and T. Loiseau, *Angew. Chem., Int. Ed.*, 1999, **38**, 3268.
5 J. B. Parise, *Inorg. Chem.*, 1985, **24**, 4312; Y. Guangdi, F. Shouhua and X. Ruren, *J. Chem. Soc., Chem. Commun.*, 1987, 1254.
6 S. Natarajan, M. P. Attfield and A. K. Cheetham, *Angew. Chem., Int. Ed. Engl.*, 1997, **36**, 978.
7 C. Cleitzer, *Eur. J. Solid State Inorg. Chem.*, 1991, **28**, 77; K.-W. Lii, *J. Chem. Soc., Dalton Trans.*, 1996, 819; G. Férey, *J. Fluorine Chem.*, 1995, **72**, 187.
8 P. Y. Feng, X. H. Bu and G. D. Stucky, *Nature*, 1997, **388**, 735.
9 N. Rajic, N. Z. Logar and V. Kaucic, *Zeolites*, 1995, **15**, 672.
10 V. Soghomonian, Q. Chen, R. C. Haushalter, J. Zubieta and J. O'Connor, *Science*, 1993, **259**, 1596.
11 S. S. Dhingra and R. C. Haushalter, *J. Chem. Soc., Chem. Commun.*, 1993, 1665.
12 P. Smith-Verdier and S. Garcia-Blanco, *Z. Kristallogr.*, 1980, **151**, 175.
13 N. Rajic, A. Ristic and V. Kaucic, *Zeolites*, 1996, **17**, 304.
14 P. Kierkegaard and M. Westerlund, *Acta Chem. Scand.*, 1964, **18**, 2217; G. Costentin, A. Laclaire, M. M. Borel, A. Grandin and B. Raveau, *Rev. Inorg. Chem.*, 1993, **13**, 77.
15 S. Fernández, J. L. Mesa, J. L. Pizarro, L. Lezama, M. I. Arriortua, R. Olazcuaga and T. Rojo, *Chem. Mater.*, 2000, **12**, 2092.
16 E. V. Anokhina, C. S. Day, M. W. Essig and A. Lachgar, *Angew. Chem., Int. Ed.*, 2000, **39**, 1047.
17 R. J. Francis, P. S. Halasyamani and D. O'Hare, *Chem. Mater.*, 1998, **10**, 3131.
18 W. Schnick and J. Lücke, *Angew. Chem., Int. Ed. Engl.*, 1992, **31**, 213.
19 A. Choudhury, J. Krishnamoorthy and C. N. R. Rao, *Chem Commun.*, 2001, 2610.
20 R. L. Bedard, S. T. Wilson, L. D. Vail, J. M. Bennett and E. M. Flanigen, *Stud. Surf. Sci. Catal. A*, 1989, **49**, 375; O. M. Yaghi, Z. Sun, D. A. Richardson and T. L. Groy, *J. Am. Chem. Soc.*, 1994, **116**, 807.
21 W. T. A. Harrison, M. L. F. Phillips, J. Stanchfield and T. M. Nenoff, *Angew. Chem., Int. Ed.*, 2000, **39**, 3808.
22 J. D. Martin and K. B. Greenwood, *Angew. Chem., Int. Ed. Engl.*, 1997, **36**, 2072.
23 X.-H. Bu, P.-Y. Feng and G. D. Stucky, *J. Am. Chem. Soc.*, 1998, **120**, 11204.
24 T. E. Gier, X.-H. Bu, P.-Y. Feng and G. D. Stucky, *Nature*, 1998, **395**, 154.
25 K. R. Dunbar and R. A. Heintz, *Prog. Inorg. Chem.*, 1997, **45**, 283.

26 J. W. Johnson, A. J. Jacobson, W. M. Butler, S. E. Rosenthal, J. F. Brody and J. T. Lewandowsky, *J. Am. Chem. Soc.*, 1989, **111**, 381.
27 D. Riou, O. Roubeau and G. Férey, *Microporous Mesoporous Mater.*, 1998, **23**, 23; F. Serpaggi and G. Férey, *J. Mater. Chem.*, 1998, **8**, 2749; S. Drumel, P. Janvier, P. Barboux, M. Bujoli-Doeuff and B. Bujoli, *Inorg. Chem.*, 1995, **34**, 148.
28 A. Choudhury, S. Natarajan and C. N. R. Rao, *J. Solid State Chem.*, 1999, **146**, 538.
29 P. J. Hagrman, D. Hagrman and J. Zubieta, *Angew. Chem., Int. Ed.*, 1999, **38**, 2638.
30 C. Janiak, *Dalton Trans.*, 2003, 2781.
31 M. Eddaoudi, J. Kim, N. Rosi, D. Vodak, J. Wachter, M. O'Keeffe and O. M. Yaghi, *Science*, 2002, **295**, 469; H. Li, M. Eddaoudi, M. O'Keeffe and O. M. Yaghi, *Nature*, 1999, **402**, 276.
32 N. L. Rosi, J. Eckert, M. Eddaoudi, D. T. Vodak, J. Kim, M. O'Keefe and O. M. Yaghi, *Science*, 2003, **300**, 1127.
33 O. M. Yaghi, M. O'Keefe, N. W. Ocwig, H. K. Chae, M. Eddaoudi and J. Kim, *Nature*, 2003, **423**, 705.
34 B. Moulton and M. J. Zaworotko, *Chem. Rev.*, 2001, **101**, 1629.
35 M. Eddaoudi, D. B. Moler, H. L. Li, B. L. Chen, T. M. Reineke, M. O'Keeffe and O. M. Yaghi, *Acc. Chem. Res.*, 2001, **34**, 319.
36 R. Robson, *J. Chem. Soc., Dalton Trans.*, 2000, 3735.
37 M. J. Zaworotko, *Angew. Chem., Int. Ed.*, 2000, **39**, 3052.
38 O. M. Yaghi, H. L. Li, C. Davis, D. Richardson and T. L. Groy, *Acc. Chem. Res.*, 1998, **31**, 474.
39 A. J. Blake, N. R. Champness, P. Hubberstey, W.-S. Li, M. A. Withersby and M. Schröder, *Coord. Chem. Rev.*, 1999, **183**, 117.
40 C. N. R. Rao, S. Natarajan and R. Vaighyanathan, *Angew. Chem., Int. Ed.*, 2004, **43**, 1466.
41 For a general review of the state-of-art of the field, see: A. Nangia, *Curr. Opin. Solid State Mater. Sci.*, 2001, **5**, 115; P. J. Langley and J. Hulliger, *Chem. Soc. Rev.*, 1999, **28**, 279; G. R. Desiraju, *Curr. Opin. Solid State Mater Sci.*, 1997, **2**, 451.
42 For selected examples of purely organic channel-like structures, see: J.-H. Fournier, T. Maris and J. D. Wuest, *J. Org. Chem.*, 2004, **69**, 1762; D. Laliberté, T. Maris and J. D. Wuest, *J. Org. Chem.*, 2004, **69**, 1776; E. Demers, T. Maris and J. D. Wuest, *Cryst. Growth Des.*, 2005, **5**, 1227; D. Laliberté, T. Maris, A. Sirois and J. D. Wuest, *Org. Lett.*, 2003, **5**, 4787; H. Sauriat-Dorizon, T. Maris, J. D. Wuest and G. D. Enright, *J. Org. Chem.*, 2003, **68**, 240; Y. Miyahara, K. Abe and T. Inazu, *Angew. Chem., Int. Ed.*, 2002, **41**, 3020; D. T. Bong and M. R. Ghadiri, *Angew. Chem., Int. Ed.*, 2001, **40**, 2163; K. Sada, M. Sugahara, K. Kato and M. Miyata, *J. Am. Chem. Soc.*, 2001, **123**, 4386; Y.-H. Kiang, S. Lee, Z. Xu, W. Choe and G. B. Gardner, *Adv. Mater.*, 2000, **12**, 767; T. Müller, J. Hulliger, W. Seichter, E. Weber, T. Weber and M. Wübbenhorst, *Chem. Eur. J.*, 2000, **6**, 54; K. Kobayashi, T. Shirasaka, A. Sato, E. Horn and N. Furukawa, *Angew. Chem., Int. Ed.*, 1999, **38**, 3483; K. Biradha, D. Dennis, V. A. MacKinnon, C. V. K. Sharma and M. J. Zaworotko, *J. Am. Chem. Soc.*, 1998, **120**, 11894; V. A. Russel, C. C. Evans, W. J. Li and M. D. Ward, *Science*, 1997, **276**, 575.
43 B. T. Ibragimov, S. A. Talipov and T. F. Aripov, *J. Inclusion Phenom. Mol. Recognit. Chem.*, 1994, **17**, 317.
44 A. T. Ung, D. Gizachew, R. Bishop, M. L. Scudder, I. G. Dance and D. C. Craig, *J. Am. Chem. Soc.*, 1995, **117**, 8745; P. Brunet, M. Simard and J. D. Wuest, *J. Am. Chem. Soc.*, 1997, **119**, 2737; O. Saied, T. Maris, X. Wang, M. Simard and J. D. Wuest, *J. Am. Chem. Soc.*, 2005, **127**, 10008.
45 P. Sozzani, A. Comotti, R. Simonutti, T. Meersmann, J. W. Logan and A. Pines, *Angew. Chem., Int. Ed.*, 2000, **39**, 2695; T. Hertzsch, F. Budde, E. Weber and J. Hulliger, *Angew. Chem., Int. Ed.*, 2002, **41**, 2281.
46 N. Malek, T. Maris, M. Simard and J. D. Wuest, *J. Am. Chem. Soc.*, 2005, **127**, 5910.
47 M. Kondo, T. Yoshitomi, K. Seki, H. Matsuzaka and S. Kitagawa, *Angew. Chem., Int. Ed. Engl.*, 1997, **36**, 1725; M. Kondo, T. Okubo, A. Asami, S.-I. Noro, T. Yoshitomi, S. Kitagawa, T. Ishii, H. Matsuzaka and K. Seki, *Angew. Chem., Int. Ed.*, 1999, **38**, 140; S.-I. Noro, S. Kitagawa, M. Kondo and K. Seki, *Angew. Chem., Int. Ed.*, 2000, **39**, 2081; M. Eddaoudi, J. Kim, N. Rosi, D. Vodak, J. Wachter, M. O'Keeffe and O. M. Yaghi, *Science*, 2002, **295**, 469.
48 U. Mueller, M. Schubert, F. Teich, H. Puetter, K. Scielre-Arndt and J. Pastré, *J. Mater. Chem.*, 2006, **16**, 626.
49 For recent studies on H_2 adsorption, see: Y. Gogotsi, R. K. Dash, G. Yushin, T. Yildirim, G. Laudisio and J. E. Fischer, *J. Am. Chem. Soc.*, 2005, **127**, 16006; J. Perles, M. Iglesias, M.-A. Martin-Luengo, M. A. Monge, C. Ruiz-Valero and N. Snejko, *Chem. Mater.*, 2005, **17**, 5837; J. L. C. Rowsell, J. Eckert and O. M. Yaghi, *J. Am. Chem. Soc.*, 2005, **127**, 14904; K. W. Chapman, P. D. Southon, C. L. Weeks and C. J. Kepert, *Chem. Commun.*, 2005, 3322; S. Bordiga, J. G. Vitillo, G. Ricchiardi, L. Regli, D. Cocina, A. Zecchina, B. Arstad, M. Bjorgen, J. Hafizovic and K. P. Lillerud, *J. Phys. Chem. B*, 2005, **109**, 18237; T. Mueller and G. Ceder, *J. Phys. Chem. B*, 2005, **109**, 17974; M. Dinca and J. R. Long, *J. Am. Chem. Soc.*, 2005, **127**, 9376; H. Chun, D. N. Dybtsev, H. Kim and K. Kim, *Chem. Eur. J.*, 2005, **11**, 3521; S. S. Kaye and J. R. Long, *J. Am. Chem. Soc.*, 2005, **127**, 6506; B. Panella and M. Hirscher, *Adv. Mater.*, 2005, **17**, 538; E. Y. Lee, S. Y. Jang and M. P. Suh, *J. Am. Chem. Soc.*, 2005, **127**, 6374; J. L. C. Rowsell, A. R. Millward, K. S. Park and O. M. Yaghi, *J. Am. Chem. Soc.*, 2004, **126**, 5666; L. Pan, M. B. Sander, X. Huang, J. Li, M. Smith, E. Bittner, B. Bockrath and J. K. Johnson, *J. Am. Chem. Soc.*, 2004, **126**, 1308; P. M. Forster, J. Eckert, J.-S. Chang, S.-E. Park, G. Férey and A. K. Cheetham, *J. Am. Chem. Soc.*, 2003, **125**, 1309; D. N. Dybtsev, H. Chun and K. Kim, *Angew. Chem., Int. Ed.*, 2004, **43**, 5033; E. Y. Lee and M. P. Suh, *Angew. Chem., Int. Ed.*, 2004, **43**, 2798; G. Férey, M. Latroche, C. Serre, F. Millange, T. Loiseau and A. Percheron-Guégan, *Chem. Commun.*, 2003, 2976; M. Eddaoudi, H. Li and O. M. Yaghi, *J. Am. Chem. Soc.*, 2000, **122**, 1391; K. Seki and W. Mori, *J. Phys. Chem. B*, 2002, **106**, 1380; M. Kondo, T. Okubo, A. Asami, S. Noro, T. Yoshitomi, S. Kitagawa, T. Ishii, H. Matsuzaka and K. Seki, *Angew. Chem., Int. Ed.*, 1999, **38**, 140; Q. M. Wang, D. Shen, M. Bulow, M. L. Lau, S. Deng, F. R. Fitch, N. O. Lemcoff and J. Semanscin, *Microporous Mesoporous Mater.*, 2002, **55**, 217; R. Kitaura, K. Seki, G. Akiyama and S. Kitagawa, *Angew. Chem., Int. Ed.*, 2003, **42**, 428; H. Li, M. Eddaoudi, T. L. Groy and O. M. Yaghi, *J. Am. Chem. Soc.*, 1998, **120**, 8571.
50 S. M. Kuznicki, V. A. Bell, S. Nair, H. W. Hillhouse, R. M. Jacubinas, C. M. Braunbarth, B. H. Toby and M. Tsapatsis, *Nature*, 2001, **412**, 720; L. Pan, K. M. Adams, H. E. Hernandez, X. Wang, C. Zheng, Y. Hattori and K. Kaneko, *J. Am. Chem. Soc.*, 2003, **125**, 3062; D. N. Dybtsev, H. Chun, S. H. Yoon, D. Kim and K. Kim, *J. Am. Chem. Soc.*, 2004, **126**, 32.
51 For purely inorganic systems, see: C. B. Amphlett, *Inorganic Ion Exchangers*, Elsevier, Amsterdam, 1964; A. Clearfield, in *Inorganic Ion Exchange Materials*, CRC Press, Boca Raton, FL, 1982; A. Clearfield, *Chem. Rev.*, 1988, **88**, 125; R. Paterson and H. Rahman, *J. Colloid Interface Sci.*, 1984, **97**, 421; A. Clearfield, G. H. Nancollas and R. H. Blessing, in *Ion Exchange and Solvent Extraction*, ed. J. A. Marinsky and Y. Marcus, M. Dekker, New York, 1973, vol. 5, ch. 1; P. Maireles-Torres, P. Olivera-Pastor, E. Rodríguez-Castellón, A. Jiménez-López and A. A. G. Tomlinson, in *Recent Developments in Ion Exchange*, ed. P. A. Williams and M. J. Hudson, Elsevier, London, 1990, **vol. 2**.
52 For metal–organic systems, see: K.-M. Park and T. Iwamoto, *J. Chem. Soc., Chem. Commun.*, 1992, 72; J. Kim, D. Whang, J. I. Lee and K. Kim, *J. Chem. Soc., Chem. Commun.*, 1993, 1400; O. M. Yaghi and H. Li, *J. Am. Chem. Soc.*, 1995, **117**, 10401; O. M. Yaghi and H. Li, *J. Am. Chem. Soc.*, 1996, **118**, 295; K. S. Min and M. P. Suh, *J. Am. Chem. Soc.*, 2000, **122**, 6834; A. Kamiyama, T. Noguchi, T. Kajiwara and T. Ito, *Angew. Chem., Int. Ed.*, 2000, **39**, 3130.
53 K. Uemura, S. Kitagawa, M. Kondo, K. Fukui, R. Kitaura, H.-C. Chang and T. Mizutani, *Chem. Eur. J.*, 2002, **8**, 3586.
54 For metal–organic systems, see: M. Fujita, Y. J. Kwon, S. Washizu and K. Ogura, *J. Am. Chem. Soc.*, 1994, **116**, 1151; T. Sawaki and Y. Aoyama, *J. Am. Chem. Soc.*, 1999, **121**, 4793.
55 S. Kitagawa, R. Kitaura and S.-i. Noro, *Angew. Chem., Int. Ed.*, 2004, **43**, 2334; N. R. Champness, *Dalton Trans.*, 2006, 877; C. Kepert, *Chem. Commun.*, 2006, 695.

56 D. R. Corbin, J. F. Whitney, W. C. Fultz, G. D. Stucky, M. M. Eddy and A. K. Cheetham, *Inorg. Chem.*, 1986, **25**, 2279.
57 R. C. Haushalter and L. A. Mundi, *Chem. Mater.*, 1992, **4**, 31; H. E. King, Jr., L. A. Mundi, K. G. Strohmaier and R. C. Haushalter, *J. Solid State Chem.*, 1991, **92**, 154; L. A. Meyer and R. C. Haushalter, *Inorg. Chem.*, 1993, **32**, 1579.
58 V. Soghomonian, Q. Chen, R. C. Haushalter and J. Zubieta, *Angew. Chem., Int. Ed.*, 1993, **32**, 610; T. Loiseau and G. Férey, *J. Solid State Chem.*, 1994, **111**, 416; D. Riou and G. Férey, *J. Solid State Chem.*, 1994, **111**, 422.
59 Y. Zhang and A. Clearfield, *Inorg. Chem.*, 1992, **31**, 2821; Y. Zhang, K. J. Scott and A. Clearfield, *Chem. Mater.*, 1993, **5**, 495.
60 N. Zabukovec, L. Goliz, P. Fajdiga and V. Kaucic, *Zeolites*, 1995, **15**, 104.
61 V. Soghomonian, Q. Chen, R. C. Haushalter, J. Zubieta, C. J. O'Connor and Y.-S. Lee, *Chem. Mater.*, 1993, **5**, 1690.
62 J. Chen, R. H. Jones, S. Natarajan, M. B. Hursthouse and J. M. Thomas, *Angew. Chem., Int. Ed.*, 1994, **33**, 639.
63 J. L. Bideau, C. Payen, P. Palvadeau and B. Bujoli, *Inorg. Chem.*, 1994, **33**, 4885.
64 M. Riou-Cavellec, D. Riou and G. Férey, *Inorg. Chim. Acta*, 1999, **291**, 317.
65 K.-H. Lii, Y.-F. Huang, V. Zima, C.-Y. Huang, H.-M. Lin, Y.-C. Jiang, F.-L. Liao and S.-L. Wang, *Chem. Mater.*, 1998, **10**, 2599.
66 J. B. Goodenough, *Magnetism and the Chemical Bond*, Interscience, New York, 1963, p. 180.
67 P. W. Anderson, *Magnetism*, ed. G. Rado and H. Suhl, Academic Press, New York, 1963, **vol. 1**, p. 25.
68 A. Mgaidi, H. Boughzala, A. Driss, R. Clerac and C. Coulon, *J. Solid State Chem.*, 1999, **144**, 163.
69 A. Goñi, L. Lezama, A. Espina, C. Trobajo, J. R. García and T. Rojo, *J. Mater. Chem.*, 2001, **11**, 2315.
70 A. Choudhury and S. Natarajan, *Int. J. Inorg. Mater.*, 2000, **2**, 217.
71 P. D. Battle, A. K. Cheetham, W. T. A. Harrison and G. L. Long, *J. Solid State Chem.*, 1986, **62**, 16.
72 T. Moya-Pizzaro, R. Salmon, L. Fournes, G. Le Flem, B. Wanklyn and P. Hagenmuller, *J. Solid State Chem.*, 1984, **53**, 387.
73 D. Beltran-Porter, R. Olazcuaga, L. Fournes, F. Menil and G. Le Flem, *Rev. Phys. Appl.*, 1980, **15**, 1155.
74 Y. Song, P. Y. Zavalij, M. Suzuki and M. S. Whittingham, *Inorg. Chem.*, 2002, **41**, 5778.
75 J. L. Guth, H. Kessler and R. Wey, *Stud. Surf. Sci. Catal.*, 1986, **28**, 121; G. Férey, T. Loiseau and D. Riou, *Mater. Sci. Forum*, 1994, **152**, 125.
76 M. Cavellec, D. Riou, J. M. Grenèche and G. Férey, *J. Magn. Magn. Mater.*, 1996, **163**, 173.
77 M. Cavellec, C. Egger, J. Linares, M. Nogues, F. Varret and G. Férey, *J. Solid State Chem.*, 1997, **134**, 349.
78 S. Mandal, S. K. Pati, M. A. Green, S.-L. Wang and S. Natarajan, *Z. Anorg. Allg. Chem.*, 2003, **629**, 2549.
79 A. Choudhury and S. Natarajan, *J. Solid State Chem.*, 2000, **154**, 507.
80 J. R. D. Debord, W. M. Reiff, C. J. Warren, R. C. Haushalter and J. Zubieta, *Chem. Mater.*, 1997, **9**, 1994; C. Y. Huang, S. L. Wang and K.-H. Lii, *J. Porous Mater.*, 1998, **5**, 147.
81 A. Choudhury and S. Natarajan, *Proc. Indian Acad. Sci. (Chem. Sci.)*, 1999, **111**, 627.
82 M. Cavellec, D. Riou, C. Ninclaus, J. M. Grenèche and G. Férey, *Zeolites*, 1996, **17**, 250.
83 S. Mandal, M. A. Green and S. Natarajan, *J. Solid State Chem.*, 2004, **177**, 1117.
84 M. Cavellec, J. M. Grenèche and G. Férey, *Microporous Mesoporous Mater.*, 1998, **20**, 45.
85 A. Choudhury, S. Natarajan and C. N. R. Rao, *Chem. Commun.*, 1999, 1305.
86 S. Mandal, M. A. Green, S. Natarajan and S. K. Pati, *J. Phys. Chem. B*, 2004, **108**, 20351.
87 M. Cavellec, D. Riou, J. M. Grenèche and G. Férey, *Inorg. Chem.*, 1997, **36**, 2187.
88 S. Mandal, S. Natarajan, W. Klein, M. Panthöfer and M. Jansen, *J. Solid State Chem.*, 2003, **173**, 367.
89 M. Cavellec, J. M. Grenèche, D. Riou and G. Férey, *Microporous Mater.*, 1997, **8**, 103.
90 J. R. D. DeBord, W. M. Reiff, R. C. Haushalter and J. Zubieta, *J. Solid State Chem.*, 1996, **125**, 186.
91 M. Riou-Cavellec, J. M. Grenèche, D. Riou and G. Férey, *Chem. Mater.*, 1998, **10**, 2434.
92 S. Mandal, S. Natarajan, J. M. Grenèche, M. Riou-Cavellec and G. Férey, *Chem. Mater.*, 2002, **14**, 3751.
93 S. S. Lin and H. S. Weng, *Appl. Catal. A.*, 1993, **105**, 289; J. Chen, G. Sankar, J. M. Thomas, R. Xu, G. N. Greaves and D. Walter, *Chem. Mater.*, 1992, **4**, 1373.
94 S. Neeraj, S. Natarajan and C. N. R. Rao, *Angew. Chem., Int. Ed.*, 1999, **38**, 3480; C. N. R. Rao, S. Natarajan and S. Neeraj, *J. Solid State Chem.*, 2000, **152**, 302.
95 S. Natarajan, S. Neeraj and C. N. R. Rao, *Solid State Sci.*, 2000, **2**, 87; C. N. R. Rao, S. Natarajan and S. Neeraj, *J. Am. Chem. Soc.*, 2000, **122**, 2810.
96 H.-M. Yuan, J.-S. Chen, G.-S. Zhu, J.-Y. Li, J.-H. Yu, G.-D. Yang and R.-R. Xu, *Inorg. Chem.*, 2000, **39**, 1476.
97 For open-framework cobalt phosphates in which no magnetic properties have been measured, see: S. Natarajan, S. Neeraj, A. Choudhury and C. N. R. Rao, *Inorg. Chem.*, 2000, **39**, 1426; X. Bu, P. Feng, T. E. Gier and G. D. Stucky, *J. Solid State Chem.*, 1998, **136**, 210; X. Bu, P. Feng and G. D. Stucky, *J. Solid State Chem.*, 1997, **131**, 387; Y. Shan and S. D. Huang, *Acta Crystallogr., Sect. C*, 1999, **55**, 921; A. Guesmi, M. F. Zid and A. Driss, *Acta Crystallogr., Sect. C*, 2000, **56**, 511; R. Hammond and J. Barbier, *Acta Crystallogr., Sect. B*, 1996, **52**, 440; A. M. Chippindale, A. R. Cowley, J. Chen, Q. Gao and R. Xu, *Acta Crystallogr., Sect. C*, 1999, **55**, 845; P. F. Henry, E. M. Hughes and M. T. Weller, *J. Chem. Soc., Dalton Trans.*, 2000, 555; R.-K. Chiang, *J. Solid State Chem.*, 2000, **153**, 180; D. Kobashi, S. Kohara, J. Yamakawa and A. Kawahara, *Acta Crystallogr., Sect. C*, 1998, **54**, 7; S. Neeraj, M. L. Noy, C. N. R. Rao and A. K. Cheetham, *J. Solid State Chem.*, 2002, **167**, 344; S. Neeraj, C. N. R. Rao and A. K. Cheetham, *J. Mater. Chem.*, 2004, **14**, 814; F. Sanz, C. Parada, U. Amador, M. A. Monge and C. R. Valero, *J. Solid State Chem.*, 1996, **123**, 129.
98 A. Choudhury, S. Natarajan and C. N. R. Rao, *J. Solid State Chem.*, 2000, **155**, 62.
99 R. P. Bontchev, M. N. Iliev, L. M. Dezaneti and A. J. Jacobson, *Solid State Sci.*, 2001, **3**, 133.
100 P. Feng, X. Bu, S. H. Tolbert and G. D. Stucky, *J. Am. Chem. Soc.*, 1997, **119**, 2497.
101 W. M. Meier, D. H. Olsen and C. Baerlocher, *Atlas of Zeolite Structure Types*, Elsevier, London, 1996.
102 P. Feng, X. Bu and G. D. Stucky, *J. Solid State Chem.*, 1997, **129**, 328.
103 R.-K. Chiang, C.-C. Huang and C.-R. Lin, *J. Solid State Chem.*, 2001, **156**, 242.
104 J. R. D. DeBord, R. C. Haushalter and J. Zubieta, *J. Solid State Chem.*, 1996, **125**, 270.
105 P. Feng, X. Bu and G. D. Stucky, *J. Solid State Chem.*, 1997, **131**, 160.
106 R.-K. Chiang, *Inorg. Chem.*, 2000, **39**, 4985.
107 A. Choudhury, S. Neeraj, S. Natarajan and C. N. R. Rao, *Angew. Chem., Int. Ed.*, 2000, **39**, 3091.
108 R. Stief, C. Frommen, J. Pebler and W. Massa, *Z. Anorg. Allg. Chem.*, 1998, **624**, 461.
109 K. O. Kongshaug, H. Fjellvag and K. P. Lillerud, *J. Solid State Chem.*, 2001, **156**, 32.
110 C. V. K. Sharma, C. C. Chusuei, R. Clérac, T. Möller, K. R. Dunbar and A. Clearfield, *Inorg. Chem.*, 2003, **42**, 8300.
111 A. M. Chippindale, F. O. M. Gaslain, A. D. Bond and A. V. Powell, *J. Mater. Chem.*, 2003, **13**, 1950.
112 J. Escobal, J. L. Pizarro, J. L. Mesa, L. Lezama, R. Olazcuaga, M. I. Arriortua and T. Rojo, *Chem. Mater.*, 2000, **12**, 376.
113 A. M. Chippindale, F. O. M. Gaslain, A. R. Cowley and A. V. Powell, *J. Mater. Chem.*, 2001, **11**, 3172.
114 Y. Song, P. Y. Zavalij, N. A. Chernova and M. S. Whittingham, *Chem. Mater.*, 2003, **15**, 4968.
115 J. Escobal, J. L. Mesa, J. L. Pizarro, L. Lezama, R. Olazcuaga and T. Rojo, *J. Mater. Chem.*, 1999, **9**, 2691.

116 F. Sanz, C. Parada, J. M. Rojo and C. Ruiz-Valero, *Chem. Mater.*, 2001, **13**, 1334.
117 S. Neeraj, M. L. Noy and A. K. Cheetham, *Solid State Sci.*, 2002, **4**, 397.
118 N. Guillou, Q. Gao, M. Nogues, R. E. Morris, M. Hervieu, G. Férey and A. K. Cheetham, *C. R. Acad. Sci., Ser. IIc: Chim.*, 1999, 387.
119 N. Guillou, Q. Gao, P. M. Forster, J.-S. Chang, M. Noguès, S.-E. Park, G. Férey and A. K. Cheetham, *Angew. Chem., Int. Ed.*, 2001, **40**, 2831.
120 S. H. Jhung, J. W. Yoon, J.-S. Hwang, A. K. Cheetham and J.-S. Chang, *Chem. Mater.*, 2005, **17**, 4455.
121 S. Hwa Jhung, J.-S. Chang, S.-E. Park, P. M. Forster, G. Férey and A. K. Cheetham, *Chem. Mater.*, 2004, **16**, 1394.
122 J.-S. Chang, S.-E. Park, Q. Gao, G. Férey and A. K. Cheetham, *Chem. Commun.*, 2001, 859.
123 X. Wang and Q. Gao, *Mater. Lett.*, 2005, **59**, 446.
124 P. M. Forster, J. Eckert, J.-S. Chang, S.-E. Park, G. Férey and A. K. Cheetham, *J. Am. Chem. Soc.*, 2003, **125**, 1309.
125 S. H. Jhung, J.-S. Chang, J. W. Yoon, J.-M. Grenèche, G. Férey and A. K. Cheetham, *Chem. Mater.*, 2004, **16**, 5552; L. Xie, Q. Gao, X. Su, P. Wang and J. Shi, *Microporous Mesoporous Mater.*, 2004, **75**, 135; S. H. Jhung, J.-S. Chang, Y. K. Hwang, J.-M. Grenèche, G. Férey and A. K. Cheetham, *J. Phys. Chem. B*, 2005, **109**, 845.
126 A. Goñi, J. L. Pizarro, L. M. Lezama, G. E. Barberis, M. I. Arriortua and T. Rojo, *J. Mater. Chem.*, 1996, **6**, 421; A. Goñi, J. Rius, M. Insausti, L. M. Lezama, J. L. Pizarro, M. I. Arriortua and T. Rojo, *Chem. Mater.*, 1996, **8**, 1052; W. Liu, X. X. Yang, H. H. Chen, Y. X. Huang, W. Schnelle and J. T. Zhao, *Solid State Sci.*, 2004, **6**, 1375; N. Hamanaka and H. Imoto, *Inorg. Chem.*, 1998, **37**, 5844.
127 F. Sanz, C. Parada, J. M. Rojo and C. Ruiz-Valero, *Chem. Mater.*, 1999, **11**, 2673.
128 A. Daidouh, J. L. Martinez, C. Pico and M. L. Veiga, *J. Solid State Chem.*, 1999, **144**, 169.
129 M. Riou-Cavellec, J.-M. Grenèche and G. Férey, *J. Solid State Chem.*, 1999, **148**, 150.
130 C.-H. Lin and S.-L. Wang, *Chem. Mater.*, 2002, **14**, 96; A. D. Bond, A. M. Chippindale, A. R. Cowley and J. E. Readman, *Zeolites*, 1997, **19**, 326; C.-H. Lin and S.-L. Wang, *Inorg. Chem.*, 2005, **44**, 251; K.-F. Hsu and S.-L. Wang, *Chem. Commun.*, 2000, 135; P. Feng, X. Bu and G. D. Stucky, *Nature*, 1997, **388**, 735; A. R. Cowley and A. M. Chippindale, *Chem. Commun.*, 1996, 673; A. M. Chippindale, A. R. Cowley and R. I. Watson, *J. Mater. Chem.*, 1996, 661; A. M. Chippindale and A. R. Cowley, *Zeolites*, 1997, **18**, 176; M. Mrak, N. N. Tusar, A. Ristic, I. Arcon, F. Thibault-Starzyk and V. Kaucic, *Microporous Mesoporous Mater.*, 2002, **56**, 257; A. R. Cowley and A. M. Chippindale, *Microporous Mesoporous Mater.*, 1999, **28**, 163; A. M. Chippindale and R. I. Walton, *J. Chem. Soc., Chem. Commun.*, 1994, 2453.
131 P. Feng, X. Bu and G. D. Stucky, *Science*, 1997, **278**, 2080; N. Zabukovez, L. Goliè, P. Fajdiga and V. Kauèiè, *Zeolites*, 1995, **15**, 104; B. M. Lok, C. A. Messina, R. L. Patton, R. T. Gajek, T. R. Cannan and E. M. Flanigen, *J. Am. Chem. Soc.*, 1984, **106**, 6092; C. Borges, M. F. Ribeiro, C. Henriques, J. P. Lourenco, D. M. Murphy, A. Louati and Z. Gabelica, *J. Phys. Chem. B*, 2004, **108**, 8344; J. P. Hirst, J. B. Claridge, M. J. Rosseinsky and P. Bishop, *Chem. Commun.*, 2003, 684; C. Panz, K. Polborn and P. Bechrens, *Inorg. Chim. Acta*, 1998, **269**, 73; D. Goldfarb, *Zeolites*, 1989, **9**, 509; C. V. A. Duke, S. J. Hill and C. D. Williams, *Zeolites*, 1995, **15**, 413; N. Rajic, D. Stojakovic, S. Hocevar and V. Kaucic, *Zeolites*, 1993, **13**, 384.
132 Y.-H. Sun, X.-B. Cui, J.-Q. Xu, L. Ye, Y. Li, J. Lu, H. Ding and H.-Y. Bie, *J. Solid State Chem.*, 2004, **177**, 1811; C. du Peloux, P. Mialane, A. Dolbecq, J. Marrot, E. Riviere and F. Sécheresse, *J. Mater. Chem.*, 2001, **11**, 3392; J. J. Lu, Y. Xu, N. K. Goh and L. S. Chia, *Chem. Commum.*, 1998, 1709; C. du Peloux, P. Milane, A. Dolbecq, J. Marrot, E. Rivière and F. Sécheresse, *J. Mater. Chem.*, 2001, **11**, 3392.
133 M. B. Sorensen, R. G. Hazell, A. Bentien, A. D. Bond and T. R. Jensen, *Dalton Trans.*, 2004, 598.
134 A. M. Chippindale, A. D. Bond and A. R. Cowley, *Chem. Mater.*, 1997, **9**, 2830.
135 L. Liu, H. Meng, G. Li, Y. Cui, H. Ding, Y. Xing and W. Pang, *Mater. Lett.*, 2005, **59**, 1752.
136 V. Soghomonian, R. C. Haushalter, J. Zubieta and C. J. O'Connor, *Inorg. Chem.*, 1996, **35**, 2826; Y.-C. Yang, L.-I. Hung and S.-L. Wang, *Chem. Mater.*, 2005, **17**, 2833; E. Alba, S. Fernández, J. L. Mesa, J. L. Pizarro, V. Jubera and T. Rojo, *Mater. Res. Bull.*, 2002, **37**, 2355.
137 E. Alda, B. Bazán, J. L. Mesa, J. L. Pizarro, M. I. Arriortua and T. Rojo, *J. Solid State Chem.*, 2003, **173**, 101.
138 C. Serre, F. Taulelle and G. Férey, *Chem. Commun.*, 2003, 2755; C. Serre, F. Taulelle and G. Férey, *Chem. Mater.*, 2002, **14**, 998; D. M. Poojary, A. I. Bortun, L. N. Bortun and A. Clearfield, *J. Solid State Chem.*, 1997, **132**, 213; C. Serre and G. Férey, *C. R. Acad. Sci., Ser. IIc: Chim.*, 1999, 85; Y. Liu, Z. Shi, L. Zhang, Y. Fu, J. Chen, B. Li, J. Hua and W. Pang, *Chem. Mater.*, 2001, **13**, 2017.
139 S. Ekambaram and S. C. Sevov, *Angew. Chem., Int. Ed.*, 1999, **38**, 372; S. Ekambaram, C. Serre, G. Férey and S. C. Sevov, *Chem. Mater.*, 2000, **12**, 444.
140 S. Neeraj, T. Loiseau, C. N. R. Rao and A. K. Cheetham, *Solid State Sci.*, 2004, **6**, 1169.
141 S. C. Sevov, *Angew. Chem., Int. Ed. Engl.*, 1996, **35**, 2630.
142 R. Kniep, H. Engelhardt and C. Hauf, *Chem. Mater.*, 1998, **10**, 2930.
143 For examples of transition-metal ions based borophosphates in which not magnetic measurements have been done, see: R. Kniep, H. G. Will, I. Boy and C. Rohr, *Angew. Chem., Int. Ed.*, 1997, **36**, 1013; G. Schäfer, H. Borrmann and R. Kniep, *Z. Anorg. Allg. Chem.*, 2001, **627**, 61; I. Boy, G. Schäfer and R. Kniep, *Z. Anorg. Allg. Chem.*, 2001, **627**, 139; C. J. Warren, R. C. Haushalter, D. J. Rose and J. Zubieta, *Chem. Mater.*, 1997, **9**, 2694; R. Kniep and G. Schäfer, *Z. Anorg. Allg. Chem.*, 2000, **626**, 141; G. Schäfer, H. Borrmann and R. Kniep, *Microporous Mesoporous Mater.*, 2000, **41**, 161.
144 Y. X. Huang, G. Shäfer, W. Carrillo-Cabrera, R. Cardoso, W. Schnelle, J.-T. Zhao and R. Kniep, *Chem. Mater.*, 2001, **13**, 4348.
145 A. Yilmaz, L. T. Yildirim, X. Bu, M. Kizilyalli and G. D. Stucky, *Cryst. Res. Technol.*, 2005, **40**, 579; A. Yilmaz, X. Bu, M. Kizilyalli and G. D. Stucky, *Chem. Mater.*, 2000, **12**, 3243; H. Engelhardt, H. Borrmann, W. Schnelle and R. Kniep, *Z. Anorg. Allg. Chem.*, 2000, **626**, 1647.
146 R. P. Bontchev and A. J. Jacobson, *Mater. Res. Bull.*, 2002, **37**, 1997; H. Engelhardt, W. Schnelle and R. Kniep, *Z. Anorg. Allg. Chem.*, 2000, **626**, 1380.
147 M. Shieh, K. J. Martin, P. J. Squattrito and A. Clearfield, *Inorg. Chem.*, 1990, **29**, 958.
148 G. Bonavia, J. DeBord, R. C. Haushalter, D. Rose and J. Zubieta, *Chem. Mater.*, 1995, **7**, 1995.
149 W. Liu, H.-H. Chen, X.-X. Yang and J.-T. Zhao, *Eur. J. Inorg. Chem.*, 2005, 946.
150 S. Fernández, J. L. Mesa, J. L. Pizarro, L. Lezama, M. I. Arriortua and T. Rojo, *Angew. Chem., Int. Ed.*, 2002, **41**, 3683.
151 S. Fernández-Armas, J. L. Mesa, J. L. Pizarro, L. Lezama, M. I. Arriortua and T. Rojo, *J. Solid State Chem.*, 2004, **177**, 765.
152 S. Fernández, J. L. Mesa, J. L. Pizarro, L. Lezama, M. I. Arriortua and T. Rojo, *Chem. Mater.*, 2003, **15**, 1204.
153 S. Fernández, J. L. Mesa, J. L. Pizarro, A. Peña, J. Gutiérrez, M. I. Arriortua and T. Rojo, *J. Magn. Magn. Mater.*, 2004, **272–276**, 1113.
154 U.-C. Chung, J. L. Mesa, J. L. Pizarro, L. Lezama, J. S. Garitaonandia, J. P. Chapman and M. I. Arriortua, *J. Solid State Chem.*, 2004, **177**, 2705.
155 S. Fernández, J. L. Pizarro, J. L. Mesa, L. Lezama, M. I. Arriortua and T. Rojo, *Int. J. Inorg. Mater.*, 2001, **3**, 331.
156 S. Fernández-Armas, J. L. Mesa, J. L. Pizarro, A. Peña, J. P. Chapman and M. I. Arriortua, *Mater. Res. Bull.*, 2004, **39**, 1779.
157 S. Shi, L. Wang, H. Yuan, G. Li, J. Xu, G. Zhu, T. Song and S. Qiu, *J. Solid State Chem.*, 2004, **177**, 4183; D. Zhang, H. Yue, Z. Shi, M. Guo and S. Feng, *Microporous Mesoporous Mater.*, 2005, **82**, 209; R.-K. Chiang and N.-T. Chuang, *J. Solid State Chem.*, 2005, **178**, 3040.
158 S. Fernández, J. L. Mesa, J. L. Pizarro, L. Lezama, M. I. Arriortua and T. Rojo, *Chem. Mater.*, 2002, **14**, 2300.

159 Y. Fan, T. Song, G. Li, Z. Shi, G. Yu, J. Xu and S. Feng, *Inorg. Chem. Commun.*, 2005, **8**, 661.
160 Z.-E. Lin, J. Zhang, S.-T. Zheng and G.-Y. Yang, *J. Mater. Chem.*, 2004, **14**, 1652; S. Suhua, Q. Wei, L. Guanghua, W. Li, Y. Hongming, X. Jianing, Z. Guangshan, S. Tianyou and Q. Shilun, *J. Solid State Chem.*, 2004, **177**, 3038.
161 S. Ekambaram and S. C. Sevoc, *Inorg. Chem.*, 2000, **39**, 2405.
162 B. Bazán, J. L. Mesa, J. L. Pizarro, L. Lezama, M. I. Arriortua and T. Rojo, *Inorg. Chem.*, 2000, **39**, 6056.
163 J. L. Mesa, A. Goñi, A. L. Brandl, N. O. Moreno, G. E. Barberis and T. Rojo, *J. Mater. Chem.*, 2000, **10**, 2779.
164 R. D. Adams and R. Layland, *Polyhedron*, 1996, **15**, 1235; C.-Y. Cheng and S.-L. Wang, *J. Chem. Soc., Dalton Trans.*, 1992, 2395.
165 S. Chakrabarti, S. K. Pati, M. A. Green and S. Natarajan, *Eur. J. Inorg. Chem.*, 2004, 3846; S. Chakrabarti, S. K. Pati, M. A. Green and S. Natarajan, *Eur. J. Inorg. Chem.*, 2003, 3820.
166 M. Ulutagay-Kartin, S.-J. Hwu and J. A. Clayhold, *Inorg. Chem.*, 2003, **42**, 2405.
167 S.-J. Hwu, M. Ulutagay-Kartin, J. A. Clayhold, R. Mackay, T. A. Wardojo, C. J. O'Connor and M. Krawiec, *J. Am. Chem. Soc.*, 2002, **124**, 12404; J. A. Clayhold, M. Ulutagay-Kartin, S.-J. Hwu, H.-J. Koo, M.-H. Whangbo, A. Voigt and K. Eaiprasertsak, *Phys. Rev. B: Condens. Matter*, 2002, **66**, 052403.
168 R. J. B. Jakeman, M. J. Kwiecien, W. M. Reiff, A. K. Cheetham and C. C. Torardi, *Inorg. Chem.*, 1991, **30**, 2806.
169 B. Bazán, J. L. Mesa, J. L. Pizarro, A. T. Aguayo, M. I. Arriortua and T. Rojo, *Chem. Commun.*, 2003, 622.
170 B. Bazán, J. L. Mesa, J. L. Pizarro, J. Rodríguez-Fernández, J. Sánchez-Marcos, A. Roig, E. Molins, M. I. Arriortua and T. Rojo, *Chem. Mater.*, 2004, **16**, 5249.
171 S.-H. Luo, Y.-C. Jiang, S.-L. Wang, H.-M. Kao and K.-H. Lii, *Inorg. Chem.*, 2001, **40**, 5381; B. Bazán, J. L. Mesa, J. L. Pizarro, A. Goñi, L. Lezama, M. I. Arriortua and T. Rojo, *Inorg. Chem.*, 2001, **40**, 5691; B. Bazán, J. L. Mesa, J. L. Pizarro, L. Lezama, J. S. Garitaonandia, M. I. Arriortua and T. Rojo, *Solid State Sci.*, 2003, **5**, 1291.
172 N. Stock, G. D. Stucky and A. K. Cheetham, *J. Phys. Chem. Solids*, 2001, **62**, 1457; S.-L. Wang, J.-C. Horng and Y.-H. Lee, *J. Chem. Soc., Dalton Trans.*, 1994, 1825; S.-L. Wang and W.-J. Tsai, *J. Solid State Chem.*, 1996, **122**, 36.
173 B. Bazan, J. L. Mesa, J. L. Pizarro, A. Peña, M. I. Arriortua and T. Rojo, *Z. Anorg. Allg. Chem.*, 2005, **631**, 2026.
174 G. Paul, A. Choudhury and C. N. R. Rao, *J. Chem. Soc., Dalton Trans.*, 2002, 3859.
175 G. Paul, A. Choudhury and C. N. R. Rao, *Chem. Commun.*, 2002, 1904.
176 C. N. R. Rao, E. V. Sampathkumaran, R. Natarajan, G. Paul, J. N. Behera and A. Choudhury, *Chem. Mater.*, 2004, **16**, 1441.
177 J. N. Behera, G. Paul, A. Choudhury and C. N. R. Rao, *Chem. Commun.*, 2004, 456.
178 G. Paul, A. Choudhury, E. V. Sampathkumaran and C. N. R. Rao, *Angew. Chem., Int. Ed.*, 2002, **41**, 4297.
179 J. E. Greedan, *J. Mater. Chem.*, 2001, **11**, 37; A. P. Ramirez, *Annu. Rev. Mater. Sci.*, 1994, **24**, 453.
180 G. Paul, A. Choudhury and C. N. R. Rao, *Chem. Mater.*, 2003, **15**, 1174.
181 J. N. Behera, K. V. Gopalkrishnan and C. N. R. Rao, *Inorg. Chem.*, 2004, **43**, 2636.
182 Y. Fan, G. H. Li, L. Yang, Z. M. Zhang, Y. Chen, T. Y. Song and S. H. Feng, *Eur. J. Inorg. Chem.*, 2005, 3359.
183 Y.-P. Yuan, R.-Y. Wang, D.-Y. Kong, J.-G. Mao and A. Clearfield, *J. Solid State Chem.*, 2005, **178**, 2030; L. Liu, H. Meng, G. Li, Y. Cui, X. Wang and W. Pang, *J. Solid State Chem.*, 2005, **178**, 1003.
184 Anonymous, *Miscellanea Berolinensia ad incrementum scientiarum*, Berlin, 1710, vol. **1**, p. 377.
185 H. J. Buser, D. Schwarzenbach, W. Petter and A. Ludi, *Inorg. Chem.*, 1977, **16**, 2704.
186 K. R. Dunbar and R. A. Heintz, *Prog. Inorg. Chem.*, 1997, **45**, 283, and references therein.
187 M. Verdaguer, A. Bleuzen, V. Marvaud, J. Vaissermann, M. Seuleima, C. Desplanches, A. Scuiller, C. Train, R. Garde, G. Gelly, C. Lomenech, I. Rosenman, P. Veillet, C. Cartier and F. Villain, *Coord. Chem. Rev.*, 1999, **190–192**, 1023, and references therein.
188 S. Ferlay, T. Mallah, R. Ouahès, P. Veillet and M. Verdaguer, *Nature*, 1995, **378**, 701; T. Mallah, S. Thiébaut, M. Verdaguer and P. Veillet, *Science*, 1993, **262**, 1554; W. R. Entley and G. S. Girolami, *Science*, 1995, **268**, 397; Ø. Hatlevik, W. E. Buschmann, J. Zhang, J. L. Manson and J. S. Miller, *Adv. Mater.*, 1999, **11**, 914; S. M. Holmes and G. S. Girolami, *J. Am. Chem. Soc.*, 1999, **121**, 5593; O. Sato, T. Iyoda, A. Fujishima and K. Hashimoto, *Science*, 1996, **272**, 704; E. Dujardin, S. Ferlay, X. Phan, C. Desplanches, C. Cartier dit Moulin, P. Sainctavit, F. Baudelet, E. Dartyge, P. Veillet and M. Verdaguer, *J. Am. Chem. Soc.*, 1998, **120**, 11347.
189 G. B. Seifer, *Russ. J. Inorg. Chem.*, 1962, **7**, 899.
190 P. Cartraud, A. Cointot and A. Renaud, *J. Chem. Soc., Faraday Trans.*, 1981, **77**, 1561.
191 G. Boxhoorn, J. Mooljuysen, J. G. F. Coolegem and R. A. van Santen, *J. Chem. Soc., Chem. Commun.*, 1985, 1305.
192 J. Kuyper and G. Boxhoorn, *J. Catal.*, 1987, **105**, 163.
193 S. S. Kaye and J. R. Long, *J. Am. Chem. Soc.*, 2005, **127**, 6506; K. W. Chapman, P. D. Southon, C. L. Weeks and C. J. Kepert, *Chem. Commun.*, 2005, 3322.
194 F. Herren, P. Fischer, A. Ludi and W. Hälg, *Inorg. Chem.*, 1980, **19**, 956; G. B. Seifer, *Russ. J. Inorg. Chem.*, 1959, **4**, 841.
195 B. Mayoh and P. Day, *J. Chem. Soc., Dalton Trans.*, 1976, 1483; A. Ito, M. Suenaga and K. Ono, *J. Chem. Phys.*, 1968, **48**, 3597.
196 L. G. Beauvais and J. R. Long, *J. Am. Chem. Soc.*, 2002, **124**, 12096.
197 Z. Lü, X. Wang, Z. Liu, F. Liao, S. Gao, R. Xiong, H. Ma, D. Zhang and D. Zhu, *Inorg. Chem.*, 2006, **45**, 999.
198 W. Dong, L.-N. Zhu, Y.-Q. Sun, M. Liang, Z.-Q. Liu, D.-Z. Liao, Z.-H. Jiang, S.-P. Yan and P. Cheng, *Chem. Commun.*, 2003, 2544; J. Larionova, R. Clérac, B. Donnadieu, S. Willemin and C. Guérin, *Cryst. Growth Des.*, 2003, **3**, 267; J. Y. Yang, M. P. Shores, J. J. Sokol and J. R. Long, *Inorg. Chem.*, 2003, **42**, 1403; F.-T. Chen, D.-F. Li, S. Gao, X.-Y. Wang, Y.-Z. Li, L.-M. Zheng and W. X. Tang, *Dalton Trans.*, 2003, 3283.
199 M. P. Shores, L. G. Beauvais and J. R. Long, *J. Am. Chem. Soc.*, 1999, **121**, 775; M. V. Bennet, L. G. Beauvais, M. P. Shores and J. R. Long, *J. Am. Chem. Soc.*, 2001, **123**, 8022; M. V. Bennett, L. G. Beauvais, M. P. Shores and J. R. Long, *J. Am. Chem. Soc.*, 2001, **123**, 8022; L. G. Beauvais, M. P. Shores and J. R. Long, *J. Am. Chem. Soc.*, 2000, **122**, 2763; B. Yan, H. Zhou and A. Lachgar, *Inorg. Chem.*, 2003, **42**, 8818; E. G. Tulsky, N. R. M. Crawford, S. A. Baudron, P. Batail and J. R. Long, *J. Am. Chem. Soc.*, 2003, **125**, 15543; S.-M. Park, Y. Kim and S.-J. Kim, *Eur. J. Inorg. Chem.*, 2003, 4117.
200 J. A. Real, A. B. Gaspar and M. C. Muñoz, *Dalton Trans.*, 2005, 2062.
201 V. Niel, J. M. Martínez-Agudo, M. C. Muñoz, A. B. Gaspar and J. A. Real, *Inorg. Chem.*, 2001, **40**, 3838.
202 A. Schmidt and R. Glaum, *Inorg. Chem.*, 1997, **36**, 4883; X. Wang, L. Liu and A. J. Jacobson, *J. Am. Chem. Soc.*, 2002, **124**, 7812.
203 M. A. Monge, E. Gutiérrez-Puebla, C. Cascales and J. A. Campa, *Chem. Mater.*, 2000, **12**, 1926.
204 K. Barthelet, J. Marrot, D. Riou and G. Férey, *J. Solid State Chem.*, 2001, **162**, 266.
205 P. M. Almond, R. E. Sykora, S. Skanthakumar, L. Soderholm and T. E. Albrecht-Schmitt, *Inorg. Chem.*, 2004, **43**, 958.
206 W. Yang, C. Lu, Q. Zhang, S. Chen, X. Zhan and J. Liu, *Inorg. Chem.*, 2003, **42**, 7309.
207 H.-O. Stephan and M. G. Kanatzidis, *J. Am. Chem. Soc.*, 1996, **118**, 12226.
208 A. Choudury, U. Kuma and C. N. R. Rao, *Angew. Chem., Int. Ed.*, 2001, **41**, 158.
209 D. Riou, F. Belier, C. Serre, M. Nogues, D. Vichard and G. Férey, *Int. J. Inorg. Mater.*, 2000, **2**, 29.
210 D. Riou, C. Serre, J. Provost and G. Férey, *J. Solid State Chem.*, 2000, **155**, 238.
211 A. Choudhury, S. Natarajan and C. N. R. Rao, *Chem. Mater.*, 1999, **11**, 2316.
212 A. Choudhury and S. Natarajan, *J. Mater. Chem.*, 1999, **9**, 3113.
213 A. Choudhury, S. Natarajan and C. N. R. Rao, *Chem. Eur. J.*, 2000, **6**, 1168.

214 Y.-C. Jiang, S.-L. Wang and K.-H. Lii, *Chem. Mater.*, 2003, **15**, 1633.
215 Z. A. D. Lethbridge, S. K. Tiwary, A. Harrison and P. Lightfoot, *J. Chem. Soc., Dalton Trans.*, 2001, 1904.
216 Z. A. D. Lethbridge, A. D. Hillier, R. Cywinsky and P. Lightfoot, *J. Chem. Soc., Dalton Trans.*, 2000, 1595.
217 P. Yin, L.-M. Zheng, S. Gao and X.-Q. Xin, *Chem. Commun.*, 2001, 2346.
218 Z. Shi, G. Li, D. Zhang, J. Hua and S. Feng, *Inorg. Chem.*, 2003, **42**, 2357.
219 L.-I. Hung, S.-L. Wang, H. M. Kao and K.-H. Lii, *Inorg. Chem.*, 2002, **41**, 3929.
220 A. Rujiwatra, C. J. Kepert and M. J. Rosseinsky, *Chem. Commun.*, 1999, 2307.
221 A. Rujiwatra, C. J. Kepert, J. B. Claridge, M. J. Rosseinsky, H. Kumagai and M. Kurmoo, *J. Am. Chem. Soc.*, 2001, **123**, 10584.
222 M. Kurmoo, H. Kumagai, S. M. Hughes and C. J. Kepert, *Inorg. Chem.*, 2003, **42**, 6709.
223 K. Barthelet, K. Adil, F. Millange, C. Serre, D. Riou and G. Férey, *J. Mater. Chem.*, 2003, **13**, 2208.
224 D. J. Price, S. Tripp, A. K. Powell and P. T. Wood, *Chem. Eur. J.*, 2001, **7**, 200.
225 C. Serre, F. Millange, S. Surblé, J.-M. Grenèche and G. Férey, *Chem. Mater.*, 2004, **16**, 2706.
226 M. Sanselme, J.-M. Grenèche, M. Riou-Cavellec and G. Férey, *Solid State Sci.*, 2004, **6**, 853.
227 M. Kurmoo, H. Kumagai, K. W. Chapman and C. J. Kepert, *Chem. Commun.*, 2005, 3012; S. O. H. Gutschke, M. Molinier, A. K. Powell and P. T. Wood, *Angew. Chem., Int. Ed. Engl.*, 1997, **36**, 991.
228 S. O. H. Gutschke, D. J. Price, A. K. Powell and P. T. Wood, *Angew. Chem., Int. Ed.*, 2001, **40**, 1920.
229 Y.-Q. Zheng and H.-Z. Xie, *J. Solid State Chem.*, 2004, **177**, 1352.
230 N. Guillou, S. Pastre, C. Livage and G. Férey, *Chem. Commun.*, 2002, 2358.
231 F. Millange, C. Serre and G. Férey, *Chem. Commun.*, 2002, 822; C. Serre, F. Millange, C. Thouvenot, M. Noguès, G. Marsolier, D. Louër and G. Férey, *J. Am. Chem. Soc.*, 2002, **124**, 13519.
232 K. Barthelet, J. Marrot, D. Riou and G. Férey, *Angew. Chem., Int. Ed.*, 2002, **41**, 281.
233 C.-Z. Lu, C.-D. Wu, S.-F. Lu, J.-C. Liu, Q.-J. Wu, H.-H. Zhuang and J.-S. Huang, *Chem. Commun.*, 2002, 152.
234 M. Riou-Cavellec, M. Sanselme, M. Nogués, J.-M. Grenèche and G. Férey, *Solid State Sci.*, 2002, **4**, 619.
235 A. Choudhury, S. Natarajan and C. N. R. Rao, *J. Solid State Chem.*, 1999, **146**, 538.
236 W. Zhao, Y. Song, T. Okamura, J. Fan, W.-Y. Sun and N. Ueyama, *Inorg. Chem.*, 2005, **44**, 3330.
237 F. Lloret, M. Julve, R. Ruiz, Y. Journaux, K. Nakatani, O. Kahn and J. Sletten, *Inorg. Chem.*, 1993, **32**, 27; K. Nakatani, J. Y. Carriat, Y. Journaux, O. Kahn, F. Lloret, J. P. Renard, Y. Pei, J. Sletten and M. Verdaguer, *J. Am. Chem. Soc.*, 1989, **111**, 5739; S. Turner, O. Kahn and L. Rabardel, *J. Am. Chem. Soc.*, 1996, **118**, 6428.
238 O. Kahn, J. Larionova and J. V. Yakhmi, *Chem. Eur. J.*, 1999, **5**, 3443.
239 J. Larionova, S. A. Chavan, J. V. Yakhmi, A. G. Frøystein, J. Sletten, C. Sourisseau and O. Kahn, *Inorg. Chem.*, 1997, **36**, 6374.
240 J. D. Woodward, R. Backov, K. A. Abboud, H. Ohnuki, M. W. Meisel and D. R. Talham, *Polyhedron*, 2003, **22**, 2821; Z. Huang, H.-B. Song, M. Du, S.-T. Chen, X.-H. Bu and J. Ribas, *Inorg. Chem.*, 2004, **43**, 931; M. Du, Y.-M. Guo, S.-T. Chen, X.-H. Bu, S. R. Batten, J. Ribas and S. Kitagawa, *Inorg. Chem.*, 2004, **43**, 1287; D. M. Shin, I. S. Lee and Y. K. Chung, *Inorg. Chem.*, 2003, **42**, 8838.
241 D. N. Dybtsev, H. Chun, S. H. Yoon, D. Kim and K. Kim, *J. Am. Chem. Soc.*, 2004, **126**, 32.
242 R. P. Farrell, T. W. Hambley and P. A. Lay, *Inorg. Chem.*, 1995, **34**, 757.
243 E. Coronado and J. R. Galán-Mascarós, *J. Mater. Chem.*, 2005, **15**, 66; E. Coronado and P. Day, *Chem. Rev.*, 2004, **104**, 5419.
244 E. Coronado, J. R. Galán-Mascarós, C. J. Gómez-García and V. Laukhin, *Nature*, 2000, **408**, 447.
245 Z. Wang, B. Zhang, T. Otsuka, K. Inoue, H. Kobayashi and M. Kurmoo, *Dalton Trans.*, 2004, 2209.
246 X.-Y. Wang, L. Gan, S.-W. Zhang and S. Gao, *Inorg. Chem.*, 2004, **43**, 4615.
247 M. Viertelhaus, P. Adler, R. Clérac, C. E. Anson and A. K. Powell, *Eur. J. Inorg. Chem.*, 2005, 692.
248 Z. Wang, B. Zhang, H. Fujiwara, H. Kobayashi and M. Kurmoo, *Chem. Commun.*, 2004, 416.
249 A. Cornia, A. Caneschi, P. Dapporto, A. C. Fabretti, D. Gatteschi, W. Malavasi, C. Sangregorio and R. Sessoli, *Angew. Chem., Int. Ed.*, 1999, **38**, 1780.
250 T. Lancaster, S. J. Blundell, F. L. Pratt, E. Coronado and J. R. Galán-Mascarós, *J. Mater. Chem.*, 2004, **14**, 1518; T. Hashiguchi, Y. Miyazaki, K. Asano, M. Nakano, M. Sorai, H. Tamaki, N. Matsumoto and H. Okawa, *J. Chem. Phys.*, 2003, **119**, 6856; E. Coronado, J. R. Galán-Mascarós, C. J. Gómez-García and J. M. Martínez-Agudo, *Synth. Met.*, 2001, **122**, 501; A. Bhattacharjee, R. Feyerherm and M. Steiner, *J. Magn. Magn. Mater.*, 1999, **195**, 336; G. Antorrena, F. Palacio, M. Castro, R. Pellaux and S. Decurtins, *J. Magn. Magn. Mater.*, 1999, **196–197**, 581; C. J. Nuttall and P. Day, *Chem. Mater.*, 1998, **10**, 3050; R. Pellaux, H. W. Schmalle, R. Huber, P. Fischer, T. Hauss, B. Ouladdiaf and S. Decurtins, *Inorg. Chem.*, 1997, **36**, 2301; S. Decurtins, H. W. Schmalle, R. Pellaux, A. Hauser, M. E. von Arx and P. Fischer, *Synth. Met.*, 1997, **85**, 1689; R. Pellaux, H. W. Schmalle, S. Decurtins, P. Fischer, F. Fauth, B. Ouladdiaf and T. Hauss, *Physica B*, 1997, **234–236**, 783; S. Decurtins, H. W. Schmalle, R. Pellaux, R. Huber, P. Fischer and B. Ouladdiaf, *Adv. Mater.*, 1996, **8**, 647.
251 E. Coronado, J. R. Galán-Mascarós, C. J. Gómez-García, E. Martínez-Ferrero, M. Almeida and J. C. Waerenborgh, *Eur. J. Inorg. Chem.*, 2005, 2064; R. Andrés, M. Brissard, M. Gruselle, C. Train, J. Vaissermann, B. Malézieux, J.-P. Jamet and M. Verdaguer, *Inorg. Chem.*, 2001, **40**, 4633; E. Coronado, J. R. Galán-Mascarós, C. J. Gómez-García and J. M. Martínez-Agudo, *Inorg. Chem.*, 2001, **40**, 113; R. Sieber, S. Decurtins, H. Stoeckli-Evans, C. Wilson, D. Yufit, J. A. K. Howard, S. C. Capelli and A. Hauser, *Chem. Eur. J.*, 2000, **6**, 361; M. Hernández-Molina, F. Lloret, C. Ruiz-Pérez and M. Julve, *Inorg. Chem.*, 1998, **37**, 4131; S. Decurtins, H. W. Schmalle, R. Pellaux, P. Schneuwly and A. Hauser, *Inorg. Chem.*, 1996, **35**, 1451; S. Decurtins, H. W. Schmalle, R. Pellaux, R. Huber, P. Fischer and B. Ouladdiaf, *Adv. Mater.*, 1996, **8**, 647; S. Decurtins, H. W. Schmalle, P. Schneuwly, J. Ensling and P. Gutlicht, *J. Am. Chem. Soc.*, 1994, **116**, 9521; S. Decurtins, H. W. Schmalle, P. Schneuwly and H. R. Oswald, *Inorg. Chem.*, 1993, **32**, 1888.
252 D. Armentano, G. De Munno, F. Lloret, A. V. Palii and M. Julve, *Inorg. Chem.*, 2002, **41**, 2007.
253 D. Armentano, G. De Munno, T. F. Mastropietro, M. Julve and F. Lloret, *J. Am. Chem. Soc.*, 2005, **127**, 10778.
254 H.-Y. Shen, W.-M. Bu, D.-Z. Liao, Z.-H. Jiang, S.-P. Yan and G.-L. Wang, *Inorg. Chem.*, 2000, **39**, 2239.
255 R.-K. Chiang, C.-C. Huang and C.-S. Wur, *Inorg. Chem.*, 2001, **40**, 3237.
256 K. P. Mörtl, J.-P. Sutter, S. Golhen, L. Ouahab and O. Kahn, *Inorg. Chem.*, 2000, **39**, 1626.
257 T.-F. Liu, H.-L. Sun, S. Gao, S. W. Zhang and T.-C. Lau, *Inorg. Chem.*, 2003, **42**, 4792.
258 P. M. Forster and A. K. Cheetham, *Angew. Chem., Int. Ed.*, 2002, **41**, 457.
259 N. Guillou, C. Livage, M. Drillon and G. Férey, *Angew. Chem., Int. Ed.*, 2003, **42**, 5314.
260 S. J. Rettig, R. C. Thompson, J. Trotter and S. Xia, *Inorg. Chem.*, 1999, **38**, 1360.
261 For a review on transition metal oxalates, see: S. Decurtins, R. Pellaux, G. Antorrena and F. Palacio, *Coord. Chem. Rev.*, 1999, **190–192**, 841.
262 S. O. Nikolaï, V. D. Makhaev, S. M. Aldoshin, P. Gredin, K. Boubekeur, C. Train and M. Gruselle, *Dalton Trans.*, 2005, 3101; M. Gruselle, R. Thouvenot, B. Malézieux, C. Train, P. Gredin, T. V. Demeschik, L. L. Troitskaya and V. I. Sokolov, *Chem. Eur. J.*, 2004, **10**, 4763; I. D. Watts, S. G. Carling and

P. Day, *J. Chem. Soc., Dalton Trans.*, 2002, 1429; E. Coronado, J. R. Galán-Mascarós, C. J. Gómez-García, J. M. Martínez-Agudo, E. Martínez-Ferrero, J. C. Waerenborgh and M. Almeida, *J. Solid State Chem.*, 2001, **159**, 391; B. Malézieux, R. Andrés, M. Brissard, M. Gruselle, C. Train, P. Herson, L. L. Troitskaya, V. I. Sokolov, S. T. Ovseenko, T. V. Demeschik, N. S. Ovanesyan and I. A. Mamed'yarova, *J. Organomet. Chem.*, 2001, **637–639**, 182; E. Coronado, J. R. Galán-Mascarós, C. J. Gómez-García, J. Ensling and P. Gütlich, *Chem. Eur. J.*, 2000, **6**, 552; E. Coronado, J. R. Galán-Mascarós, C. J. Gómez-García and J. M. Martínez-Agudo, *Adv. Mater.*, 1999, **11**, 558; J. Larionova, B. Mombelli, J. Sanchiz and O. Kahn, *Inorg. Chem.*, 1998, **37**, 679; M. Clemente-León, E. Coronado, J. R. Galán-Mascarós and C. J. Gómez-García, *Chem. Commun.*, 1997, 1727; S. G. Carling, C. Mathonière, P. Day, K. M. A. Malik, S. J. Coles and M. B. Hursthouse, *J. Chem. Soc., Dalton Trans.*, 1996, 1839; C. Mathonière, C. J. Nuttall, S. G. Carling and P. Day, *Inorg. Chem.*, 1996, **35**, 1201; S. Decurtins, H. W. Schmalle and H. R. Oswald, *Inorg. Chim. Acta*, 1994, **216**, 65; C. Mathonière, S. G. Carling, D. Yusheng and P. Day, *J. Chem. Soc., Chem. Commun.*, 1994, 1551; L. O. Atovmyan, G. V. Shilov, R. N. Lyubovskaya, E. I. Zhilyaeva, N. S. Ovanesyan, S. I. Pirumova, I. G. Gusakovskaya and Y. G. Morozov, *JETP Lett.*, 1993, **58**, 766; H. Tamaki, Z. J. Zhong, N. Matsumoto, S. Kida, M. Koikawa, N. Achiwa, Y. Hashimoto and H. Okawa, *J. Am. Chem. Soc.*, 1992, **114**, 6974.

263 T. K. Maji, S. Sain, G. Mostafa, T.-H. Lu, J. Ribas, M. Montfort and N. R. Chaudhuri, *Inorg. Chem.*, 2003, **42**, 709.

264 S. Sain, T. K. Maji, G. Mostafa, T.-H. Lu and N. R. Chaudhuri, *New J. Chem.*, 2003, **27**, 185.

265 F. S. Delgado, J. Sanchiz, C. Ruiz-Pérez, F. Lloret and M. Julve, *Inorg. Chem.*, 2003, **42**, 5938.

266 S. Konar, P. S. Mukherjee, M. G. B. Drew, J. Ribas and N. R. Chaudhuri, *Inorg. Chem.*, 2003, **42**, 2545; S. Konar, S. C. Manna, E. Zangrando, T. Mallah, J. Ribas and N. R. Chaudhury, *Eur. J. Inorg. Chem.*, 2004, 4202; Q. Liu, Y.-z. Li, Y. Song, H. Liu and Z. Xu, *J. Solid State Chem.*, 2004, **177**, 4701.

267 L.-S. Long, X.-M. Chen, M.-L. Tong, Z.-G. Sun, Y.-P. Ren, R.-B. Huang and L.-S. Zheng, *J. Chem. Soc., Dalton Trans.*, 2001, 2888.

268 Y. J. Kim and D.-Y. Jung, *Bull. Korean Chem. Soc.*, 1999, **20**, 827.

269 Y.-Q. Zheng, J.-L. Lin and Z.-P. Kong, *Inorg. Chem.*, 2004, **43**, 2590.

270 E. Lee, Y. Kim and D.-Y. Jung, *Inorg. Chem.*, 2002, **41**, 501.

271 H. Kumagai, C. J. Kepert and M. Kurmoo, *Inorg. Chem.*, 2002, **41**, 3410.

272 Y.-L. Wang, D.-Q. Yuan, W.-H. Bi, X. Li, X.-J. Li, F. Li and R. Cao, *Cryst. Growth Des.*, 2005, **5**, 1849.

273 X.-Y. Wang, H.-Y. Wei, Z.-M. Wang, Z.-D. Chen and S. Gao, *Inorg. Chem.*, 2005, **44**, 572.

274 J. Y. Lu, M. A. Lawandy, J. Li, T. Yuen and C. L. Lin, *Inorg. Chem.*, 1999, **38**, 2695; T. Yuen, C. L. Lin, T. W. Mihalisin, M. A. Lawandy and J. Li, *J. Appl. Phys.*, 2000, **87**, 6001.

275 L.-M. Zheng, X. Fang, K.-H. Lii, H.-H. Song, X.-Q. Xin, H.-K. Fun, K. Chinnakali and I. A. Razak, *J. Chem. Soc., Dalton Trans.*, 1999, 2311.

276 G. De Mundo, M. Julve, F. Nicolo, F. Lloret, J. Faus, R. Ruiz and E. Sinn, *Angew. Chem., Int. Ed. Engl.*, 1993, **32**, 613; G. De Mundo, R. Ruiz, F. Lloret, J. Faus, R. Sessoli and M. Julve, *Inorg. Chem.*, 1995, **34**, 408.

277 N. Guillou, C. Livage, W. van Beek, M. Nogués and G. Férey, *Angew. Chem., Int. Ed.*, 2003, **42**, 644.

278 H. Kumagai, M. Akita-Tanaka, K. Inoue and M. Kurmoo, *J. Mater. Chem.*, 2001, **11**, 2146.

279 M. Riou-Cavellec, C. Albinet, C. Livage, N. Guillou, M. Noguès, J. M. Grenèche and G. Férey, *Solid State Sci.*, 2002, **4**, 267.

280 C. Livage, N. Guillou, J. Marrot and G. Férey, *Chem. Mater.*, 2001, **13**, 4387.

281 M. E. Chapman, P. Ayyappan, B. M. Foxman, G. T. Yee and W. Lin, *Cryst. Growth Des.*, 2001, **1**, 159.

282 Y.-H. Liu, Y.-L. Lu, H.-L. Tsai, J.-C. Wang and K.-L. Lu, *J. Solid State Chem.*, 2001, **158**, 315.

283 Secondary building units (SBUs) are molecular complexes and cluster entities in which ligand coordination modes and metal coordination environments can be utilized in the transformation of these fragments into extended porous networks using polytopic linkers. See ref. 35.

284 S. S.-Y. Chui, S. M.-F. Lo, J. P. H. Charmant, A. G. Orpen and I. D. Williams, *Science*, 1999, **283**, 1148.

285 X. X. Zhang, S. S.-Y. Chui and I. D. Williams, *J. Appl. Phys.*, 2000, **87**, 6007.

286 B. Moulton, J. Lu, R. Hajndl, S. Hariharan and M. J. Zaworotko, *Angew. Chem., Int. Ed.*, 2002, **41**, 2821; J. L. Atwood, *Nat. Mater.*, 2002, **1**, 91.

287 S. A. Bourne, J. Lu, A. Mondal, B. Moulton and M. J. Zaworotko, *Angew. Chem., Int. Ed.*, 2001, **40**, 2111.

288 H. Srikanth, R. Hajndl, B. Moulton and M. J. Zaworotko, *J. Appl. Phys.*, 2003, **93**, 7089.

289 B. Chen, M. Eddaoudi, T. M. Reineke, J. W. Kampf, M. O'Keeffe and O. M. Yaghi, *J. Am. Chem. Soc.*, 2000, **122**, 11559.

290 R. Cao, Q. Shi, D. Sun, M. Hong, W. Bi and Y. Zhao, *Inorg. Chem.*, 2002, **41**, 6161.

291 J. P. García-Terán, O. Castillo, A. Luque, U. García-Couceiro, P. Román and L. Lezama, *Inorg. Chem.*, 2004, **43**, 4549.

292 Y. Li, N. Hao, Y. Lu, E. Wang, Z. Kang and C. Hu, *Inorg. Chem.*, 2003, **42**, 3119; Y. Li, H. Zhang, E. Wang, N. Hao, C. Hu, Y. Yan and D. Hall, *New J. Chem.*, 2002, **26**, 1619.

293 Y.-Q. Zheng and E.-B. Ying, *Polyhedron*, 2005, **24**, 397; Y.-Q. Zheng, J.-L. Lin and Z.-P. Kong, *Inorg. Chem.*, 2004, **43**, 2590.

294 Y.-H. Liu, H.-L. Tsai, Y.-L. Lu, Y.-S. Wen, J.-C. Wang and K.-L. Lu, *Inorg. Chem.*, 2001, **40**, 6426.

295 W. Lin, O. R. Evans and G. T. Yee, *J. Solid State Chem.*, 2000, **152**, 152; R.-K. Chiang, N.-T. Chuang, C.-S. Wur, M.-F. Chong and C.-R. Lin, *J. Solid State Chem.*, 2002, **166**, 158; B.-Q. Ma, D.-S. Zhang, S. Gao, T.-Z. Jin, C.-H. Yan and G.-X. Xu, *Angew. Chem., Int. Ed.*, 2000, **39**, 3644; X.-J. Zheng, L.-P. Jin and S. Gao, *Inorg. Chem.*, 2004, **43**, 1600.

296 K. Barthelet, D. Riou and G. Férey, *Chem. Commun.*, 2002, 1492.

297 S. Xiang, X. Wu, J. Zhang, R. Fu, S. Hu and X. Zhang, *J. Am. Chem. Soc.*, 2005, **127**, 16352.

298 J. W. Ko, K. S. Min and M. P. Suh, *Inorg. Chem.*, 2002, **41**, 2151; T.-B. Lu, H. Xiang, R. L. Luck, L. Jiang, Z.-W. Mao and L.-N. Ji, *New J. Chem.*, 2002, **26**, 969; D. Cheng, M. A. Khan and R. P. Houser, *J. Chem. Soc., Dalton Trans.*, 2002, 4555.

299 H. J. Choi and M. P. Suh, *J. Am. Chem. Soc.*, 1998, **120**, 10622.

300 C. Livage, N. Guillou, J. Marrot and G. Férey, *Chem. Mater.*, 2001, **13**, 4387.

301 L.-J. Zhang, J.-Q. Xu, Z. Shi, X.-L. Zhao and T.-G. Wang, *J. Solid State Chem.*, 2003, **32**, 32.

302 H. Grove, J. Sletten, M. Julve, F. Lloret and L. Lezama, *Inorg. Chim. Acta*, 2000, **310**, 217; N. Masciocchi, S. Galli, A. Sironi, E. Barea, J. A. R. Navarro, J. M. Salas and L. C. Tabares, *Chem. Mater.*, 2003, **15**, 2153.

303 G. J. Halder, C. J. Kepert, B. Moubaraki, K. S. Murray and J. D. Cashion, *Science*, 2002, **298**, 1762.

304 Y. Q. Tian, C.-X. Cai, X.-M. Ren, C.-Y. Duan, Y. Xu, S. Gao and X.-Z. You, *Chem. Eur. J.*, 2003, **9**, 5673.

305 B.-B. Ding, Y.-Q. Weng, Z.-W. Mao, C.-K. Lam, X.-M. Chen and B.-H. Ye, *Inorg. Chem.*, 2005, **44**, 8836.

306 Y.-Q. Zheng and Z.-P. Kong, *Z. Anorg. Allg. Chem.*, 2003, **629**, 1469.

307 S. Konar, M. Corbella, E. Zangrado, J. Ribas and N. R. Chaudhuri, *Chem. Commun.*, 2003, 1424; S. C. Manna, E. Zangrado, J. Ribas and N. R. Chaudhuri, *Inorg. Chim. Acta*, 2005, **358**, 4497.

308 J. Greve, I. Jeβ and C. Näther, *J. Solid State Chem.*, 2003, **175**, 328.

309 A. Caneschi, D. Gatteschi, R. Sessoli and P. Rey, *Acc. Chem. Res.*, 1989, **22**, 392.

310 O. Kahn, *Molecular Magnetism*, Wiley-VCH, New York, 1993; J. S. Miller and M. Drillon, *Magnetism: Molecules to Materials II*, Wiley-VCH, Weinheim, 2001; M. M. Turnbull, T. Sugimoto and L. K. Thompson, *Molecule-based Magnetic Materials: Theory, Techniques and Applications*, ACS Publications, Washington D.C., 1996; K. Itoh and M. Kinoshita, *Molecular Magnetism: New Magnetic Materials*, Kodansha, Tokyo, 2000; J. Veciana, C. Rovira and D. B. Amabilino, *Supramolecular Engineering of Synthetic Metallic Materials: Conductors and Magnets*, Kluwer Academics Publishers, Dordrecht, 1999.

311 D. Maspoch, N. Domingo, D. Ruiz-Molina, K. Wurst, J. Tejada, C. Rovira and J. Veciana, *C. R. Chem.*, 2005, **8**, 1213.
312 D. Maspoch, D. Ruiz-Molina, K. Wurst, N. Domingo, M. Cavallini, F. Biscarini, J. Tejada, C. Rovira and J. Veciana, *Nat. Mater.*, 2003, **2**, 190.
313 D. Maspoch, D. Ruiz-Molina, K. Wurst, C. Rovira and J. Veciana, *Chem. Commun.*, 2004, 1164.
314 D. Maspoch, N. Domingo, D. Ruiz-Molina, K. Wurst, J. M. Hernández, G. Vaughan, C. Rovira, F. Lloret, J. Tejada and J. Veciana, *Chem. Commun.*, 2005, 5035.
315 J. Omata, T. Ishida, D. Hashizume, F. Iwasaki and T. Nogami, *Inorg. Chem.*, 2001, **40**, 3954; T. Ishida, J. Omata and T. Nogami, *Polyhedron*, 2003, **22**, 2133; H.-H. Lin, S. Mohanta, C.-J. Lee and H.-H. Wei, *Inorg. Chem.*, 2003, **42**, 1584.
316 M. Ballester, *Acc. Chem. Res.*, 1985, **12**, 380.
317 D. Maspoch, N. Domingo, D. Ruiz-Molina, K. Wurst, J. Tejada, C. Rovira and J. Veciana, *J. Am. Chem. Soc.*, 2004, **126**, 730.
318 D. Maspoch, N. Domingo, D. Ruiz-Molina, K. Wurst, G. Vaughan, J. Tejada, C. Rovira and J. Veciana, *Angew. Chem., Int. Ed.*, 2004, **43**, 1828.
319 D. Maspoch, L. Catala, P. Gerbier, D. Ruiz-Molina, J. Vidal-Gancedo, K. Wurst, C. Rovira and J. Veciana, *Chem. Eur. J.*, 2002, **8**, 3635.
320 B. Kesanli and W. Lin, *Coord. Chem. Rev.*, 2003, **246**, 305.
321 W. Lin, *J. Solid State Chem.*, 2005, **178**, 2486.
322 V. L. Pecoraro, J. J. Bodwin and A. D. Cutland, *J. Solid State Chem.*, 2000, **152**, 68.
323 D. Bradshaw, J. B. Claridge, E. J. Cussen, T. J. Prior and M. J. Rosseinsky, *Acc. Chem. Res.*, 2005, **38**, 273.
324 D. Bradshaw, T. J. Prior, E. J. Cussen, J. B. Claridge and M. J. Rosseinsky, *J. Am. Chem. Soc.*, 2004, **126**, 6106.
325 W. T. A. Harrison, T. E. Gier, G. D. Stucky, R. W. Broach and R. A. Bedard, *Chem. Mater.*, 1996, **8**, 145.
326 S. Ayyappan, X. Bu, A. K. Cheetham and C. N. R. Rao, *Chem. Mater.*, 1998, **10**, 3308.
327 G. Schäfer, W. Carrillo-Cabrera, S. Leoni, H. Borrmann and R. Kniep, *Z. Anorg. Allg. Chem.*, 2002, **628**, 67.
328 B. F. Abrahams, P. A. Jackson and R. Robson, *Angew. Chem., Int. Ed.*, 1998, **37**, 2656.
329 K. Biradha, C. Seward and M. J. Zaworotko, *Angew. Chem., Int. Ed.*, 1999, **38**, 492.
330 A. J. Blake, N. R. Champness, P. A. Cooke and J. E. B. Nicolson, *Chem. Commun.*, 2000, 665.
331 M. Sasa, K. Tanaka, X.-H. Bu, M. Shiro and M. Shionoya, *J. Am. Chem. Soc.*, 2001, **123**, 10750.
332 M. Du, Y.-M. Guo, S.-T. Chen, X.-H. Bu, S. R. Battern, J. Ribas and S. Kitagawa, *Inorg. Chem.*, 2004, **43**, 1287.
333 S. M. Stalder and A. P. Wilkinson, *Chem. Mater.*, 1997, **9**, 2168.
334 C. J. Kepert and M. J. Rosseinsky, *Chem. Commun.*, 1998, 31.
335 C. J. Kepert, T. J. Prior and M. J. Rosseinsky, *J. Am. Chem. Soc.*, 2000, **122**, 5158.
336 J. S. Seo, D. Whang, H. Lee, S. I. Jun, J. Oh, Y. J. Jeon and K. Kim, *Nature*, 2000, **404**, 982.
337 S. Thushari, J. A. K. Cha, H. H.-Y. Sung, S. S.-Y. Chui, A. L.-F. Leung, Y.-F. Yen and I. D. Williams, *Chem. Commun.*, 2005, 5515.
338 O. R. Evans, H. L. Ngo and W. Lin, *J. Am. Chem. Soc.*, 2001, **123**, 10395.
339 O. R. Evans, D. R. Manke and W. Lin, *Chem. Mater.*, 2002, **14**, 3866.
340 A. Hu, H. L. Ngo and W. Lin, *Angew. Chem., Int. Ed.*, 2003, **42**, 6000.
341 A. Hu, H. L. Ngo and W. Lin, *J. Am. Chem. Soc.*, 2003, **125**, 11490.
342 H. L. Ngo, A. Hu and W. Lin, *J. Mol. Catal. A: Chem.*, 2004, **215**, 177.
343 H. L. Ngo and W. Lin, *J. Am. Chem. Soc.*, 2002, **124**, 14298.
344 Y. Cui, O. R. Evans, H. L. Ngo, P. S. White and W. Lin, *Angew. Chem., Int. Ed.*, 2002, **41**, 1159.
345 Y. Cui, H. L. Ngo, P. S. White and W. Lin, *Chem. Commun.*, 2002, 1666.
346 Y. Cui, H. L. Ngo, P. S. White and W. Lin, *Chem. Commun.*, 2003, 994.
347 Y. Cui, H. L. Ngo, P. S. White and W. Lin, *Inorg. Chem.*, 2003, **42**, 652.
348 C.-D. Wu and W. Lin, *Inorg. Chem.*, 2005, **44**, 1178.
349 Y. Cui, S. J. Lee and W. Lin, *J. Am. Chem. Soc.*, 2003, **125**, 6014.
350 C.-D. Wu, A. Hu, L. Zhang and W. Lin, *J. Am. Chem. Soc.*, 2005, **127**, 8940.
351 R.-G. Xiong, X.-Z. You, B. F. Abrahams, Z. Xue and C.-M. Che, *Angew. Chem., Int. Ed.*, 2001, **40**, 4422.
352 Md. A. Alam, M. Nethaji and M. Ray, *Inorg. Chem.*, 2005, **44**, 1302.
353 N. G. Pschirer, D. M. Ciurtin, M. D. Smith, U. H. F. Bunz and H.-C. zur Loye, *Angew. Chem., Int. Ed.*, 2002, **41**, 583.
354 J. J. Bodwin and V. L. Pecoraro, *Inorg. Chem.*, 2000, **39**, 3434.
355 J. D. Ranford, J. J. Vittal and D. Wu, *Angew. Chem., Int. Ed.*, 1998, **37**, 1114.
356 J. D. Ranford, J. J. Vittal, D. Wu and X. Yang, *Angew. Chem., Int. Ed.*, 1999, **38**, 3498.
357 H. Shirakawa, *Angew. Chem., Int. Ed.*, 2001, **40**, 2574; A. G. MacDiarmid, *Angew. Chem., Int. Ed.*, 2001, **40**, 2581; A. J. Heeger, *Angew. Chem., Int. Ed.*, 2001, **40**, 2591.
358 R. L. Benard, S. T. Wilson, L. D. Vail, E. M. Bennet and E. M. Flanigen, *Zeolites: Facts, Figures, Future*, ed. P. A. Jacobs and R. A. Van Santen, Elsevier, Amsterdam, 1989; J. B. Parise, *Science*, 1991, **251**, 293; H.-O. Stephan and M. G. Kanatzidis, *J. Am. Chem. Soc.*, 1996, **118**, 12226.
359 For reviews, see: C. L. Bowes and G. A. Ozin, *Adv. Mater.*, 1996, **8**, 13; P. Feng, X. Bu and N. Zheng, *Acc. Chem. Res.*, 2005, **38**, 293; R. W. J. Scott, M. J. MacLachlan and G. A. Ozin, *Curr. Opin. Solid State Mater. Sci.*, 1999, **4**, 113; X. Bu, N. Zheng and P. Feng, *Chem. Eur. J.*, 2004, **10**, 3356.
360 H. Li, A. Laine, M. O'Keeffe and O. M. Yaghi, *Science*, 1999, **283**, 1145; H. Li, J. Kim, T. L. Groy, M. O'Keefe and O. M. Yaghi, *J. Am. Chem. Soc.*, 2001, **123**, 4867; X. Bu, N. Zheng, Y. Li and P. Feng, *J. Am. Chem. Soc.*, 2002, **124**, 12646; X. Bu, N. Zheng, Y. Li and P. Feng, *J. Am. Chem. Soc.*, 2003, **125**, 6024; N. Zheng, X. Bu and P. Feng, *J. Am. Chem. Soc.*, 2003, **125**, 1138; C. Wang, Y. Li, X. Bu, N. Zheng, O. Zivkovic, C.-S. Yang and P. Feng, *J. Am. Chem. Soc.*, 2001, **123**, 11506; C. L. Cahill and J. B. Parise, *J. Chem. Soc., Dalton Trans.*, 2000, 1475; H. Ahari, A. Lough, S. Petrov, G. A. Ozin and R. L. Bedard, *J. Mater. Chem.*, 1999, **9**, 1263; C. L. Cahill, Y. Ko and J. B. Parise, *Chem. Mater.*, 1998, **10**, 19.
361 N. Zheng, X. Bu, B. Wang and P. Feng, *Science*, 2002, **298**, 2366.
362 S. Dhingra and M. G. Kanatzidis, *Science*, 1992, **258**, 1769.
363 T. J. McCarthy, T. A. Tanzer and M. G. Kanatzidis, *J. Am. Chem. Soc.*, 1995, **117**, 1294.
364 E. A. Axtell, J.-H. Liao, Z. Pikramenou, Y. Park and M. G. Kanatzidis, *J. Am. Chem. Soc.*, 1993, **115**, 12191.
365 K. Chondroudis and M. G. Kanatzidis, *J. Solid State Chem.*, 1998, **136**, 328.
366 X. Bu, N. Zheng, X. Wang, B. Wang and P. Feng, *Angew. Chem., Int. Ed.*, 2004, **43**, 1502; N. Zheng, X. Bu and P. Feng, *J. Am. Chem. Soc.*, 2005, **127**, 5286; M. J. Manos, R. G. Iyer, E. Quarez, J. H. Liao and M. G. Kanatzidis, *Angew. Chem., Int. Ed.*, 2005, **44**, 3552; N. Ding and M. G. Kanatzidis, *Angew. Chem., Int. Ed.*, 2006, **45**, 1397; N. Ding, D.-Y. Chung and M. G. Kanatzidis, *Chem. Commun.*, 2004, 1170; Y. Dong, Q. Peng, R. Wang and Y. Li, *Inorg. Chem.*, 2003, **42**, 1794; M. Wu, W. Su, N. Jasutkar, X. Huang and J. Li, *Mater. Res. Bull.*, 2005, **40**, 21.
367 W. Su, X. Huang, J. Li and H. Fu, *J. Am. Chem. Soc.*, 2002, **124**, 12944.
368 U. Simon, F. Schüth, S. Schunk, X. Wang and F. Liebau, *Angew. Chem., Int. Ed.*, 1997, **36**, 1121.
369 F. Starrost, E. E. Krasovskii, W. Schattke, J. Jockel, U. Simon, X. Wang and F. Liebau, *Phys. Rev. Lett.*, 1998, **80**, 3316.
370 J. A. Hanko and M. G. Kanatzidis, *Angew. Chem., Int. Ed.*, 1998, **37**, 342.
371 A. E. C. Palmqvist, B. B. Iversen, E. Zanghellini, M. Behm and G. D. Stucky, *Angew. Chem., Int. Ed.*, 2004, **43**, 700.
372 H. Ahari, G. A. Ozin, R. L. Bedard, S. Petrov and D. Young, *Adv. Mater.*, 1995, **7**, 370.
373 N. Zheng, X. Bu, H. Vu and P. Feng, *Angew. Chem., Int. Ed.*, 2005, **44**, 5299.
374 N. Zheng, X. Bu and P. Feng, *Chem. Commun.*, 2005, 2805.
375 N. Zheng, X. Bu and P. Feng, *Nature*, 2003, **426**, 428.
376 N. Zheng, X. Bu and P. Feng, *Angew. Chem., Int. Ed.*, 2004, **43**, 4753.

377 For some examples, see: G. S. Goplakrishna, S. P. Madhu, M. Mahendra, B. H. Doreswamy, M. J. Mahesh, M. A. Sridhar and J. S. Prasad, *Mater. Lett.*, 2006, **60**, 613, and references thereinL. Sebastian and J. Gopalakrishnan, *J. Mater. Chem.*, 2003, **13**, 433, and references thereinC. Falah, H. Bohghzala, T. Jouini and A. Madani, *J. Solid State Chem.*, 2003, **173**, 342; R. Vaidhyanathan, S. Natarajan and C. N. R. Rao, *J. Solid State Chem.*, 2001, **162**, 150; S. Obbade, C. Dion, M. Rivenet, M. Saadi and F. Abraham, *J. Solid State Chem.*, 2004, **177**, 2058; S. Wang and S.-J. Hwu, *Chem. Mater.*, 1992, **4**, 589, and references therein.
378 J. Pang, E. J.-P. Marcotte, C. Seward, R. Stephen Brown and S. Wang, *Angew. Chem., Int. Ed.*, 2001, **40**, 4042.
379 Y. Bai, G.-j. He, Y.-g. Zhao, C.-y. Duan, D.-b. Dang and Q.-j. Meng, *Chem. Commun.*, 2006, 1530.
380 B. Zhao, X.-Y. Chen, P. Cheng, D.-Z. Liao, S.-P. Yan and Z.-H. Jiang, *J. Am. Chem. Soc.*, 2004, **126**, 15394.
381 Y. Li and C. M. Yang, *J. Am. Chem. Soc.*, 2005, **127**, 3527.
382 For Cd(II) examples, see: B. Ding, L. Yi, Y. Wang, P. Cheng, D.-Z. Liao, S.-P. Yan, Z.-H. Jiang, H.-B. Song and H.-G. Wang, *Dalton Trans.*, 2006, 665; W.-G. Lu, L. Jiang, X.-L. Feng and T.-B. Lu, *Cryst. Growth Des.*, 2006, **6**, 564; L. Wen, Y. Li, Z. Lu, J. Lin, C. Duan and Q. Meng, *Cryst. Growth Des.*, 2006, **6**, 530; L.-L. Wen, D.-B. Dang, C.-Y. Duan, Y.-Z. Li, Z.-F. Tian and Q.-J. Meng, *Inorg. Chem.*, 2005, **44**, 7161; X. Li, R. Cao, W. Bi, D. Yuan and D. Sun, *Eur. J. Inorg. Chem.*, 2005, 3156; J. Lu, K. Zhao, Q.-R. Fang, J.-Q. Xu, J.-H. Yu, X. Zhang, H.-Y. Bie and T.-G. Wang, *Cryst. Growth Des.*, 2005, **5**, 1091; J.-C. Dai, X.-T. Wu, S.-M. Hu, Z.-Y. Fu, J.-J. Zhang, W.-X. Du, H.-H. Zhang and R.-Q. Sun, *Eur. J. Inorg. Chem.*, 2004, 2096; Q. Fang, G. Zhu, X. Shi, G. Wu, G. Tian, R. Wang and S. Qiu, *J. Solid State Chem.*, 2004, **177**, 1060; J.-X. Chen, S.-X. Liu and E.-Q. Gao, *Polyhedron*, 2004, **23**, 1877; J. Luo, M. Hong, R. Wang, R. Cao, L. Han and Z. Lin, *Eur. J. Inorg. Chem.*, 2003, 2705; J.-C. Dai, S.-M. Hu, X.-T. Wu, Z.-Y. Fu, W.-X. Du, H.-H. Zhang and R.-Q. Sun, *New J. Chem.*, 2003, **27**, 914; J.-C. Dai, X.-T. Wu, Z.-Y. Fu, C.-P. Cui, S.-M. Hu, W.-X. Du, L.-M. Wu, H.-H. Zhang and R.-Q. Sun, *Inorg. Chem.*, 2002, **41**, 1391; J.-C. Dai, X.-T. Wu, Z.-Y. Fu, S.-M. Hu, W.-X. Du, C.-P. Cui, L.-M. Wu, H.-H. Zhang and R.-Q. Sun, *Chem. Commun*, 2002, 12.
383 For Zn(II) examples, see: Y.-F. Zhou, B.-Y. Lou, D.-Q. Yuan, Y.-Q. Xu, F.-L. Jiang and M.-C. Hong, *Inorg. Chim. Acta*, 2005, **358**, 3057; L. Xua, B. Liua, F.-K. Zhenga, G.-C. Guoa and J.-S. Huang, *J. Solid State Chem.*, 2005, **178**, 3306; M.-S. Wang, G.-C. Guo, L.-Z. Cai, W.-T. Chen, B. Liu, A.-Q. Wu and J.-S. Huang, *Dalton Trans.*, 2004, 2230; C. Jiang, Z. Yu, S. Wang, C. Jiao, J. Li, Z. Wang and Y. Cui, *Eur. J. Inorg. Chem.*, 2004, 3662; W. Chen, J.-Y. Wang, C. Chen, Q. Yue, H.-M. Yuan, J.-S. Chen and S.-N. Wang, *Inorg. Chem.*, 2003, **42**, 944.
384 C.-G. Zheng, Y.-L. Xie, R.-G. Xiong and X.-Z. You, *Inorg. Chem. Commun.*, 2001, **4**, 405.
385 Q. Fang, G. Zhu, M. Xue, J. Sun, F. Sun and S. Qiu, *Inorg. Chem.*, 2006, **45**, 3582.
386 R.-Q. Zou, Y. Yamada and Q. Xu, *Microporous Mesoporous Mater.*, 2006, **91**, 233.
387 H.-K. Fun, S. S. S. Raj, R.-G. Xiong, J.-L. Zuo, Z. Yu and X.-Z. You, *J. Chem. Soc., Dalton Trans.*, 1999, 1915.
388 For a review, see: R. J. Hill, D.-L. Long, P. Hubberstey, M. Schröder and N. R. Champness, *J. Solid State Chem.*, 2005, **178**, 2414.
389 T. M. Reineke, M. Eddaoudi, M. Fehr, D. Kelley and O. M. Yaghi, *J. Am. Chem. Soc.*, 1999, **121**, 1651; A. Thirumurugan and S. Natarajan, *Cryst. Growth Des.*, 2006, **6**, 983; X. Guo, G. Zhu, F. Sun, Z. Li, X. Zhao, X. Li, H. Wang and S. Qiu, *Inorg. Chem.*, 2006, **45**, 2581; X. Guo, G. Zhu, Z. Li, Y. Chen, X. Li and S. Qiu, *Inorg. Chem.*, 2006, **45**, 4065; C. Serre, F. Pelle, N. Gardant and G. Ferey, *Chem. Mater.*, 2004, **16**, 1177.
390 J.-L. Song and J.-G. Mao, *Chem. Eur. J.*, 2005, **11**, 1417.
391 C. Serre, F. Millange, C. Thouvenot, N. Gardant, F. Pelléb and G. Férey, *J. Mater. Chem.*, 2004, **14**, 1540.
392 Y. Kim, M. Suh and D.-Y. Jung, *Inorg. Chem.*, 2004, **43**, 245; Z. Wanga, M. Ströbeleb, K.-L. Zhanga, H. -J. Meyerb, X.-Z. Youa and Z. Yu, *Inorg. Chem. Commun.*, 2002, **5**, 230.
393 H.-T. Zhang, Y. Song, Y.-X. Li, J.-L. Zuo, S. Gao and X.-Z. You, *Eur. J. Inorg. Chem.*, 2005, 766.
394 X. Guo, G. Zhu, Q. Fang, M. Xue, G. Tian, J. Sun, X. Li and S. Qiu, *Inorg. Chem.*, 2005, **44**, 3850.
395 L. Han, R. Wang, D. Yuan, B. Wu, B. Lou and M. Hong, *J. Mol. Struct.*, 2005, **737**, 55; M.-L. Tong, J.-X. Shi and X.-M. Chen, *New J. Chem.*, 2002, **26**, 814; M.-L. Tong, X.-M. Chen, B.-H. Ye and L.-N. Ji, *Angew. Chem., Int. Ed.*, 1999, **38**, 2237.
396 C. Seward, W.-L. Jia, R.-Y. Wang, G. D. Enright and S. Wang, *Angew. Chem., Int. Ed.*, 2004, **43**, 2933.
397 Y.-L. Shen, H.-L. Jiang, J. Xu, J.-G. Mao and K. W. Cheah, *Inorg. Chem.*, 2005, **44**, 9314.
398 A. Ferreira, D. Ananias, L. D. Carlos, C. M. Morais and J. Rocha, *J. Am. Chem. Soc.*, 2003, **125**, 14573.
399 X. Liu, G.-C. Guo, A.-Q. Wu, L.-Z. Cai and J.-S. Huang, *Inorg. Chem.*, 2005, **44**, 4282.
400 T. A. Sullensa, P. M. Almonda, J. A. Byrda, J. V. Beitzb, T. H. Braya and T. E. Albrecht-Schmitt, *J. Solid State Chem.*, 2006, **179**, 1192; T. Y. Shvareva, J. V. Beitz, E. C. Duin and T. E. Albrecht-Schmitt, *Chem. Mater.*, 2005, **17**, 6219; R. Fu, H. Zhang, L. Wang, S. Hu, Y. Li, X. Huang and X. Wu, *Eur. J. Inorg. Chem.*, 2005, 3211; H.-X. Zhang, J. Zhang, S.-T. Zheng, G.-M. Wang and G.-Y. Yang, *Inorg. Chem.*, 2004, **43**, 6148; X. Wang, L. Liu, J. Huang and A. J. Jacobson, *J. Solid State Chem.*, 2006, **177**, 2499; C. S. Liang, W. T. A. Harrison, M. M. Eddy, T. E. Gier and G. D. Stucky, *Chem. Mater.*, 1993, **5**, 917.
401 H. Hou, Y. Song, H. Xu, Y. Wei, Y. Fan, Y. Zhu, L. Li and C. Du, *Macromolecules*, 2003, **36**, 999.
402 For more information about dynamic coordination polymers, see: S. Kitagawa and K. Uemura, *Chem. Soc. Rev.*, 2005, **34**, 109.
403 M. Kurmoo, H. Kumagai, K. W. Chapman and C. J. Kepert, *Chem. Commun.*, 2005, 3012.
404 M. Kurmoo, H. Kumagai, M. Akita-Tanaka, K. Inoue and S. Takagi, *Inorg. Chem.*, 2006, **45**, 1627.
405 J. Larionova, O. Kahn, S. Gohlen, L. Ouahab and R. Clérac, *J. Am. Chem. Soc.*, 1999, **121**, 3349; J. Larionova, R. Clérac, J. Sanchiz, O. Kahn, S. Golhen and L. Ouahab, *J. Am. Chem. Soc.*, 1998, **120**, 13088.
406 S.-I. Ohkoshi, K.-I. Arai, Y. Sato and K. Hashimoto, *Nat. Mater.*, 2004, **3**, 857.
407 Y. Sato, S.-i. Ohkoshi, K.-i. Arai, M. Tozawa and K. Hashimoto, *J. Am. Chem. Soc.*, 2003, **125**, 14590.
408 Z. Lu, X. Wang, Z. Liu, F. Liao, S. Gao, R. Xiong, H. Ma, D. Zhang and D. Zhu, *Inorg. Chem.*, 2006, **45**, 999.
409 S. Bonhommeau, G. Molnár, A. Galet, A. Zwick, J. A. Real, J. J. McGarvey and A. Bousseksou, *Angew. Chem., Int. Ed.*, 2005, **44**, 4069.
410 V. Niel, A. L. Thompson, M. C. Muñoz, A. Galet, A. E. Goeta and J. A. Real, *Angew. Chem., Int. Ed.*, 2003, **42**, 3760.
411 H. Ahari, C. L. Bowes, T. Jiang, A. Lough, G. A. Ozin, R. L. Bedard, S. Petrov and D. Young, *Adv. Mater.*, 1995, **7**, 375.
412 S. Hermes, F. Schröder, R. Chelmowski, C. Wöll and R. A. Fischer, *J. Am. Chem. Soc.*, 2005, **127**, 13744.
413 M. Altman, A. D. Shkla, T. Zubkov, G. Evmenenko, P. Dutta and M. E. van der Boom, *J. Am. Chem. Soc.*, 2006, **128**, 7374.

